



**Gonçalo Amorim
Ribeiro Gomes
Pereira**

**Arquitectura WDM-PON Baseada em Componentes
Sintonizáveis**

**WDM-PON Architecture Based on Tunable
Components**



**Gonçalo Amorim
Ribeiro Gomes
Pereira**

Arquitectura WDM-PON Baseada em Componentes Sintonizáveis

WDM-PON Architecture Based on Tunable Components

Dissertação apresentada à Universidade de Aveiro para cumprimento dos requisitos necessários à obtenção do grau de Mestre em Engenharia Electrónica e Telecomunicações, realizada sob a orientação científica do Prof. Dr. António Teixeira e do Prof. Dr. Mário Lima, ambos do Departamento de Electrónica, Telecomunicações e Informática (DETI) e do Instituto de Telecomunicações (IT) da Universidade de Aveiro.

Dedico este trabalho em especial aos meus pais, mas também aos meus amigos e aos restantes membros da minha família sem os quais não me teria sido possível concretizar este percurso académico.

O Júri

Presidente

Prof. Dr. Nuno Miguel Gonçalves Borges de Carvalho
Prof. Associado com Agregação da Universidade de Aveiro

Vogal

Prof. Dr. Henrique Manuel de Castro Faria Salgado
Prof. Associado da Faculdade de Engenharia da Universidade do Porto

Orientador

Prof. Dr. Mário José Neves de Lima
Prof. Auxiliar da Universidade de Aveiro

Co-Orientador

Prof. Dr. António Luís Jesus Teixeira
Prof. Associado da Universidade de Aveiro

Agradecimentos

Esta dissertação marca o fim de um percurso de 5 anos. Um percurso que teve certamente mais altos do que baixos, e do qual levarei momentos que ficarão comigo para o resto da vida. Aproveito agora para fazer agradecimentos a algumas pessoas que me marcaram neste percurso.

Gostaria de começar por agradecer aos meus pais, Daisi e Carlos, ao meu irmão, Tiago, e também à minha avó materna, Alda. Certamente que sem eles tudo isto não teria sido possível.

Gostaria também de agradecer aos meus amigos e companheiros de vida académica, Andreia Migueis, Hugo Carvalho, Tiago Mendes e Rui Silva, por todos os momentos passados, entre noitadas (tanto de estudo como de diversão) e viagens. Certamente que em muito contribuíram para me moldar e melhorar.

Gostaria ainda de agradecer aos restantes amigos, os “de sempre”, que com maior ou menor frequência estiveram presentes e me apoiaram e ajudaram a cumprir esta caminhada: Cátia Silva, Daniela Melo, Daniela Simões, Elton Rafael, Hugo Canas, Inês Almeida, Luciana Alegre, Mário Penetra, Miguel Mestre, Nuno Seabra, Nuno Vicente, Pedro Maria, Pedro Pintado e Rui Dimas.

Não poderia também deixar de mencionar os, poucos mas bons, amigos que fiz durante a minha experiência Erasmus: Adam Urbanec, Dimitri, Joanna Drygajlo e Patrícia Carvalho.

Um agradecimento ainda para os companheiros de equipa e treinadores com os quais tive o prazer de trabalhar, tanto no Illiabum Clube como no Clube dos Galitos. Tive oportunidade de lidar com pessoas que tomo como exemplos e que me ajudaram a crescer.

Uma menção ainda para os colegas de laboratório pela paciência e cooperação, em especial Ali Shahpari e Ricardo Ferreira, uma vez que sem estes teria sido mais difícil ultrapassar alguns obstáculos.

Por fim, um agradecimento especial aos meus orientadores, Prof. Dr. António Teixeira e Prof. Dr. Mário Lima, pela disponibilidade e tempo despendido durante este ano lectivo, ajudando-me continuamente a melhorar o meu trabalho e a ultrapassar as dificuldades encontradas.

Palavras-chave

Lasers sintonizáveis, NGPON, QPSK, receptores sintonizáveis, redes de acesso, redes ópticas passivas, transceivers incolores, UDWDM-PON, WDM-PON.

Resumo

O tema principal abordado neste trabalho é a tecnologia WDM-PON como próxima geração de redes de acesso. Começou por ser feita uma abordagem geral a este tópico, servindo esta como ponto de partida para a parte experimental. Foi proposta e demonstrada uma arquitectura WDM-PON bidirecional directamente modulada baseada em lasers sintonizáveis e receptores sintonizáveis no terminal do utilizador, e um divisor de potência no nó de acesso. Foram também apontados possíveis melhoramentos ao hardware desta arquitectura.

Dois formatos de modulação avançados – QPSK e Duobinário – foram abordados, no contexto dos sistemas WDM-PON. Assim sendo, foram testados um sistema coerente QPSK e um sistema UDWDM-QPSK e foram apresentados os resultados obtidos.

Keywords

Access networks, colorless transceivers, NGPON, passive optical networks, QPSK, tunable lasers, tunable receivers, UDWDM-PON, WDM-PON.

Abstract

The main topic of this work is WDM-PON as a technology for next generation access networks. It was first made a general approach to this topic, serving as starting point to the experimental part. It was proposed and demonstrated a bidirectional directly modulated WDM-PON architecture based on tunable lasers and tunable receivers at the users' end, and a splitter at the Remote Node. Possible improvements to this architecture's hardware were also pointed out.

Two advanced modulation formats – QPSK and Duobinary – were addressed, in the context of WDM-PON systems. Thus, we tested a coherent QPSK and a UDWDM QPSK system and present the obtained results.

Table of Contents

Table of Contents	I
List of Figures.....	IV
List of Tables	VI
List of Acronyms	VII
1. Introduction	1
1.1. Context and Motivation	1
1.2. Structure and Objectives.....	4
1.3. Contributions.....	5
2. An Overview on WDM-PON	7
2.1. Introduction.....	7
2.2. Key Features and Issues	7
2.2.1. Challenges to Overcome.....	9
2.2.1.1. Standardization	9
2.2.1.2. Equipment Cost.....	9
2.2.1.3. Investment	10
2.2.2. Market Drivers	10
2.2.2.1. Bandwidth.....	10
2.2.2.2. Total Cost of Ownership (TCO)	10
2.2.2.3. Scalability	11
2.3. Approaches	11
2.3.1. Tunable Lasers (and Receivers)	14
2.3.2. Spectrum Slicing (with BLS)	17
2.3.3. Injection Locking.....	18
2.3.3.1. With BLS Seeding.....	18
2.3.3.2. With Modulated Downstream Signal	19
2.3.4. Reflective	20
2.3.4.1. RSOA with BLS Seeding	20

2.3.4.2.	RSOA with Laser Array Seeding	21
2.3.4.3.	RSOA with Self Seeding	22
2.3.4.4.	RSOA with Remodulation	23
2.4.	Market Status.....	24
2.4.1.	Vendors	24
2.4.1.1.	SFPs	25
2.4.1.2.	UDWDM-PON	27
2.4.2.	Service Providers.....	28
3.	Modulation.....	31
3.1.	Introduction.....	31
3.2.	Direct Modulation Vs. External	31
3.3.	Direct Detection Vs. Coherent.....	33
3.4.	Advanced Modulation Formats.....	35
3.4.1.	QPSK	35
3.4.2.	Duobinary	37
4.	Proposed Architecture	41
4.1.	Introduction	41
4.2.	Components.....	42
4.2.1.	Lasers.....	42
4.2.1.1.	DFB Laser (OLT)	42
4.2.1.2.	Tunable Laser (ONU).....	44
4.2.2.	Receivers	49
4.2.2.1.	Tunable Receiver (ONU)	49
4.2.2.2.	APD (OLT).....	50
4.2.3.	Others.....	51
4.2.3.1.	AWG (OLT).....	51
4.2.3.2.	SMF.....	52
4.2.3.3.	Power Splitter.....	52
4.2.3.4.	Circulator (ONU).....	53
4.3.	Configurations and Link Budgets.....	54
4.3.1.	Downstream Transmission	54
4.3.2.	Upstream Transmission	55
5.	Experimental Results.....	57

5.1.	Introduction.....	57
5.2.	Proposed Architecture	57
5.2.1.	Conditions of Measurements.....	57
5.2.2.	Downstream Transmission.....	58
5.2.3.	Upstream Transmission	60
5.3.	QPSK Systems.....	63
5.3.1.	General Specifications.....	63
5.3.2.	Coherent QPSK System	65
5.3.2.1.	Setup.....	65
5.3.2.2.	Results	65
5.3.2.2.1.	Without Adjacent Channel	65
5.3.2.2.2.	With Adjacent Channel	67
5.3.3.	Coherent UDWDM QPSK System.....	70
5.3.3.1.	Setup.....	70
5.3.3.2.	Results	71
6.	Conclusions and Future Work.....	75
6.1.	Conclusions	75
6.2.	Future Work.....	77
	References.....	79

List of Figures

FIGURE 1.1.1 – NETWORK ARCHITECTURE OF A TDM-PON [1].	2
FIGURE 1.1.2 – ACCESS NETWORK CAPACITY BY APPLICATION AND TECHNOLOGY [4].	3
FIGURE 2.2.1 EXPECTED PON DEPLOYMENT [3].	8
FIGURE 2.2.2.2.1 – TCO COMPARISON FOR DIFFERENT ACCESS NETWORKS [11].	11
FIGURE 2.3.1 – APPLICATIONS AND ISSUES FOR TWO TYPES OF WDM-PON [12].	12
FIGURE 2.3.2 – APPROACHES TO REALIZE COLORLESS ONUS [12].	13
FIGURE 2.3.3 – COMPARISON OF COLORLESS LIGHT SOURCES [13].	14
FIGURE 2.3.1.1 – EXPERIMENTAL SETUP FOR DOWNSTREAM TRANSMISSION USED IN [15].	15
FIGURE 2.3.1.2 – EXPERIMENTAL SETUP FOR UPSTREAM TRANSMISSION USED IN [15].	16
FIGURE 2.3.2.1 – EXPERIMENTAL SETUP USED IN [17].	17
FIGURE 2.3.3.1.1 – EXPERIMENTAL SETUP USED IN [18].	18
FIGURE 2.3.3.2.1 – EXPERIMENTAL SETUP USED IN [19].	19
FIGURE 2.3.4.1.1 – EXPERIMENTAL SETUP USED IN [20].	20
FIGURE 2.3.4.2.1 – EXPERIMENTAL SETUP USED IN [22].	21
FIGURE 2.3.4.3.1 – EXPERIMENTAL SETUP USED IN [23].	22
FIGURE 2.3.4.4.1 – EXPERIMENTAL SETUP USED IN [24].	23
FIGURE 2.4.1.1 – PON PORTS BY TECHNOLOGY [25].	24
FIGURE 2.4.1.2 – PONY EXPRESS 16 SYSTEM CONFIGURATION [26].	25
FIGURE 2.4.1.1.1 – GPON FOR INTERCONNECTING EPON/GPON WITH WDM-PON [28].	26
FIGURE 2.4.1.1.2 – FUNCTIONAL BLOCKS OF WTG32 X-LINK [28].	26
FIGURE 2.4.1.2.1 – HIGH-LEVEL UDWDM NETWORK CONCEPT [31].	27
FIGURE 2.4.2.1 – WDM-PON SYSTEM STATUS IN SOUTH KOREA (IS – INJECTION SEEDED; TL – TUNABLE LASER) [33].	29
FIGURE 3.2.1 – DIRECT AND EXTERNAL MODULATION (AMPLITUDE) [35].	32
FIGURE 3.2.2 – MACH-ZEHNDER INTERFEROMETER SCHEMATIC DRAWING [37].	33
FIGURE 3.3.1 – COHERENT DEMODULATION FOR A PHASE-MODULATED FORMAT [38].	34
FIGURE 3.3.2 – SCHEMATIC OF THE DSP BLOCKS IN A DIGITAL COHERENT RECEIVER [40].	35
FIGURE 3.4.1.1 – CONSTELLATION DIAGRAM FOR QPSK WITH GRAY ENCODING (EACH ADJACENT SYMBOL ONLY DIFFERS BY ONE BIT) [42].	36
FIGURE 3.4.1.2 – NESTED MZM AS A MODULATOR FOR QPSK SIGNALS [38].	36
FIGURE 3.4.1.3 – ERROR VECTOR MAGNITUDE AND RELATED QUANTITIES [43].	37
FIGURE 3.4.2.1 – NRZ AND DUOBINARY EYE DIAGRAM COMPARISON [46].	38
FIGURE 3.4.2.2 – INTENSITY AND PHASE CHARACTERISTICS OF STANDARD DUOBINARY AND PSBT PULSES IN A ‘1110010100111’ SEQUENCE [45].	39
FIGURE 3.4.2.3 – CONFIGURATION OF DIFFERENT DUOBINARY TRANSMITTERS [45].	39
FIGURE 4.1.1 – EXPERIMENTAL SETUP PROPOSED.	42
FIGURE 4.2.1.1.1 – POWER VARIATION WITH BIAS CURRENT FOR THE 1547.7 NM CHANNEL.	43
FIGURE 4.2.1.1.2 – WAVELENGTH VARIATION WITH BIAS CURRENT FOR THE 1549.3 NM CHANNEL.	43
FIGURE 4.2.1.1.3 – RF RESPONSE FOR THE 1546.9 NM CHANNEL.	44
FIGURE 4.2.1.2.1 – WAVELENGTH VARIATION WITH HEATER PARAMETER FOR TL3.	45
FIGURE 4.2.1.2.2 – POWER VARIATION WITH WAVELENGTH FOR TL3.	46
FIGURE 4.2.1.2.3 – RF RESPONSE FOR TL1.	46
FIGURE 4.2.1.2.4 – POWER DRIFT OVER TIME FOR TL2.	48
FIGURE 4.2.2.1.1 – RF RESPONSE FOR TR1 @ 1547.7 NM.	50
FIGURE 4.2.2.2.1 – RF RESPONSE FOR APD1 @ 1546.9 NM.	50

FIGURE 4.2.2.2.2 – RF RESPONSE FOR APD1 @ 1547.7 NM.....	51
FIGURE 4.2.3.3.1 – 1:32 SPLITTER CONFIGURATION USED.....	52
FIGURE 4.2.3.4.1 – OPTICAL CIRCULATOR.	53
FIGURE 5.2.2.1 – BER VS OPTICAL BUDGET FOR DOWNSTREAM TRANSMISSION @ 1.25 GBPS.	58
FIGURE 5.2.2.2 – EYE DIAGRAM FOR 40 KM AND 38.0 DB OPTICAL BUDGET @ 1.25 GBPS...59	59
FIGURE 5.2.2.3 – BER VS OPTICAL BUDGET FOR DOWNSTREAM TRANSMISSION @ 2.5 GBPS.	59
FIGURE 5.2.2.4 – EYE DIAGRAM FOR 40 KM AND 37.0 DB OPTICAL BUDGET @ 2.5 GBPS....	60
FIGURE 5.2.3.1 – BER VS OPTICAL BUDGET FOR UPSTREAM TRANSMISSION @ 1.25 GBPS. 61	61
FIGURE 5.2.3.2 – EYE DIAGRAM FOR 20 KM AND 26.0 DB OPTICAL BUDGET @ 1.25 GBPS...61	61
FIGURE 5.2.3.3 – EYE DIAGRAM FOR 0 KM AND 22.0 DB OPTICAL BUDGET @ 2.5 GBPS.....62	62
FIGURE 5.2.3.4 – EYE DIAGRAM FOR 0 KM AND 22.0 DB OPTICAL BUDGET @ 2 GBPS.....62	62
FIGURE 5.3.1.1 – CONFIGURATION OF A POLARIZATION/PHASE DIVERSITY HOMODYNE RECEIVER [38].....	64
FIGURE 5.3.2.1.1 – COHERENT QPSK SYSTEM EXPERIMENTAL SETUP.....	65
FIGURE 5.3.2.2.1.1 – SIGNAL STATUS AFTER COMPENSATION FOR BACK-TO-BACK (VITERBITAP = 8).....	66
FIGURE 5.3.2.2.1.2 – SIGNAL STATUS AFTER COMPENSATION FOR 20 KM (VITERBITAP = 8).67	67
FIGURE 5.3.2.2.2.1 – EVM Vs. QPSK SIGNAL WAVELENGTH WITH A NRZ ADJACENT CHANNEL @ 1550.12 NM AND WORKING @ 6 GBPS (FOR 3 DIFFERENT OUTPUT POWERS OF THIS CHANNEL).....	68
FIGURE 5.3.2.2.2.2 – EVM Vs. QPSK SIGNAL WAVELENGTH WITH A NRZ ADJACENT CHANNEL @ 1550.12 NM AND WORKING @ 10 GBPS (FOR 3 DIFFERENT OUTPUT POWERS OF THIS CHANNEL).....	69
FIGURE 5.3.2.2.2.3 – EVM Vs. QPSK SIGNAL WAVELENGTH WITH A NRZ ADJACENT CHANNEL @ 1550.12 NM AND WORKING @ 40 GBPS (FOR 3 DIFFERENT OUTPUT POWERS OF THIS CHANNEL).....	69
FIGURE 5.3.2.2.2.4 – EVM Vs. QPSK SIGNAL WAVELENGTH WITH A NRZ ADJACENT CHANNEL @ 1550.12 NM AND FOR 16 DBM OUTPUT POWER (FOR 3 DIFFERENT BIT RATES OF THIS CHANNEL).....	70
FIGURE 5.3.3.1.1 – COHERENT UDWDM QPSK SYSTEM EXPERIMENTAL SETUP.....	71
FIGURE 5.3.3.2.1 – CARRIER'S SPECTRUM; ONE OF THE CHANNEL'S SPECTRUM AFTER FILTERING (CUTOFF FREQUENCY = 0.75×622 MHz).....	71
FIGURE 5.3.3.2.2 – SIGNAL SIGNAL STATUS AFTER COMPENSATION FOR BACK-TO-BACK (VITERBITAP = 8).....	72
FIGURE 5.3.3.2.3 – SIGNAL SIGNAL STATUS AFTER COMPENSATION FOR 20 KM (VITERBITAP = 8).....	73

List of Tables

TABLE 4.2.1.2.1 – APPROXIMATE VALUES OF THE FIXED PARAMETERS FOR EACH TL.	45
TABLE 4.2.1.2.2 – WAVELENGTH VARIATION WITH HEATER PARAMETER FOR TL3.	45
TABLE 4.2.1.2.3 – POWER VARIATION WITH LD BIAS FOR TL3 @ 1531.1 NM.	47
TABLE 4.2.1.2.4 – POWER VARIATION WITH LD MODULATION FOR TL3 @ 1531.1 NM.	47
TABLE 4.2.1.2.5 – POWER VARIATION WITH LD TEC FOR TL3 @ 1531.1 NM.	47
TABLE 4.2.1.2.6 – WAVELENGTH VARIATION WITH LD TEC FOR TL3 @ 1531.1 NM.	47
TABLE 4.2.1.2.7 – POWER VARIATION WITH ECL TEC FOR TL3 @ 1531.1 NM.	48
TABLE 4.2.1.2.8 – WAVELENGTH VARIATION WITH ECL TEC FOR TL3 @ 1531.1 NM.	48
TABLE 4.2.1.2.9 – WAVELENGTH DRIFT OVER TIME FOR TL2.	49
TABLE 4.2.3.3.1 – 1:4 SPLITTER LOSSES BY PORT.	53
TABLE 4.2.3.3.2 – 1:8 SPLITTER LOSSES BY PORT.	53
TABLE 4.3.1.1 – LASER CONFIGURATION FOR DOWNSTREAM TRANSMISSION.	54
TABLE 4.3.1.2 – LINK BUDGET FOR DOWNSTREAM TRANSMISSION.	54
TABLE 4.3.2.1 – LASER CONFIGURATION FOR UPSTREAM TRANSMISSION.	55
TABLE 4.3.2.2 – LINK BUDGET FOR UPSTREAM TRANSMISSION.	55
TABLE 5.3.1.1 – RELATION BETWEEN BER AND EVM.	63
TABLE 5.3.2.2.1.1 – EVM FOR DIFFERENT VITERBITAP VALUES (BACK-TO-BACK SCENARIO).	66
TABLE 5.3.2.2.1.2 – EVM FOR DIFFERENT VITERBITAP VALUES (20 KM FIBER LENGTH).	67
TABLE 5.3.3.2.1 – SINGLE CHANNEL AND MULTI CHANNEL EVM RESULTS FOR DIFFERENT VITERBITAP VALUES (BACK-TO-BACK SCENARIO).	72
TABLE 5.3.3.2.2 – SINGLE CHANNEL AND MULTI CHANNEL EVM RESULTS FOR DIFFERENT VITERBITAP VALUES (20 KM FIBER LENGTH).	73

List of Acronyms

<u>#</u>	10G-EPON 3DTV	10 Gbps Ethernet Passive Optical Network 3D Television
<u>A</u>	A/D ADC AN APD APON ASE ATM AWG	Add-Drop Analog-to-Digital Converter Access Node Avalanche Photodiode ATM Passive Optical Network Amplified Spontaneous Emission Asynchronous Transfer Mode Arrayed Waveguide Grating
<u>B</u>	BER BERT BLS BPF BPON BPSK	Bit Error Rate Bit Error Rate Tester Broadband Light Source Band Pass Filter Broadband Passive Optical Network Binary Phase-Shift Keying
<u>C</u>	CATV CD CDR CMA CML CMOS CO CW	Cable Television Chromatic Dispersion Clock/Data Recovery Constant Modulus Algorithm Chirp Managed Laser Complementary Metal-Oxide-Semiconductor Central Office Continuous Wave
<u>D</u>	DBR DEMUX DFB DM DPCC DPSK DQPSK DSL DSP DWDM	Distributed Bragg Reflector Demultiplexer Distributed Feedback Direct Modulation/Modulated Dispersion Precompensation Circuit Differential Phase-Shift Keying Differential Quadrature Phase-Shift Keying Digital Subscriber Line Digital Signal Processor Dense Wavelength Division Multiplexing
<u>E</u>	EAM ECL EDC EDF EDFA	Electro-Absorption Modulator External Cavity Laser Electronic Dispersion Compensator Erbium Doped Fiber Erbium Doped Fiber Amplifier

	EFM	Ethernet in the First Mile
	EPON	Ethernet Passive Optical Network
	EOM	Electro-Optic Modulator
	EVM	Error Vector Magnitude
<u>F</u>	FEC	Forward Error Correction
	FM	Fiber Mirror
	FP	Fabry-Pérot
	FSAN	Full Service Access Network
	FTTB	Fiber-to-the-Building
	FTTC	Fiber- to-the -Curb
	FTTH	Fiber- to-the -Home
	FTTx	Fiber- to-the -x
<u>G</u>	Gbps	Gigabit per second
	GPON	Gigabit-capable Passive Optical Network
<u>H</u>	HDTV	High-Definition Television
<u>I</u>	IEEE	Institute of Electrical and Electronics Engineers
	IPTV	Internet Protocol Television
	ISI	Intersymbol Interference
	ITU	International Telecommunication Union
<u>L</u>	LD	Laser Diode
	LED	Light Emitting Diode
	LO	Local Oscillator
<u>M</u>	Mbps	Megabit per second
	MEMS	Microelectromechanic System
	MSM	Metal-Semiconductor-Metal
	MUX	Multiplexer
	MZM	Mach-Zehnder Modulator
<u>N</u>	NGPON	Next-Generation Passive Optical Network
	NRZ	Non-Return-to-Zero
<u>O</u>	ODN	Optical Distribution Network
	OLT	Optical Line Terminal
	ONT	Optical Network Terminal
	ONU	Optical Network Unit
	OOK	On-Off Keying
	OSA	Optical Spectrum Analyzer
	OSR	Optical Spectrum Reshaper
	OTG	Optical Transceiver Group
<u>P</u>	P2P	Point-to-Point
	PBS	Polarization Beam Splitter
	PC	Polarization Controller
	PD	Photodiode

	PG	Pattern Generator
	PIN	Positive-Intrinsic-Negative (Photodiode)
	PM	Power Meter
	PPG	Pulse Pattern Generator
	PON	Passive Optical Network
	PRBS	Pseudo Random Bit Sequence
	PSBT	Phase-Shaped Binary Transmission
	PSK	Phase Shift Keying
<u>Q</u>	QPSK	Quadrature Phase-Shift Keying
<u>R</u>	REAM	Reflective Electro-Absorption Modulator
	RF	Radio Frequency
	RIN	Relative Intensity Noise
	RN	Remote Node
	RSOA	Reflective Semiconductor Optical Amplifier
	Rx	Receiver
<u>S</u>	SFP	Small Form-Factor Pluggable
	SLED/SLD	Superluminescent Diode
	SMF	Single-Mode Optical Fiber
	SMSR	Single-Mode Suppression Ratio
<u>T</u>	T-ECL	Tunable External Cavity Laser
	TCO	Total Cost of Ownership
	TDM	Time Division Multiplexing
	TDM-PON	Time Division Multiplexed Passive Optical Network
	TDMA	Time Division Multiple Access
	TEC	Thermoelectric Cooler
	TIA	Trans-Impedance Amplifier
	TL	Tunable Laser
	TLS	Tunable Laser Source
	TR	Tunable Receiver
	Tx	Transmitter
<u>U</u>	UDWDM	Ultra Dense Wavelength Division Multiplexing
	USB	Universal Serial Bus
<u>V</u>	VCSEL	Vertical-Cavity Surface-Emitting Laser
	VOA	Variable Optical Attenuator
	VOD	Video on Demand
	VoIP	Voice over Internet Protocol
<u>W</u>	WDM	Wavelength Division Multiplexing
	WDM-PON	Wavelength Division Multiplexed Passive Optical Network
<u>X</u>	XG-PON	10 Gigabit-capable Passive Optical Network

“Great work is done by people who are not afraid to be great”

Fernando Flores

1. Introduction

1.1. Context and Motivation

Access networks are responsible for connecting the service providers to their customers (either business or residential). The bandwidth required by customers has been increasing quickly in the last years and is expected to keep this pace. Passive optical networks (PONs) evolved in order to provide much higher bandwidth than previously deployed access networks (DSL and CATV).

In a PON, a single fiber between the optical line terminal (OLT) and the remote node (RN) is shared by all users connected to it. The network between the OLT and the optical network units (ONUs) is passive, which means that there is no need of any power supply in this path.

PON developments started in the early 1990s, by the hands of the Full Service Access Network (FSAN) working group, and led to the creation of APON in 1995 [1]. It is based on ATM and provides 622 Mbps of downstream bandwidth and 155 Mbps of bandwidth for upstream traffic and was mostly used for serving enterprises. APON was standardized by the ITU, which then improved it and developed BPON in 1998, redefining it in 2005 to allow higher bit rates. This technology's signals operate at ATM rates, as well as in the case of APON, but in this case the maximum data rates achieved are 1.2 Gbps and 622 Mbps for downstream and upstream, respectively [1,2].

In 2001, FSAN group started the development of GPON, standardized in 2003 by the ITU, to keep pace with the increasing demand for bandwidth and allowing ATM and Ethernet convergence, since by that time the last one was already the universal standard that ATM craved to be. This later standard supports downstream bit rates up to about 2.5 Gbps and upstream bit rates up to about 1.25 Gbps. [1,3]

Roughly simultaneously to the beginning of GPON's development, the IEEE created a study group called Ethernet in the First Mile (EFM) intended to develop a PON standard exclusively based on Ethernet. This was called EPON and was formally ratified by the IEEE in June 2004. It can support a maximum 1.25 Gbps downstream and upstream traffics (1.0 Gbps of effective traffic). On the market are also available EPON products with 2.0 Gbps effective downstream bit rate. [1,3]

All currently deployed PONs based on the standards referred before are known as TDM-PON architectures since they rely on TDM technology. Upstream transmission is accomplished by time sharing the available bandwidth between all subscribers (TDMA), while downstream operation is performed by sending all data to all ONUs, being these responsible to select the data destined to the subscriber(s) associated. [1,3]

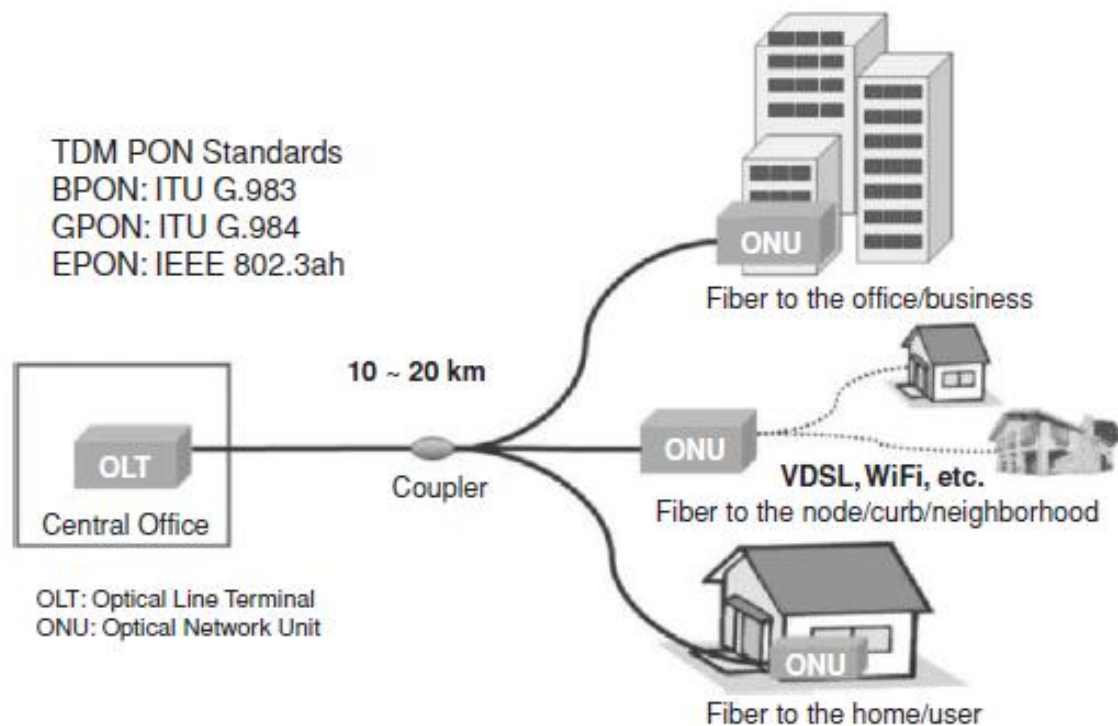


Figure 1.1.1 – Network Architecture of a TDM-PON [1].

These architectures use a maximum of three wavelengths: one for downstream transmission, other for upstream transmission and there is the possibility to add another for video transmission. Downstream data is transmitted in the 1480-1500 nm transmission window, upstream data in the 1290-1330 nm and video transmission in the 1550-1560 nm [1]. The maximum splitting ratio is 128 and the maximum transmission distance is about 60 km but the typical values are 32-64 users and 20-40 km. EPON predominates in Asia while GPON predominates in the USA and Europe [1,3].

Due to progressive massification of new types of traffic (such as 3DTV and cloud-based services) both the ITU and the IEEE have already ratified new standards, still TDM-based. Figure 1.1.2 illustrates some examples of current and future applications as well as their bandwidth requirements.

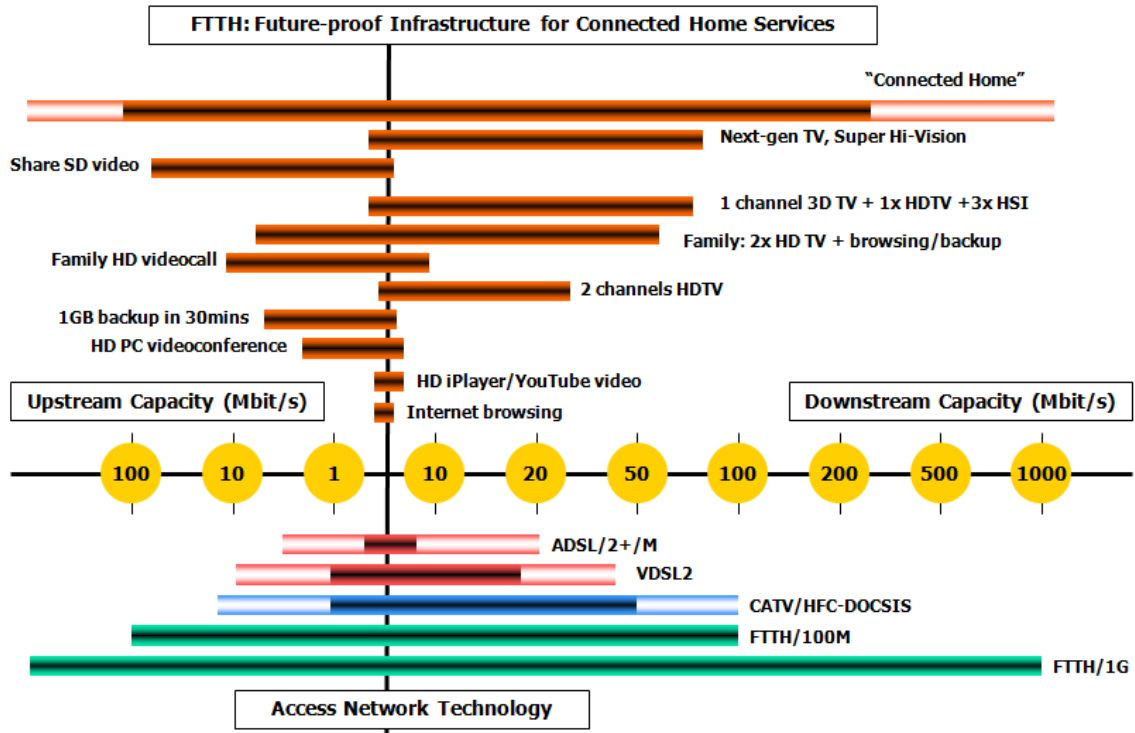


Figure 1.1.2 – Access Network Capacity by Application and Technology [4].

IEEE ratified 10G-EPON in 2009. This offers two bit rate options, one with 10 Gbps of symmetrical bandwidth, and the other with 10 Gbps for downstream transmission and 1 Gbps for upstream transmission. This standard is compatible with EPON, using separate transmission windows for 10 Gbps and 1 Gbps downstream transmissions and the same for both 10 Gbps and 1 Gbps upstream transmissions (with TDMA). 10 Gbps downstream signals are transmitted over the range 1575 to 1580 nm. [1,2,3]

Regarding the ITU, XG-PON1 was standardized in 2010. It allows 10 Gbps and 2.5 Gbps bit rates for downstream and upstream transmissions, respectively. XG-PON2 specification is also expected to be standardized soon, allowing 10 Gbps symmetrical bandwidth. Coexistence with GPON is possible given that this standard uses the 1260-1280 nm transmission window for upstream transmission and the same transmission window that the 10G-EPON standard for the downstream case. [1,2,3]

Even though the data rates offered by TDM-based standards are high, all bandwidth is shared by several users as referred before. Although end users do not sense the effect of this sharing just yet, this will happen sooner than later. So, it is hoped that future access networks to be WDM-based since WDM enables to achieve higher bit rates by transmitting multiple wavelengths on the same fiber. There is also the possibility of achieving greater transmission distances. Furthermore, WDM-PON technology is considered to be future-proof in terms of necessary bandwidth [1,5].

1.2. Structure and Objectives

This document is divided in 6 chapters, and the main objectives are the following:

- Identify the main benefits and drawbacks of WDM-PON technology;
- Identify the different possible approaches for colorless ONUs;
- Propose and demonstrate a WDM-PON architecture based on tunable components enabling 32 users;
- Study the use of advanced modulation formats in a WDM-PON system.

In this **first** chapter are presented the context along with the motivation, the structure and the objectives, as well as the contributions according to the author's opinion.

The **second** chapter presents an overview on WDM-PON, starting by its main features, issues and market drivers. After, are presented the different approaches already proposed in order to accomplish WDM-PON architectures with colorless ONUs. At the end of this chapter is described this technology's market status, regarding both vendors and service providers.

In the **third** chapter a brief approach regarding modulation is done, including the differences between direct and external modulations, as well as between direct and coherent detection types. Two different modulation formats are also briefly described.

Chapter **four** presents the architecture proposed and all its components description. The last subchapter shows the configurations of the lasers and the link budgets for both downstream and upstream transmission scenarios.

In the **fifth** chapter are firstly presented the experimental results for the architecture proposed, including all procedures and conditions of measurements. After are shown some tests performed using an advanced modulation format.

Ultimately, in the **sixth** chapter the conclusions taken from the work carried out are presented and some future work related to this topic is suggested.

1.3. Contributions

In the author's opinion, the main contributions to this work may be summarized as follows:

- Identification of the benefits and drawbacks associated with WDM-PON's implementation;
- Description of the approaches that can provide WDM-PON architectures with colorless ONUs;
- Demonstration of a WDM-PON architecture based on tunable components, analyzing the impact of each of its elements;
- Use of advanced modulation formats to later on improve the proposed architecture in terms of performance.

Additionally to the already mentioned contributions, the following paper was published in the "X Symposium on Enabling Optical Networks and Sensors 2012":

- G. Pereira, A. Shahpari, M. Lima, and A. Teixeira, "Bidirectional Directly Modulated WDM-PON Architecture Based on Tunable Components".

2. An Overview on WDM-PON

2.1. Introduction

In this chapter an overview on WDM-PON is presented, starting by its main features and issues. This includes what still needs to be improved and also the reasons that can make it prevail in the market. After this first part, different approaches will be presented in order to realize a WDM-PON architecture. Along with each of the approaches presented there is also an application example, proving its functionality. The last subchapter is regarding WDM-PON market status, including different solutions provided by vendors as well as already employed access networks.

2.2. Key Features and Issues

WDM allows transmitting multiple wavelengths on the same fiber simultaneously, making use of its huge capacity. WDM-PON is a logical P2P scheme, since there is no time sharing of bandwidth, with each subscriber provided with its own wavelength (and its full bandwidth, of course).

The benefits of using the WDM technology in a PON are plenty, including [1,5,6]:

- Higher bit rates and more effective use of fiber (by transmitting several wavelengths on a single fiber);
- No need for bandwidth scheduling (contrary to TDM-PON technologies);
- Ability to achieve greater transmission distance (by using AWGs, which will be explained later).

According to Analysys Mason's report for Ofcom from 2010 [3], WDM-PON should start its deployment under the second phase of next-generation PONs – NGPON2. Figure 2.2.1 shows the expected PON deployment made by Analysys Mason contained in the document previously referred.

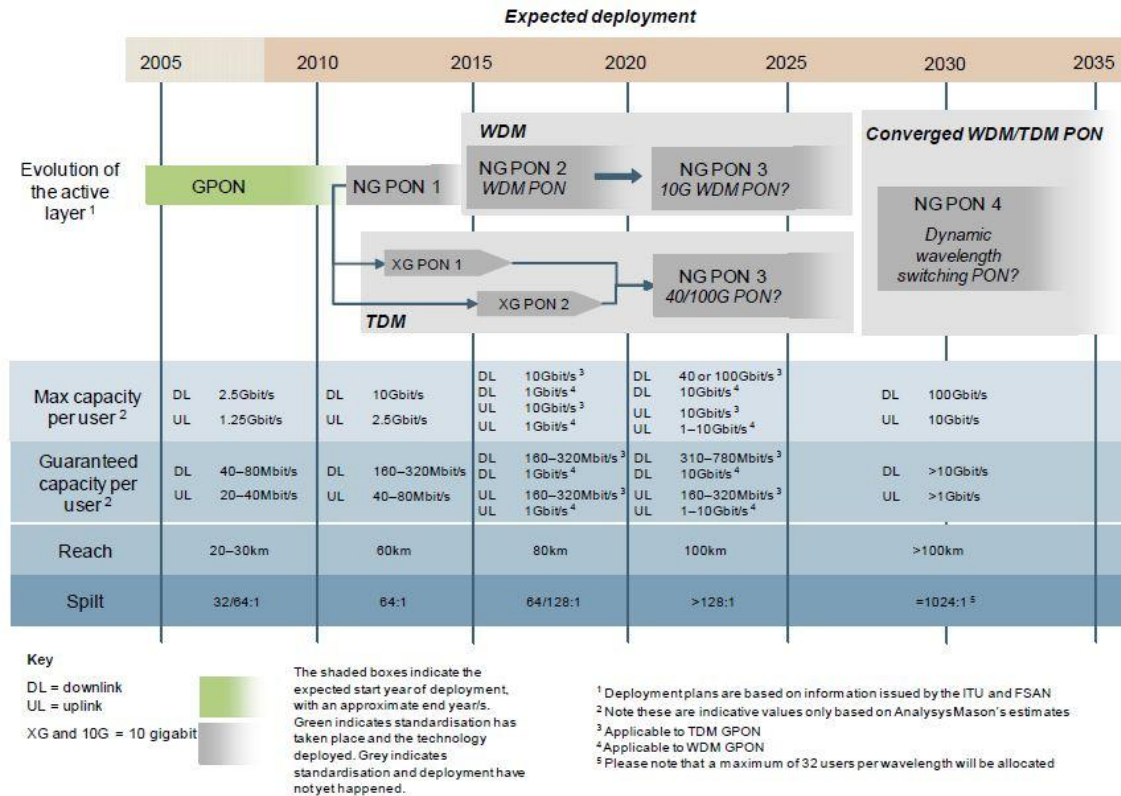


Figure 2.2.1 Expected PON Deployment [3].

Along with this prediction, which pointed the expected start year of deployment in 2015, was to guess that this technology would be standardized in the meantime. However, more recent information tells us that this may not happen even until 2020 meaning that it will not happen under NGPON2 [7]. Standardization is one of the challenges to overcome in order to make the commercial widespread happen. This and other issues will be addressed below, followed by the strengths that may allow it to avenge in the market.

2.2.1. Challenges to Overcome

2.2.1.1. Standardization

Efforts leading to standardization of WDM-PON are being carried out by FSAN since 2010. FSAN is a working group which mission is to drive applicable standards and develop new technical specifications for PONs with the goal of better defining the Full Service Access Network [8].

In order to keep reduced costs, manufacturers started using their proprietary equipment in WDM-PON development but, by now, service providers are demanding standardized equipment. The actions taken by manufacturers resulted in scalability issues and worked as an obstacle to the standardization of this technology, but they have already realized that standardization is fundamental for having success [9].

Some defend ONU standardization, after which they see no reasons to wait for WDM-PON deployment considering the advantages provided [5], while others defend standardization is not fundamental since, for example GPON's fully standardization still did not lead to universal interoperability among vendors [6]. Even so, Jorge Bonifácio, from Portugal Telecom, reminds its importance stating that the standards are the driver for the mass market. Nevertheless, he also refers that Portugal Telecom will deploy this technology when it is economically viable [7].

2.2.1.2. Equipment Cost

The equipment cost is the main obstacle regarding this technology these days. One of the factors contributing to this is the need to have one laser at the OLT for each wavelength. Another problem is regarding the ONT (the same as ONU) since WDM-PON ONT is significantly more expensive than TDM-PON technologies' ONT. According to [4], ONT standardization would result in larger scale production which in turn would result in cost reductions for manufacturers. Standardization would also help to reduce deployment, maintenance and sparing costs.

According to an article recently submitted by GigaWam regarding WDM-PON [10], the only available equipment in the market (by the time that paper was written) has an optics cost of about two times that of EPON and GPON. This means that despite being aware of the advantages,

services providers will hardly carry out large-scale WDM-PON deployments until its price becomes competitive.

2.2.1.3. Investment

WDM-PON commercially widespread implies large share of investment by service providers. Since large amount investments were made for TDM-PON technologies' deployment, service providers want now to maximize the investments made, before migration. Governments also have an important role on this decision since many of them directly injected funds for building FTTx networks. [9]

2.2.2. Market Drivers

2.2.2.1. Bandwidth

The increasing need for bandwidth is the most important market driver for WDM-PON. This is due to wide spreading of services like IPTV, VoIP, VOD, 3DTV, HDTV, file sharing, etc. Due to its enormous capacity, this technology can help service providers to be ahead of bandwidth escalation carried out by consumers. This potentially high bandwidth available is even more attractive for business clients. [5,6,9]

2.2.2.2. Total Cost of Ownership (TCO)

According to [9], once WDM-PON has competitive prices comparing to TDM-PON technologies, service providers can attain long term savings by cutting on upgrade costs. It will also enable TCO reduction by eliminating redundancy layers and unnecessary protocol conversions. It also can make possible merging service providers' metro and access areas. According to [11], a widely deployed WDM-PON network is at least 20% cheaper than GPON. Details can be observed in Figure 2.2.2.2.1.

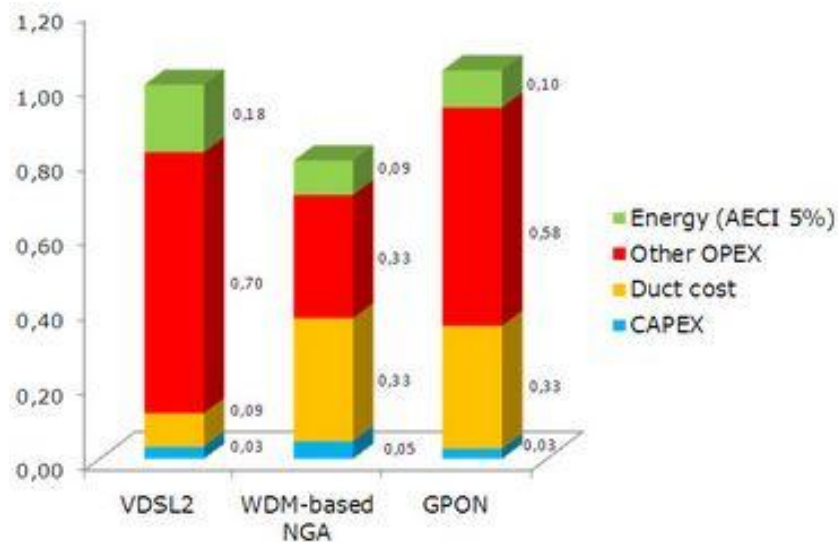


Figure 2.2.2.2.1 – TCO Comparison for Different Access Networks [11].

2.2.2.3. Scalability

Long-term scalability is a highly important market demand. Virtually, this technology has infinite scalability in terms of wavelengths and bandwidth. Bandwidth upgrades can also be done in a simpler way since each subscriber has its own dedicated wavelength [5,6,9].

2.3. Approaches

There are two ways to implement the data distribution at the optical distribution network (ODN) on a WDM-PON: using wavelength routers (usually AWGs) or using passive power splitters. Figure 2.3.1 summarizes the applications and technical issues for the two referred implementations.

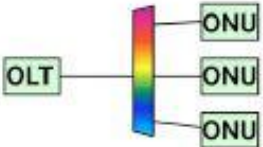
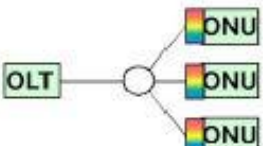
	Application	Issue	Note
Wavelength-router-based WDM-PON 	<ul style="list-style-type: none"> • Long reach (metro/access integration) • Short reach (last one mile) for greenfield 	<ul style="list-style-type: none"> • Colorless ONU • Protection for long reach 	<ul style="list-style-type: none"> • Wavelength allocation is basically static.
Power-splitter-based WDM-PON 	<ul style="list-style-type: none"> • Short reach (last one mile) for migration from legacy PONs 	<ul style="list-style-type: none"> • Colorless ONU 	<ul style="list-style-type: none"> • Dynamic wavelength allocation is possible [6].

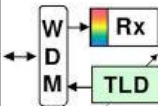
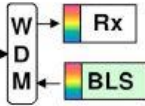
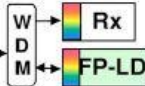
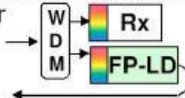
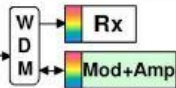
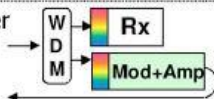
Figure 2.3.1 – Applications and Issues for Two Types of WDM-PON [12].

The second alternative is better in terms of cost since currently deployed PON infrastructures use power splitters and there will be no need to install new equipment. It is also better in terms of space: if the service provider wants to provide both services (the oldest, like for example GPON, and the most recent, WDM-PON) there is no need to have both passive splitter and wavelength router at the ODN. Another issue with using wavelength routers is that changing from one service to another would have to be done manually by disconnecting the fiber cable from the splitter and connecting it to the WDM-PON AWG, which makes this approach more expensive also in terms of human resources. [6,12]

On the other hand, using passive splitters has its own disadvantages: laser locking at the ONU is not an option, once all wavelengths reach an ONU it would not know which wavelength to lock; network security can be an issue, since all ONUs receive all wavelengths; and also lower link budget and reach for WDM-PON, since an AWG experiences significantly less attenuation than a 1:64 splitter (around 4-6 dB against 18-21 dB) [1,3,12].

In order to reduce the costs it is desirable to have colorless equipment at the ONUs. Colorless means wavelength independent or non-wavelength-specific. This results in having the same equipment across all customers, which allows a lower equipment cost due to mass production. It also allows decreasing installation, operational and maintenance expenses for both the service provider, first, and the end user, ultimately. [1,10,12]

According to [12] there are two broad categories concerning different WDM-PON approaches to realize colorless ONUs: Local Emission and Wavelength Supply. The first can be divided into two subcategories: Wavelength Tuning (using tunable lasers) and Spectrum Slicing. The second can also be divided into two subgroups: Injection Locking and Loop Back (using RSOAs or REAMs). Figure 2.3.2 gives a general idea of their differences.

	Local emission		Wavelength supply	
	Wavelength tuning	Spectrum slicing	Injection locking	Loop back
ONU configuration			1 fiber  2 fiber 	1 fiber  2 fiber 
Number of fibers	1	1	1 or 2	1 or 2
Coherency of upstream-signal light	Coherent	Incoherent	Depends on the locking condition and the type of seed light	Depends on the type of seed light
Typical transmission rate	~10 Gbps or over	~2.5 Gbps (~10 Gbps with FEC [9])	~2.5 Gbps (ASE-seeded/1-fiber)	~2.5 Gbps (ASE-seeded/1-fiber/direct-mod) ~10 Gbps (LD-seeded/2-fiber/ext-mod)
Technical issues	Low-cost implementation	<ul style="list-style-type: none">•Beat noise of BLS•Dispersion tolerance	<ul style="list-style-type: none">•Back reflection•SNR of seed light•Insufficient locking [11],[12]	<ul style="list-style-type: none">•Back reflection•SNR of seed light
Wavelength control at ONU	In the case of power-splitter-based WDM-PON, wavelength control of the TLD and wavelength selectors are needed. In the case of wavelength-router-based WDM-PON, no wavelength selectors are needed, and thus only wavelength control of the TLD is needed.			

TLD: Tunable laser diode, BLS: Broadband light source, Rx: Receiver
Mod: Modulator, Amp: Optical amplifier


 : Wavelength selector (WS)

Figure 2.3.2 – Approaches to Realize Colorless ONUs [12].

It is still possible to distinguish different kinds of seed lights according to their source: self-injection, external injection (BLS seed light injection and array laser injection) and wavelength re-use (downstream signal wavelength) [12].

The following subtopics will be regarding the 4 approaches discriminated previously. These will be addressed in greater depth and for each of them will be described a reported system, as so its advantages and disadvantages concerning topics like bit rate, transmission distance and cost (among others). Figure 2.3.3 gives a general idea of what it is expectable from each approach regarding, not only bit rate per channel and number of channels, but also pros and cons.

Scheme	Bit rate/channel	No. channels	Pros	Cons
Spectrum slicing: LED	Low, <155 Mb/s	Low, ≤ 16	Very cheap No seed needed	Poor scalability and reach
Spectrum slicing: SLED/SOA	Low, <155 Mb/s	Medium, ~ 32	Inexpensive No seed needed	Low bit rate and short reach
Injection locked FP with ASE injection	Low, ~ 1.25 Gb/s	Medium, ~ 32	Inexpensive	Non-standard FP needed (wide gain spectrum) RIN limits bit rate and transmission distance
Injection locked FP with laser injection	Medium, >2.5 Gb/s	Medium, ~ 32	Inexpensive	Non-standard FP needed (wide gain spectrum) Polarization dependent upon injection
Injection locked FP with self-seeding	Medium, >1.25 Gb/s	Medium, ~ 32	Inexpensive No seed needed	Non-standard FP needed (wide gain spectrum) Polarization dependent upon injection
RSOA: with ASE injection	Medium, <5 Gbit/s	Medium, ~ 32	Relatively high bit rate	Relatively expensive, Seed source needed Chromatic dispersion limited
RSOA: laser array seeding	Medium, <5 Gbit/s	High, >32	Relatively high bit rate	Laser bank seed source needed Polarization dependent, backscattering problem
RSOA with re-modulation	Medium, <5 Gbit/s	High, >32	Relatively high bit rate No seed source	Downstream extinction ratio is limited Backscattering affects upstream performance
REAM	High, >10 Gbit/s	Low, <32	High bit rate	Expensive; Relatively high injection power Backscatter affects upstream performance
Tuneable laser	High, ≥ 10 Gbit/s	High, ≥ 32	Good output power \Rightarrow long reach No seed needed Wavelength flexible	Expensive External modulator needed Wavelength assignment algorithm needed

Figure 2.3.3 – Comparison of Colorless Light Sources [13].

2.3.1. Tunable Lasers (and Receivers)

This approach consists on having one pair Transmitter/Receiver (Tx/Rx) per wavelength both at the OLT and the ONU. At each ONU a Tx/Rx pair can be tuned to the wavelengths assigned to that ONU with use of tunable components.

As tunable lasers are usually used DFB/DBR lasers, VCSELs or ECLs [1]. For DFB/DBR lasers the tuning is achieved by varying the temperature and the current [1]. These have the problem of limited tuning speed, which can be improved by using multisection DFB/DBR lasers. Nevertheless, these multisection lasers bear other problems related to mode hopping and electronic control. Concerning VCSELs, the ones for the desired wavelengths are not mature in the market yet. Their tuning can be done by a MEMS structure which changes the cavity length by electrostatic control [1]. ECL devices are usually more expensive and bulky than the other types but they provide high single-mode suppression ration (SMSR), narrow linewidth and low relative intensity noise (RIN) [10].

As receiver a tunable optical filter along with a broadband photodiode is usually used. Another approach is to use a MSM-based integrated CMOS wavelength-tunable optical receiver as presented in [14]. This device has the advantages of having low tuning speed (because the wavelength is set electronically), having the necessary channel spacing for the current standards, and also allowing spectral shaping. The limited scalability of its integrated interferometer is a disadvantage once this device gets more complex with increased number of wavelengths used. However, this can be softened by designing the network properly.

Using a system based on Dense WDM (DWDM), a broad range of channels need to be covered and precise wavelength needs to be achieved once the channels are separated only by 0.4 nm or 0.8 nm. The first implicates both lasers and MUXs/DEMUXs (usually AWGs) that cover a wide range of channels while the second implicates lasers with precise temperature control, which is expensive. Despite using tunable lasers solves the problem of not having specific components for each ONU, the cost of this equipment is still too high.

In [15] a WDM-PON solution was demonstrated based on low-cost tunable equipment at the ONU side with 40 Gbps aggregate bandwidth (4 channels of 10 Gbps). Figure 2.3.1.1 and Figure 2.3.1.2 present the downstream and upstream transmission architectures, respectively.

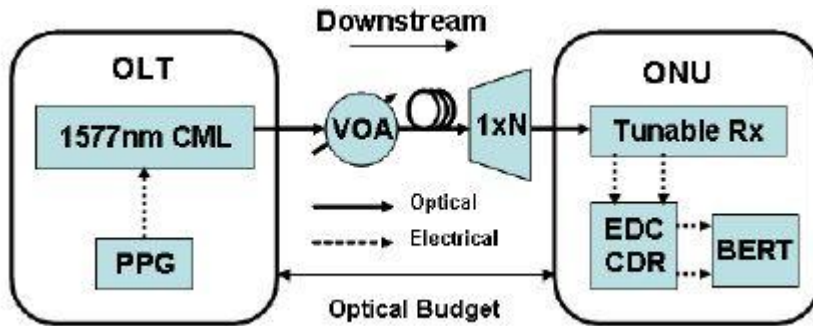


Figure 2.3.1.1 – Experimental Setup for Downstream Transmission Used in [15].

Downstream transmission was achieved by means of a chirp managed laser (CML) at the OLT, which was comprised of a directly modulated DFB laser chirp and a proprietary optical spectrum reshaper (OSR), working at 1577 nm. The pulse pattern generator (PPG) was used to directly drive the CML with a $2^{23}-1$ PRBS at 10 Gbps. The variable optical attenuator (VOA) was employed to simulate link loss.

At the ONU a tunable receiver was used, which was comprised of a tunable semiconductor thin film Fabry-Pérot (FP) filter, an APD and a trans-impedance amplifier (TIA). It was also used an electronic dispersion compensator (EDC) for bandwidth compensation since the receiver was only designed for 2.5 Gbps. There was also a clock/data recovery (CDR) and a bit error rate tester (BERT) for performance measurements.

For downstream transmission was possible to achieve good BER results with up to 40 km (having a reasonable optical budget) using NRZ modulation.

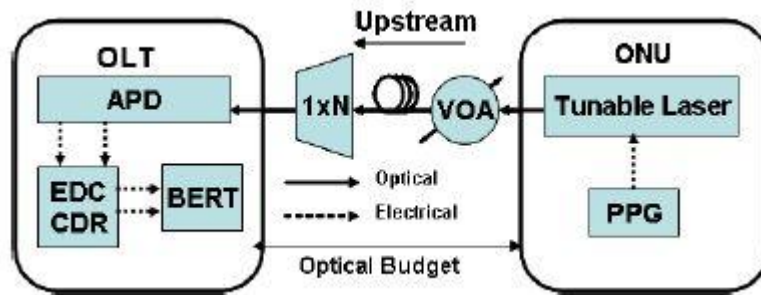


Figure 2.3.1.2 – Experimental Setup for Upstream Transmission Used in [15].

For upstream transmission was used a tunable ECL (T-ECL) at the ONU, which was composed of a SLD and a polymeric tunable Bragg reflector. This tunable laser was designed for 2.5 Gbps operation but it was driven directly at 10 Gbps by the PPG with a 2^7-1 PRBS coded in NRZ. The VOA was again used to simulate link loss.

At the OLT side was used a 10 GHz bandwidth APD as receiver, assisted by an EDC. The CDR and the BERT had the same functions as for downstream transmission. For an acceptable BER was possible to support up to 20 km of fiber.

This approach allows having high data rate at a lower cost. However, the cost may still be quite high since here was just demonstrated a 4-channel system. If we think of 32 or even 64 subscribers this would mean the same amount of lasers at the OLT (one per subscriber). The short transmission distance is also a disadvantage.

2.3.2. Spectrum Slicing (with BLS)

Having BLSs as transmitters is possible to create a WDM-PON scheme by slicing the spectrum of these sources. Considering downstream transmission, after each transmitter sends its signal, these signals need to be sliced (each on a different wavelength) and multiplexed by the AWG. The signal containing all the sliced parts of the original signals will travel along the fiber until it reaches another AWG. This will demultiplex the combined signal and distribute each of these sliced signals by the correspondent ONU, which has a specific receiver for the wavelength assigned to it.

In [16] and [17] are demonstrated WDM-PON schemes based on spectral-sliced BLSs. The solution presented in [17] used 16 channels in each direction (power budget analysis proved that the system would work to more than 40 channels for 20 km transmission distance). These channels were operating in the spectral region around 1300 nm (for both upstream and downstream). A schematic can be seen in Figure 2.3.2.1.

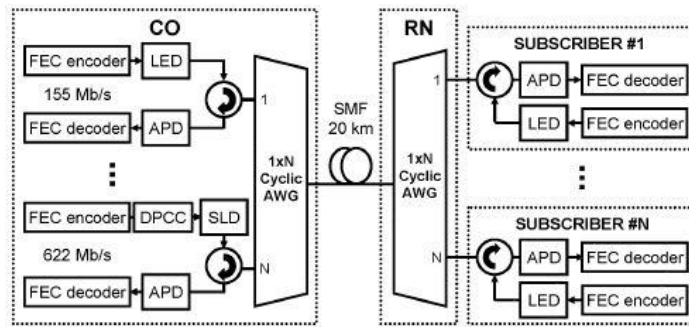


Figure 2.3.2.1 – Experimental Setup Used in [17].

Two AWGs were used (one at the CO and another at the RN) for spectrum splicing and wavelength routing. In this case, using AWGs for spectrum slicing enables using multiple peaks of the spectrum-sliced light. This improves the optical budget and allows equalization of the spectrum-sliced channels although having the con of inducing more dispersion. The spectral region was chosen in order to suppress the dispersion effect. At both OLT and ONU were used APDs and LEDs (directly modulated at 155 Mbps). It was also used FEC to improve the receiver sensitivity. 622 Mbps channels using SLDs (instead of LEDs) and DPCCs were also tested.

For the case presented, dispersion is one the biggest problems (although there are ways to overcome it, these can cause other problems). Other disadvantages are: limited modulation speed, low power and short transmission distance. The major advantages are simple implementation and low cost.

2.3.3. Injection Locking

2.3.3.1. With BLS Seeding

It is possible to injection lock a FP laser using a BLS as seeding. This seed will be coupled in the transmission fiber. In [18] an architecture based on this approach was proposed and demonstrated, using 12 channels with 50 GHz channel spacing. The experimental setup is shown in Figure 2.3.3.1.1.

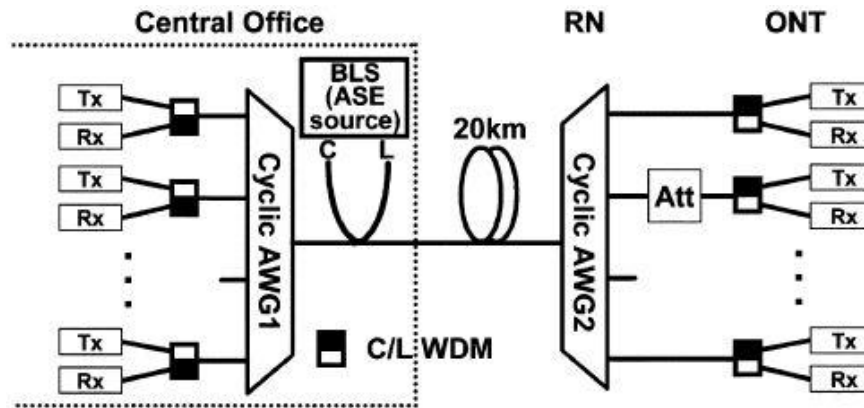


Figure 2.3.3.1.1 – Experimental Setup Used in [18].

As BLS amplified spontaneous emission (ASE) light generated by a pumped erbium doped fiber (EDF) was used. There were two BLSs at the CO, each of them operating in different bands (C and L bands), which were used as injection to lock the FP laser diodes (LDs). These were located both at the CO and the ONTs and were directly modulated at 155 Mbps. C-band was used for upstream transmission and L-band for downstream transmission. A heater was used along with each FP LD in order to reduce the wavelength variation with temperature of these devices. Both at the CO and RN were used AWGs as MUX/DEMUX. The attenuator was used for optical budget tests.

Upstream transmission will now be explained. C-band BLS was coupled into the fiber. When it reached AWG2, it was spectrally sliced and each slice was sent to the correspondent ONT. Each spectrally sliced signal would lock the mode of the FP LD which was nearest to the wavelength associated to the incoming light and each ONT had its upstream transmission wavelength assigned. The upstream signals were multiplexed by AWG2 and then transmitted through the fiber until they reached AWG1. Here they were demultiplexed and routed to the receiver which would recover the data. For downstream transmission the process was similar, with the BLS operating in the L-band.

The biggest advantage of using this approach is its low cost. Regarding cons we can notice limited bit rate and limited transmission distance (in the case presented above is used 155 Mbps bit rate and the maximum transmission distance is about 30 km including about 10 km of distribution fiber). Another disadvantage is the fact of being needed light seed.

2.3.3.2. With Modulated Downstream Signal

Another way of injection lock the FP LD is to use the data signal instead of an external seed. In [19] was presented an architecture that uses the downstream signal to injection lock the FP LD for upstream transmission. Figure 2.3.3.2.1 illustrates the setup used in this case.

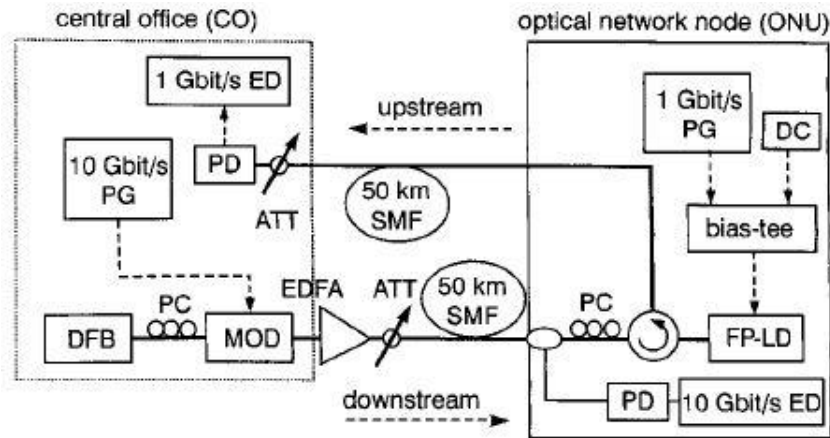


Figure 2.3.3.2.1 – Experimental Setup Used in [19].

As shown in the schematic, at the CO was used a DFB laser as light source, being this externally modulated at 10 Gbps. The fiber length from the CO until the ONU was about 50 km. At the ONU the downstream signal was splitted, 50% for data reception and other 50% to injection lock the FP LD (which was directly modulated at 1 Gbps). The optical circulator was used to separate the downstream signal from the injection-locked upstream signal. This upstream signal was transmitted over 50 km of fiber and finally received at the CO.

This is a low cost approach and using the downstream signal as seed to injection-lock the FP LDs allows eliminating the complicated synchronization process since it works for both symmetric and asymmetric two-way traffic. It also gives us better bandwidth utilization since there are no blank slots in the downstream signal reserved for upstream signal. A greater transmission distance can also be achieved when compared with using a light seed (50 km in the case presented against 30 km in the other one).

2.3.4. Reflective

2.3.4.1. RSOA with BLS Seeding

It is possible to employ a WDM-PON using reflective semiconductor optical amplifiers (RSOAs) at the receiver, seeded by a spectral sliced BLS. Comparing the RSOAs' approach with spectral sliced LEDs or FP LDs as upstream transmitters, these last ones mean low power, not very high speeds and potentially unstable behavior. The use of RSOAs allows three different things: power amplification of the incident spectral sliced signal; data modulation to the same signal; and increasing the noise margin of the system. In [20] was demonstrated an architecture using this approach and its experimental setup can be found in Figure 2.3.4.1.1.

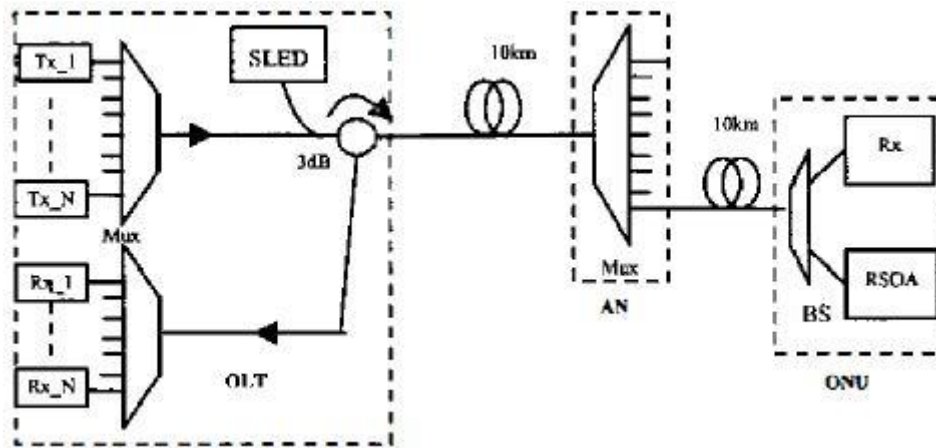


Figure 2.3.4.1.1 – Experimental Setup Used in [20].

Downstream transmission was achieved by using DFB lasers directly modulated at 1.25 Gbps as light source (one per channel). These were working over L-band and were multiplexed at the OLT and demultiplexed at the Access Node (AN) using AWGs. The total transmission distance is about 20 km and the channel separation is 100 GHz.

As we can observe in Figure 2.3.4.1.1, a single SLED was used as BLS for the RSOAs. This is sufficient to feed up to 40 users. This device emitted non polarized incoherent light and C-band was used for upstream transmission. A coupler was used to aggregate the downstream signals and the light seed. The AWG at the AN was responsible for spectrum slicing the SLED light and wavelength routing. Each ONU received a 0.4 nm bandwidth slice which was modulated (at 1.25 Gbps), amplified and reflected back at the RSOA. The AWGs were then responsible for multiplexing and demultiplexing the upstream signals, being these received by APDs. At the OLT was also used a C/L band filter to separate the downstream and upstream channels.

With this approach is possible to achieve relatively high bit rates (the case presented had a 1.25 Gbps bit rate but it's possible to achieve about 5 Gbps) but it is still a relatively expensive solution due to the price of RSOAs. Another con of this approach is the need of using a light seed.

2.3.4.2. RSOA with Laser Array Seeding

Another WDM-PON scheme using RSOAs was used in [21] and [22]. This time, the RSOAs at the receiver were seeded by an array of FP LDs. The setup presented in [22] is now analyzed. This had a self-protected architecture against fiber fault by means of a duplicated fiber between the RN and the ONUs. The following figure, Figure 2.3.4.2.1, illustrates its experimental setup.

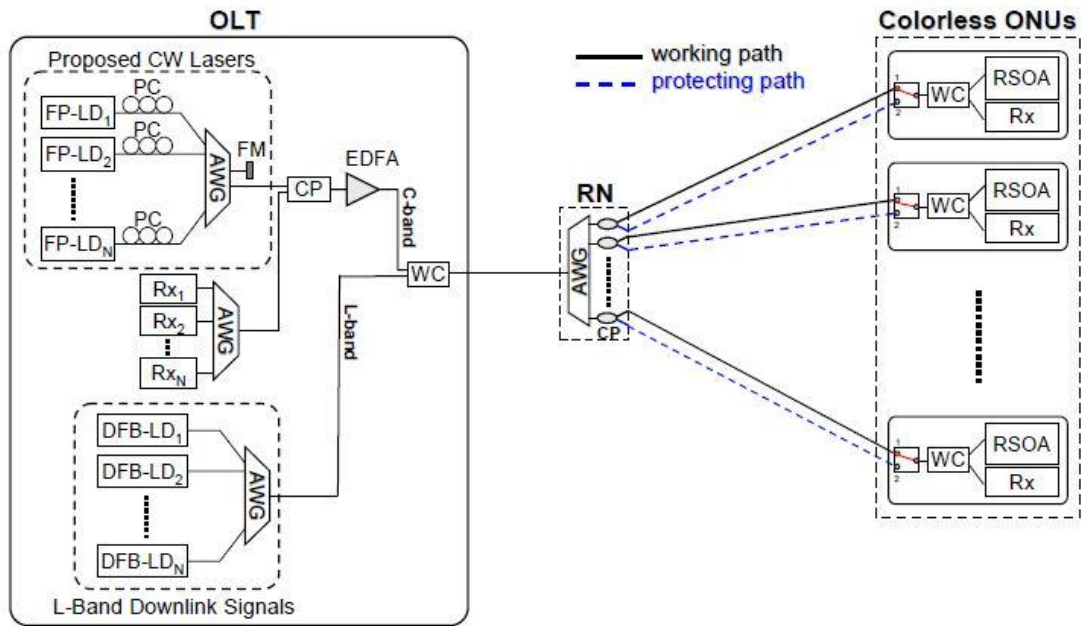


Figure 2.3.4.2.1 – Experimental Setup Used in [22].

Regarding the FP LDs, 1.38 nm channel spacing was used with C-band wavelengths while the data signals were carried by L-band wavelengths. As the schematic shows, PCs were used along with each FP LD. The fiber mirror (FM) was used to reflect light in order to seed the FP LDs. Each one of these corresponded to one wavelength which would be aggregated to the fiber by an AWG. The aggregated signal would pass through an erbium doped fiber amplifier (EDFA) in order to be amplified. There were 20km of fiber length between the OLT and the RN. At the RN the signal was splitted and at the ONUs the single-longitudinal-mode wavelengths were used to seed

the RSOAs. The RSOAs modulated (at 2.5 Gbps), amplified and reflected the signal back in the upstream direction. The AWG at the RN would aggregate the signals from each ONU and send them back to the OLT. Here the signals would be routed to different receivers by another AWG.

Downstream transmission was achieved by the means of DFB LDs, which worked in the L-band and were externally modulated (at 10 Gbps). It worked as simple as it looks in the Figure 2.3.4.2.1. The only thing new here was the possibility of using the protection fiber, which was between the RN and the ONUs, if occurred any kind of situation with the normal fiber (for example a fiber cut or a maintenance action).

With this approach is possible to get even higher bit rates than with BLS seeding but in this case, beyond the RSOAs' cost, we have also to consider the laser array seeding cost. Another problem is regarding polarization, as we can notice by the use of several PCs.

2.3.4.3. RSOA with Self Seeding

Another way of implementing a RSOA-based WDM-PON is using the ASE of the RSOAs as their own seed. This ASE light is emitted from each RSOA, spectrally sliced at the AWG present at the RN and reflected back. This approach was presented in [23] and its schematic can be observed in Figure 2.3.4.3.1.

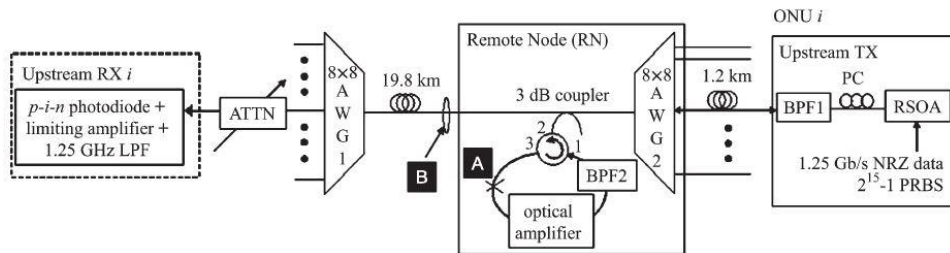


Figure 2.3.4.3.1 – Experimental Setup Used in [23].

In this particular case was used a system which enables only one spectrally sliced light to be reflected back per each output port making active temperature control not necessary. It is also noteworthy that each ONU comprised a band pass filter (BPF) and a PC, besides the RSOA. The ASE light from each RSOA was spectrally sliced by the AWG and reflected back at the RN. The RSOAs were directly modulated at 1.25 Gbps with upstream data and received at the OLT by a PIN photodiode. Each ONU and the OLT were separated by a total of 21 km of fiber.

The results of this experiment showed minimal crosstalk between the channels with separation of about 0.09 nm. This approach has the advantage of not being needed seed for the RSOAs and also active temperature control while still achieving relatively high bit rates.

2.3.4.4. RSOA with Remodulation

The last approach for WDM-PON using RSOAs uses remodulation of the downstream signal to transmit the upstream signal. This was presented in [24], where a 1.25 Gbps bidirectional system was demonstrated. The experimental setup used can be observed in Figure 2.3.4.4.1.

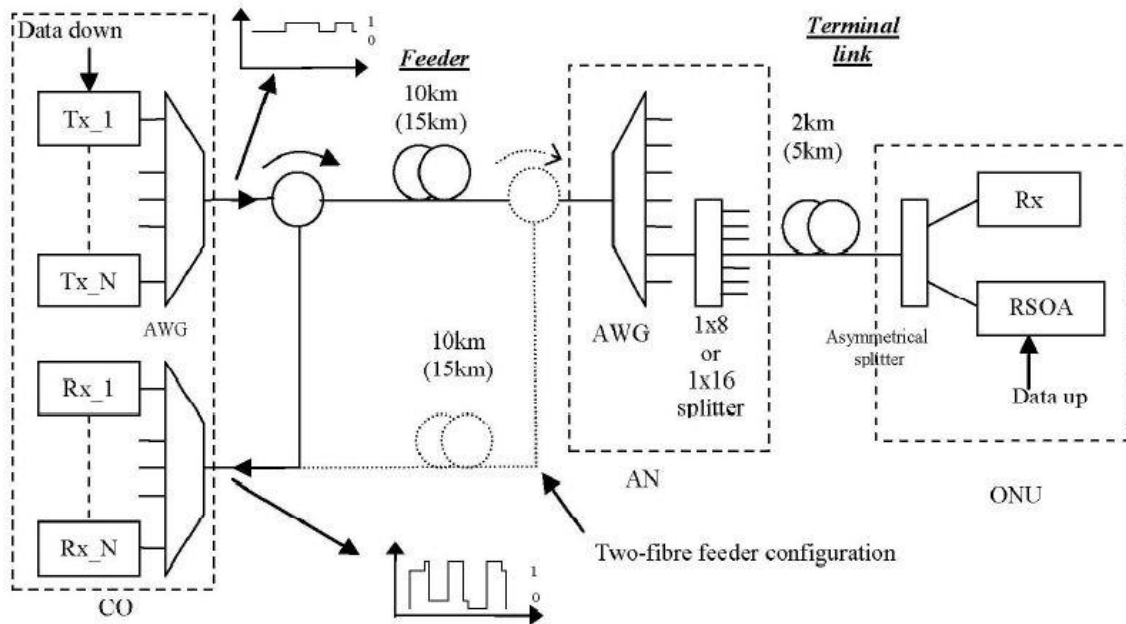


Figure 2.3.4.4.1 – Experimental Setup Used in [24].

Downstream transmission was achieved by means of directly modulated DFB LDs. The signal traveled along the fiber until reaching an AWG at the AN, which separated the different wavelengths. Each wavelength was routed to a splitter which broadcasted it to different ONUs. At each ONU the signal was splitted in two, 20% for signal detection (by means of an APD) and 80% for RSOA injection.

Regarding upstream transmission, each RSOA modulated the signal (but with higher extinction ratio in order to mask the downstream data), amplified it and reflected it back in the upstream direction. The signal would go the opposite path to the CO and reached the photo detectors (APDs) after passing through an optical circulator and an AWG.

This system does not allow so high bit rates as the first two but it has the advantage of being insensitive to polarization, excusing the PCs. Light seed is not needed as well. The biggest problem with this approach is the backscattering which can affect the upstream transmission, since both downstream and upstream signals are carried using the same wavelengths.

2.4. Market Status

2.4.1. Vendors

There are some companies providing WDM-PON solutions. TE Connectivity (formerly ADC Telecommunications), MEL, Transmode and LG-Ericsson (formerly LG-Nortel) are among them. This last one is the most popular, due to its binding with Korea Telecom, and will be addressed in the next topic. These solutions can be sold either to operators (service providers) or to enterprises directly. An estimation of the number of PON Ports by technology for a 5 year period is illustrated in Figure 2.4.1.1.

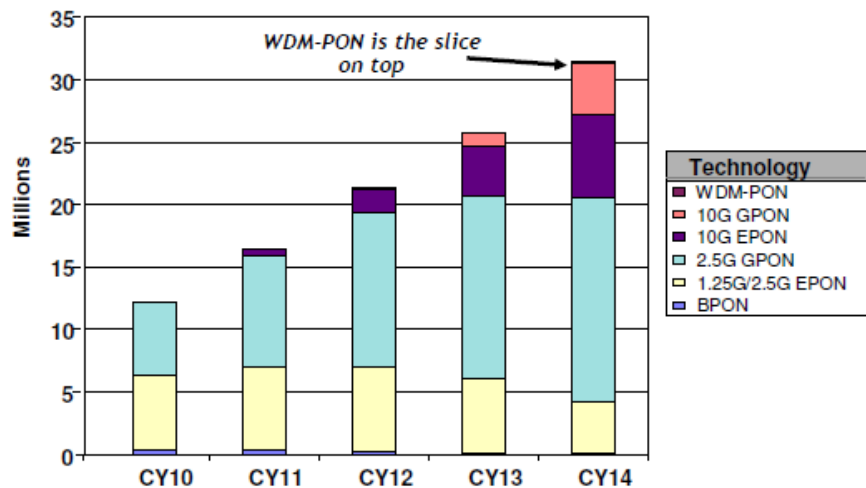


Figure 2.4.1.1 – PON Ports by Technology [25].

TE Connectivity solution is called PONy-Express. According to [26], this solution is based on wavelength-locked FP-LDs (used both at the OLT and the ONU), 2 AWGs (one at the OLT and another at the RN) and standard optical receivers at the ONUs. Each subscriber has assigned two different wavelengths for downstream and upstream transmission. It is capable of serving up to 16 ONUs simultaneously (PONy Express 16) with up to 1 Gbps of dedicated and symmetrical bandwidth per subscriber. Figure 2.4.1.2 shows PONy Express 16 system configuration.

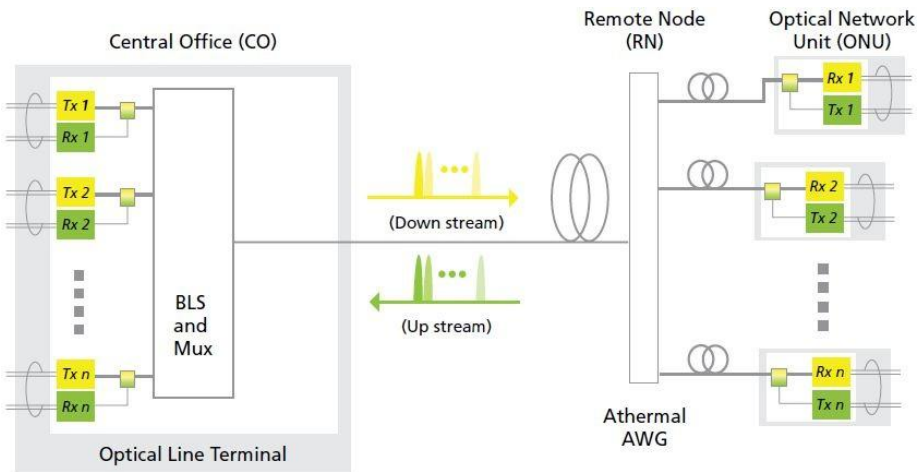


Figure 2.4.1.2 – PONy Express 16 System Configuration [26].

Regarding Transmode's solution, it is called iWDM-PON. According to [27], it is based on the same hardware than the one from TE Connectivity. This company enables operators to scale from 100 Mbps to 1 Gbps and after to 10 Gbps (and beyond, in the future). There is also a long reach version of this solution which enables the operators to choose to serve up to 50 clients and to do so over greater distances.

2.4.1.1.SFPs

Some raised the issue of WDM-PON being too large for high density applications but it can be radically reduced in size using SFPs. This is where MEL comes in, whereas the products of this company are based on this technology. MEL is spawned from a Korean government-backed research institute named ETRI (Electronics and Telecommunications Research Institute) and has as its main goal developing WDM-PON solutions.

SFPs' reduced size and amount of equipment both at the OLT and ONUs (once the line card in the OLT and the entire ONU can both be reduced to an SFP) combined with achieving GPON level costs while still providing dedicated, symmetrical and secure bandwidth are their main advantages [26].

MEL provides several products, including some that allow EPON/GPON integration [28]. One of these is an OLT transceiver (named WTG32 OLT SFP) which has an APD, able to receive GPON burst-mode 1.25 Gbps data rates, and an ECL, capable of transmitting data rates up to 2.5 Gbps with wavelength selection in L-band. This wavelength selection is performed by a

lambda-connector which is based on a wavelength-selective reflection filter. The wavelength selection range covers 32 wavelengths with 100 GHz spacing in L-band (for this product).

Another product, WTG32 X-Link, allows EPON/GPON interconnection with WDM-PON by converting the wavelengths between these two networks. This product comprises 2 transceivers, one for each link. Wavelength selection is again performed by choosing the desired wavelength at a lambda-connector, which in this case works in C-band. As it is possible to verify using Figure 2.4.1.1.1, the maximum total reach is about 40 km (20 km per link). Figure 2.4.1.1.2 presents the functional blocks of this product.

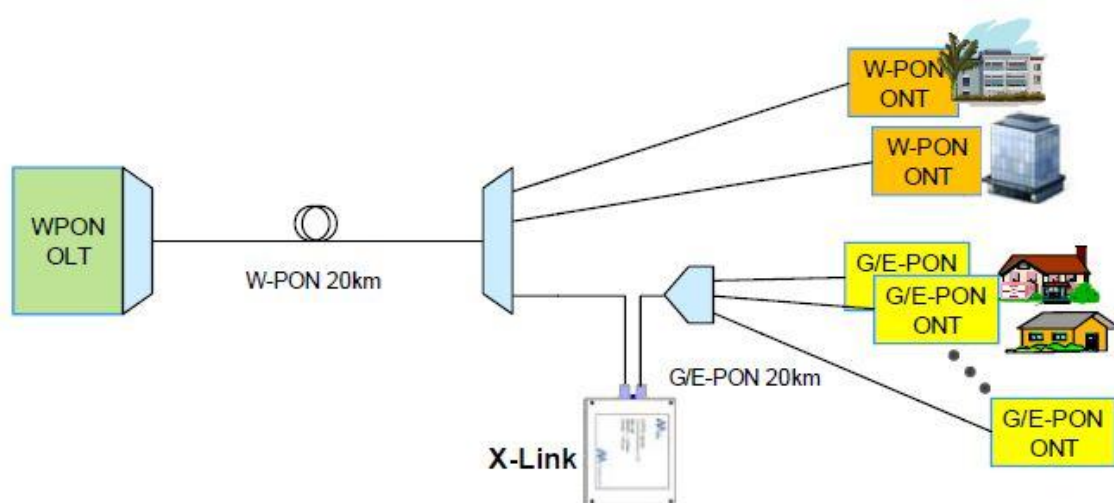


Figure 2.4.1.1.1 – GPON for Interconnecting EPON/GPON with WDM-PON [28].

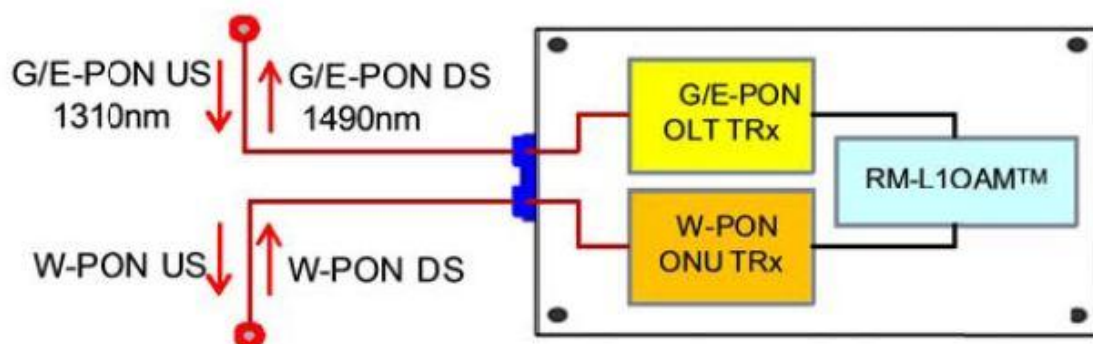


Figure 2.4.1.1.2 – Functional Blocks of WTG32 X-Link [28].

The last product produced by this company to be described is the WTG32 optical link. This is a WDM-based GPON hybrid link and comprises, not only the X-Link previously referred, but also complete WDM-PON and GPON links. At the OLT WDM-PON transceivers are used working in L-band (downstream) and C-band (upstream) and wavelength selection is performed using the same method as for the other products (with 32 channels for each band). The maximum reach is, again, 40 km.

Remaining products include a fully WDM-PON optical link based on RSOAs (both at the OLT and the ONU), and also transceivers based on ECL/APD-TIA or RSOA/PIN-TIA.

In [29] a WDM-PON based on wavelength-tunable DWDM-SFP transceivers was proposed and demonstrated. This architecture also allows integration with pre-existing PONs. In order to achieve this, data transmission occurs using L-band. Using 8 upstream channels with 50 GHz channel spacing working at 1.25 Gbps, it was possible to achieve at least 36.5 dB optical budget (for a BER value lower than 10^{-12}). For downstream transmission the results obtained were similar.

2.4.1.2.UDWDM-PON

Recently, Nokia Siemens Networks presented a PON solution based on ultra dense WDM (UDWDM) channels [30,31]. Its network concept is depicted in Figure 2.4.1.2.1. The channel spacing in this ultra dense system is 2.8 GHz, providing up to 1000 channels and offering 1 Gbps symmetrical bandwidth. The 43 dB link budget allows reaching 100 km transmission distance. Each ONU receives the wavelength assigned to it and the upstream signal is transmitted with a fixed distance to the downstream wavelength of about 1 GHz.

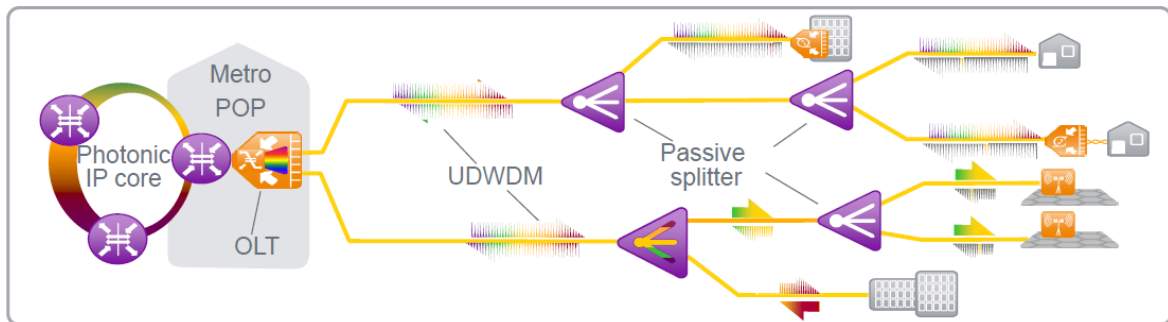


Figure 2.4.1.2.1 – High-level UDWDM Network Concept [31].

Tunable lasers are used at the OLT. These generate multiple wavelengths to reduce both cost and complexity of the system. It was concluded that the optimal number of wavelengths is 10. The module that transmits and receives multiple wavelengths was named optical transceiver group (OTG). Each OTG generates 10 DQPSK-modulated channels at 1 Gbps, using an IQ modulator. The OLT is also comprised by EDFAs (for signal amplification) and circulators (for single fiber operation).

At both the OLT and the ONU are used coherent receivers to achieve the 43 dB link budget. These receivers' sensitivity is about -46 dBm, which in combination with -3 dBm being transmitted by channel, results in 43 dB. This link budget can be used to have more subscribers or longer transmission distance.

Upstream signal generation is also performed using tunable lasers. The ONU lasers sweep the entire band being used, detecting the downstream channel and offsets this approximately 1 GHz to define its upstream channel. This results in having paired downstream and upstream channels.

It is possible to serve residential subscribers with lower bit rates by sharing the same channel between several users but also business subscribers with higher bit rate by aggregating multiple channels. This last option requires only software changes. This is a high capacity and long reach solution and enables coexistence with existing systems and smooth migration.

2.4.2. Service Providers

At the end of 2011 South Korea had about 58% market penetration of combined FTTH and FTTB subscribers, the highest in the world at that time [32]. South Korea was the first country deploying a WDM-PON system, in 2005. It was implemented by Korea Telecom using WDM-PON Ecosystem, a solution developed by LG-Ericsson. From 2008 it was also used an ONU structure from ETRI. [33]. In 2009 LG-Ericsson (by that time called LG-Nortel) and ETRI agreed a pact to promote global standardization of WDM-PON technology.

According to OASE's publication (from December 2010) there were [33]:

- 150k subscribers served by 100 Mbps as FTTC (shared by up to 24 users);
- 2k subscribers served by 100 Mbps as FTTH (one wavelength channel per user);
- 1k subscribers served by 1 Gbps as FTTB (shared by up to 24 users).

The first two slices correspond to the "Commercialized" technology presented in Figure 2.4.2.1 while the last tiny slice correspond to the two "In Pilot" technologies from the same figure. A TL approach was still in laboratory tests by that time.

	IS-WDM PON		Remodulated IS-WDM PON	TL-WDM PON
Data rate/ λ	125 Mb/s	1.25 Gb/s	1.25 Gb/s	1.25 Gb/s
WDM channels	32	16	16	16
Channel spacing	100 GHz	200 GHz	200 GHz	100 GHz
Transmission length	40 km	20 km	20 km	> 20 km
Fiber loss	12 dB	< 10 dB	< 10 dB	< 25 dB
RN Operating temp.	-40 °C ~ +65 °C	-40 °C ~ +65 °C	-40 °C ~ +65 °C	-40 °C ~ +65 °C
	Commercialized	In Pilot	In Pilot	In Labs

Figure 2.4.2.1 – WDM-PON System Status in South Korea
(IS – Injection Seeded; TL – Tunable Laser) [33].

The “Commercialized” approach is based on the same hardware than the two solutions presented before. Regarding “In Pilot” tests there are two different approaches being used. The first is also based on the same hardware than the “Commercialized” one, while the other one is a RSOA-based approach. In this case, RSOAs are used both at the OLT and the ONU, being used just one BLS. The same wavelength is used for downstream and upstream transmission, which is a worst option when comparing to the other approach since the downstream signal cannot be fully eliminated. On the other hand it means lower management cost at the ONU and fewer resources needed (half of the wavelengths).

UNET is a Danish company which also has already employed a WDM-PON system. This company’s main target market are small and medium enterprises and it is based on a FTTP infrastructure [3]. According to [34] the implemented system is also based on LG-Ericsson’s solution.

3. Modulation

3.1. Introduction

In this chapter advanced modulation formats are approached in order to later on increase transmission distance, and improve the bit rate or the spectral efficiency of a WDM-PON system.

First, basic amplitude modulation, both direct and external, is presented. Then, different types of modulation formats were considered. Having this, the native system's architecture may need to be adapted so that it can be able to work in these conditions, increasing its complexity. One of the problems relates to the fact that different receivers are required depending on the modulation format type. Therefore direct detection will be compared with coherent detection.

The last subchapter will be regarding two advanced modulation formats. These are Duobinary and QPSK. Both will be described in detail, as well as the hardware used to generate them.

3.2. Direct Modulation Vs. External

Modulation is one of the fundamental processes of any optical system. Basic amplitude modulation consists in converting the '1's and '0's from electrical domain to optical, respectively to a high and low power level. This operation can be done in two different ways, presented in Figure 3.2.1.

In direct modulation, a directly modulated laser has data input and accordingly to the data to be transmitted the output driving current (for amplitude or pulse modulation) or its own average dielectric current (for frequency modulation) is changed. This has the advantages of being simpler and cheaper than external modulation. On the other hand it inherently implies frequency chirp due to refractive index changing with bias current variation [35]. However, direct modulation is quite effective for low bit rates (till 10 Gbps [36]).

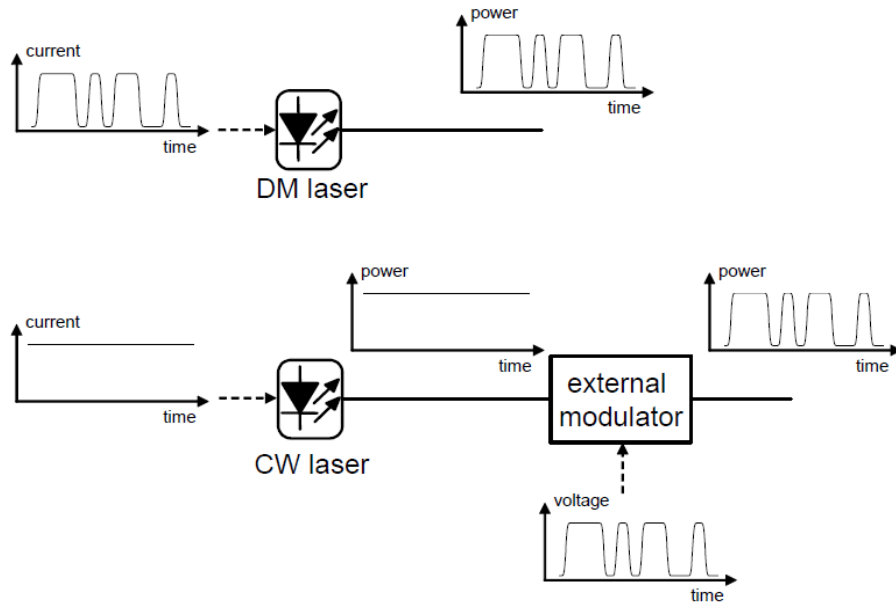


Figure 3.2.1 – Direct and External Modulation (Amplitude) [35].

For the external modulation case, a laser is fed with constant bias current, emitting a continuous wave (CW) and minimizing frequency chirp distortion (allowing higher bit rates). The modulator is then responsible to change the signal characteristics (amplitude, frequency, phase, polarization) according to the data stream (and depending on the modulation format previously chosen). [35]

There are two types of modulators: EAMs and EOMs. The first is based on the modification of the absorption spectrum caused by an applied external electric field, which changes the bandgap energy. The second is based on the change of the refractive index while subjected to an external electric field (which occurs for certain materials).

The main advantages associated with Electro-Absorption Modulators (EAMs) are their size (hence a lower cost) and compatibility for integration with lasers, since they are made using the same semiconductor material. These are also the ones expected to operate with higher efficiency in polarization-insensitive systems. Their main drawbacks are: low saturation power, large chirp, narrow optical bandwidth and their limitation to the amplitude modulation formats. [37]

The advantages pointed out for EAMs are, naturally, disadvantages of Electro-Optic Modulators (EOMs) when in comparison. These modulators are more polarization sensitive, difficult to be integrated with other components and have a higher fabrication cost in terms of large volume production. As advantages, EOMs count their low optical loss, high optical power handling capability, broad optical bandwidth, zero or tunable chirp and, finally, their ability to produce modulation formats both in amplitude and phase. [37]

The Mach-Zehnder modulator (MZM) is a well known EOM. This is based on a Mach-Zehnder interferometer, which schematic drawing is illustrated in Figure 3.2.2. A splitter at the input is responsible by dividing the optical power in two. Each portion of the signal propagates in a different path. At least one of these paths has a phase modulator, allowing modulating the optical phase of the signal by applying a voltage. At the end, the two portions are combined, interfering constructively or destructively depending on the applied electrical voltage. [35,37]

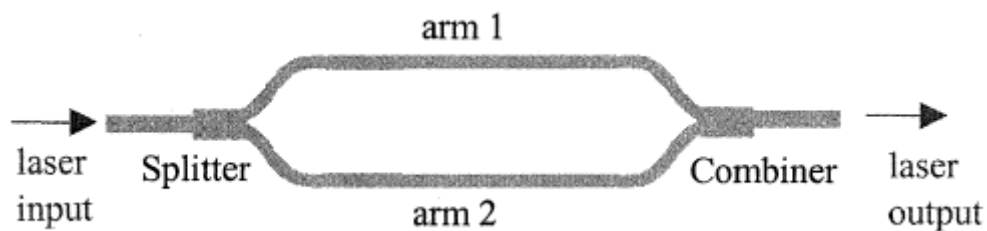


Figure 3.2.2 – Mach-Zehnder Interferometer Schematic Drawing [37].

3.3. Direct Detection Vs. Coherent

There are two different ways of receiving the optical signal and transferring it to the electric domain: direct detection and coherent detection. The first consists on generating an electrical current proportional to the incident optical power, by using a photodiode. This generated electrical current is independent of the optical phase and polarization. It is easy to conclude that this technique is used along with amplitude modulation. It is performed using PIN photodiodes or APDs.

Therefore, a modulation format that does not use only optical power as way to carry information demands additional demodulation components together with photodetection. In coherent detection, the receiver computes all properties of the signal (amplitude, frequency, phase

and polarization) by recovering the full electric field. This allows transferring all the process to the electrical domain, resulting in reduced optical complexity and making post-compensation easier.

Coherent demodulation for a phase-modulated format is illustrated in Figure 3.3.1. In this case, the signal is mixed with a local oscillator (LO), which acts as phase reference. Polarization-modulated formats require a polarization beam splitter (PBS) and frequency-modulated ones require an optical filter [38].

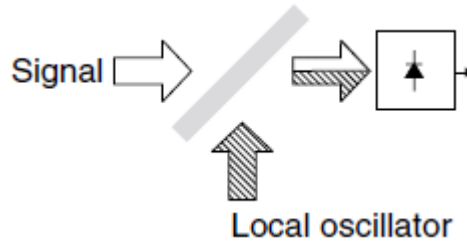


Figure 3.3.1 – Coherent Demodulation for a Phase-Modulated Format [38].

There are two different types of coherent detection receivers: heterodyne and homodyne. In the first, the local oscillator frequency is different from the signal frequency, while in the second the local oscillator frequency is similar (ideally equal) to the signal frequency. This subject will not be discussed in more detail since it is outside scope of this thesis.

According to [39], there are four main subsystems in a digital coherent receiver:

- Optical front end, which is responsible for linearly mapping the optical field of the transmitted signal into a set of electric signals;
- ADC, which converts the electrical signals in digital samples;
- Digital demodulator, which applies compensation and converts the digital samples into a set of signals sampled at the symbol rate;
- Outer receiver, which comprises FEC and whose functionality is to decode the demodulated signal in order to produce the best estimative of the data stream transmitted.

Figure 3.3.2 presents the several stages of reconstruction of the received signal, by digital signal processing. The first three blocks are fundamentally for signal conditioning in order to have all channels synchronized with the number of samples per symbol. Then, there is the digital filtering block. This is used to compensate polarization rotations and transmission impairments, like chromatic dispersion (CD). The block following this one rectifies phase and frequency mismatches between the received signal and the local oscillator. The last block is used for data recovering and FEC. [40]

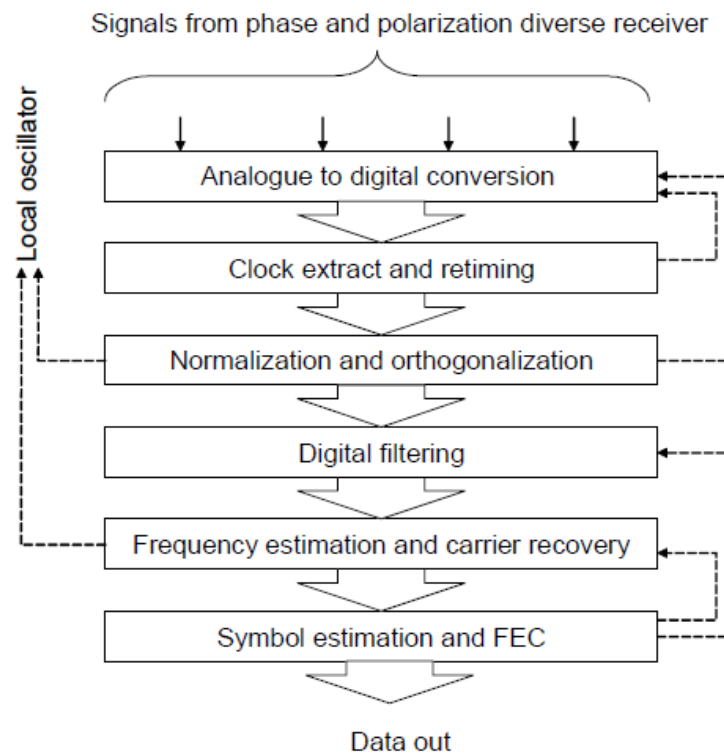


Figure 3.3.2 – Schematic of the DSP Blocks in a Digital Coherent Receiver [40].

3.4. Advanced Modulation Formats

3.4.1. QPSK

QPSK is a phase modulation format where two information bits are used to generate one symbol ('00', '01', '10' or '11') using 4 different phases, usually: 45°, 135°, 225° and 315°. This means that, instead of sending only one bit per period (which occurs for the NRZ-OOK signal, for example), it sends two. This allows doubling the bit rate while maintaining signal bandwidth, comparing to on-off keying (OOK). The constellation diagram for QPSK using Gray encoding is illustrated in Figure 3.4.1.1. Increased transmission distance is achieved due to the fact of dispersion effects being considerably less comparing to NRZ-OOK, due to the narrower spectrum associated [41].

The difference to DQPSK is, while for QPSK different phases represent different symbols, for DQPSK each symbol is encoded using a phase variation. This means that each symbol causes a different phase shift in the signal. For example, '00' not causing any phase shift, '01' causing 90° shift, '10' causing 180° shift and '11' causing 270° degree shift.

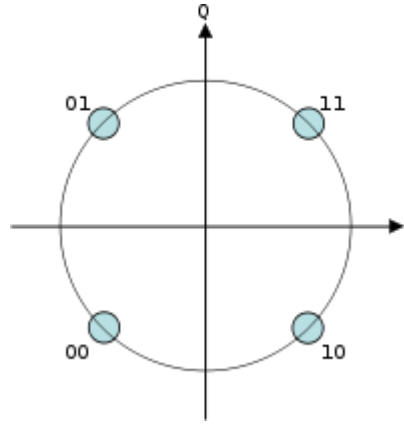


**Figure 3.4.1.1 – Constellation Diagram for QPSK with Gray Encoding
(Each Adjacent Symbol Only Differs by One Bit) [42]**

To generate a QPSK signal it is usually used a nested MZM, also called quadrature modulator or IQ modulator, depicted in Figure 3.4.1.3. This comprises two MZMs and a phase shifter. Each MZM modulates two independent bit streams on each portion of the signal, generating binary PSK (BPSK) signals. An extra 90° phase shift is applied in one of the MZM arms. At the end, the two signals are combined, resulting in a four-phase signal. [38]

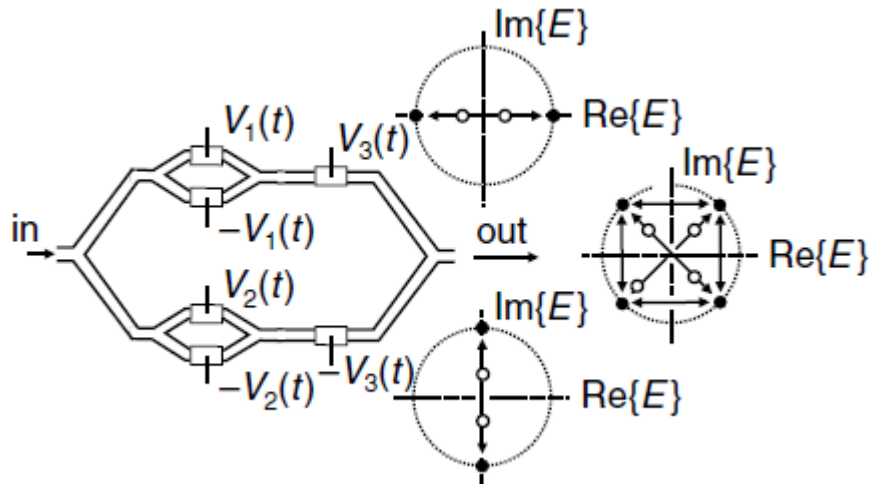


Figure 3.4.1.2 – Nested MZM as a Modulator for QPSK Signals [38].

The error vector magnitude (EVM) is usually used as performance metric for this modulation format (as well as for other phase modulation formats). It represents the magnitude of the difference between the measured signal and a signal used as reference (which represents a perfectly modulated signal). This is illustrated in Figure 3.4.1.3.

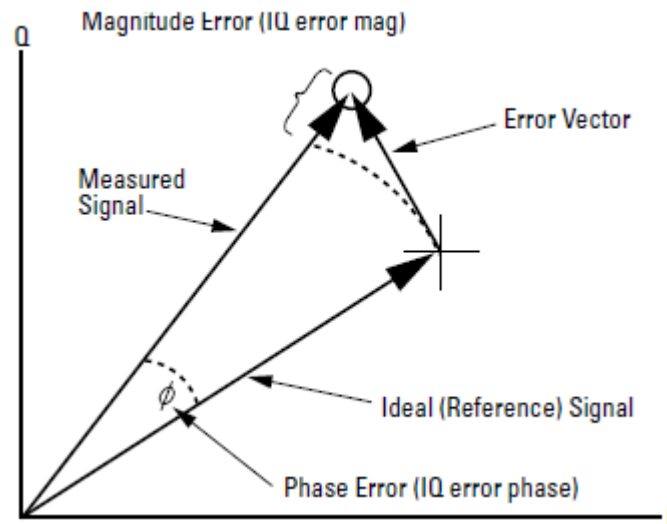


Figure 3.4.1.3 – Error Vector Magnitude and Related Quantities [43]

3.4.2. Duobinary

Duobinary is a modulation format used for transmitting R bits/s using less than $R/2$ Hz of bandwidth [44]. It can be considered an amplitude modulation format or a phase modulation format [45]. To generate a duobinary signal, a phase modulation is added when compared to a NRZ signal. Typically, the 180° phase shift occurs between two groups of '1's when the number of '0's in between is odd [45]. The symbols are usually described as '-1', '0' and '1'. To use this modulation format, first the transmitter has to receive a differentially precoded version of the data stream (converted to a three-level signal) in order to avoid error propagation at the receiver.

This modulation format has been considered one of the most promising cost-effective solutions for the deployment of high bit-rate systems [45]. Its main advantages are: higher tolerance to CD and narrow-band optical filtering, when compared to binary signaling formats (thus, allowing greater transmission distances, and improved bit rate or better spectral efficiency); and its reasonably easy implementation [44].

The first two advantages can be understood since a “1 0 1” bit pattern is encoded as “1 0 -1”. If due to dispersion or optical filtering the two ‘1’s spread into the ‘0’, this type of encoding will make them interfere destructively while, if we had a NRZ-OOK signal, the bit pattern would be encoded as “1 0 1” and the bits would interfere constructively. Besides, duobinary signals have reduced signal distortions induced by dispersion due to their narrower spectral extent (when properly filtered) [38]. Figure 3.4.1.1 illustrates the difference between the eye diagrams of a NRZ signal and a generic Duobinary signal for different transmission lengths.

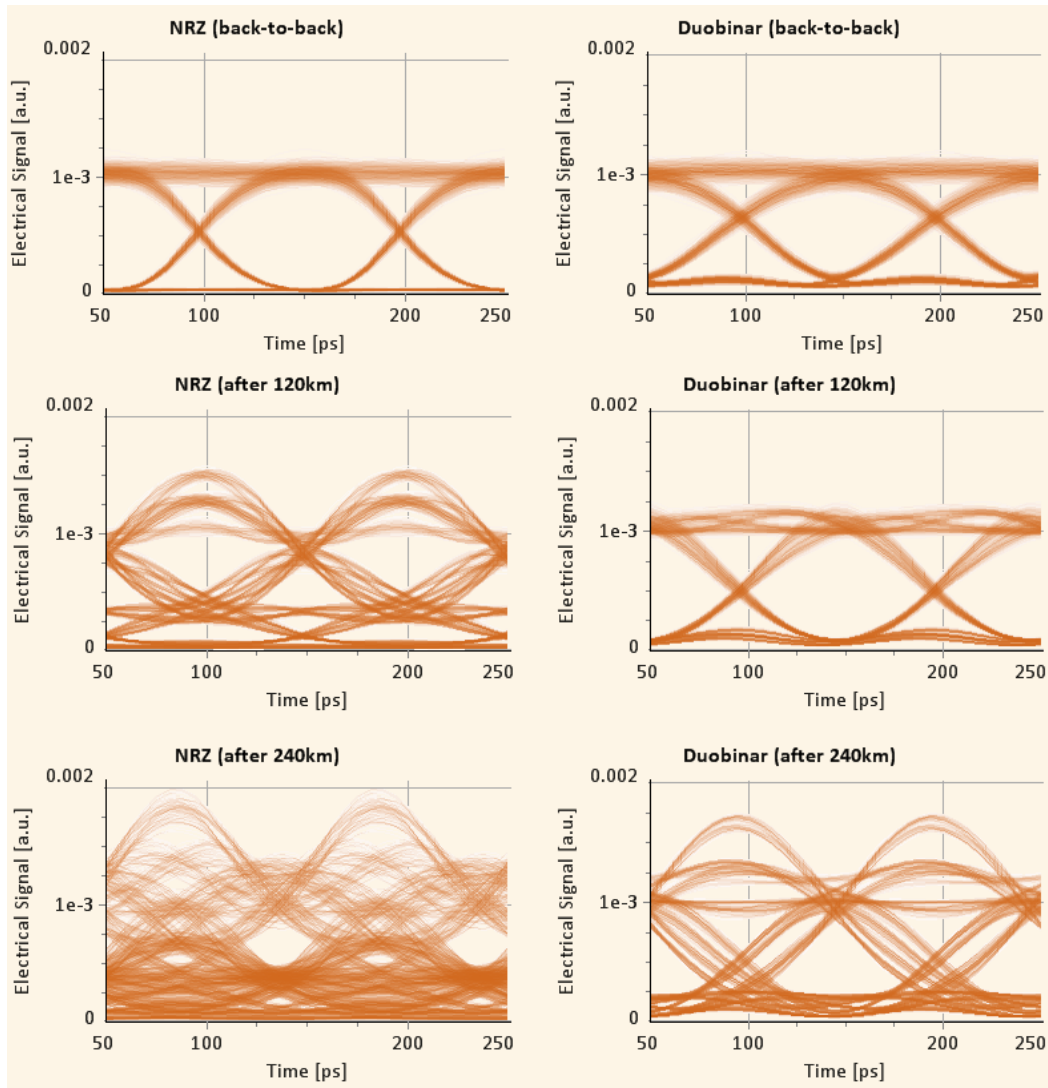


Figure 3.4.2.1 – NRZ and Duobinary Eye Diagram Comparison [46].

In [45] two different duobinary types are distinguished, referred to as standard duobinary and phase-shaped binary transmission (PSBT), and different transmitters are compared. The difference between the two will now be explained, using Figure 3.4.2.2, where are illustrated intensity and phase characteristics of standard duobinary and PSBT pulses, at 40 Gbps, in a ‘1110010100111’ sequence.

Contrarily to duobinary format (and NRZ format as well), PSBT format presents energy variations for the '0's. This, along with 180° phase shift, allows reducing ISI. On the other hand, these energy variations worsen the eye diagram opening. For the duobinary format, the 180° shift occurs between two groups of '1's when the number of '0's in between is odd. The other phase shifts do not allow reducing ISI since there is no energy associated to them. This means that the only groups of '1's resistant to ISI are the ones separated by an odd number of '0's.

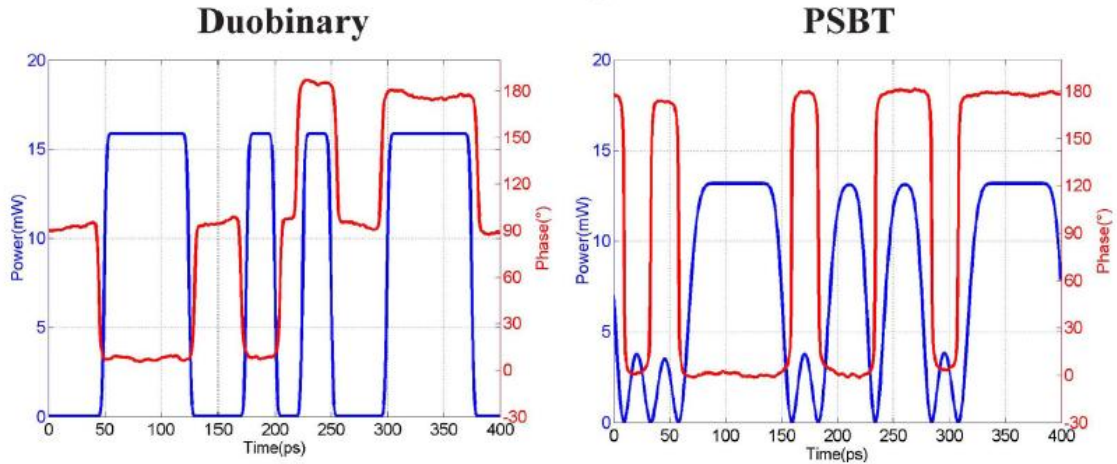


Figure 3.4.2.2 – Intensity and Phase Characteristics of Standard Duobinary and PSBT Pulses in a '1110010100111' Sequence [45].

Let us turn to the study of duobinary transmitters. The two duobinary types presented can be generated by means of electrical and/or optical filtering. Five different transmitters will now be described, including two standard duobinary transmitters ("Electrical" and "Optical") and three PSBT transmitters ("Electrical", "Optical" and "Optimum") [45]. The configuration of each of these five duobinary transmitters is depicted in Figure 3.4.2.3.

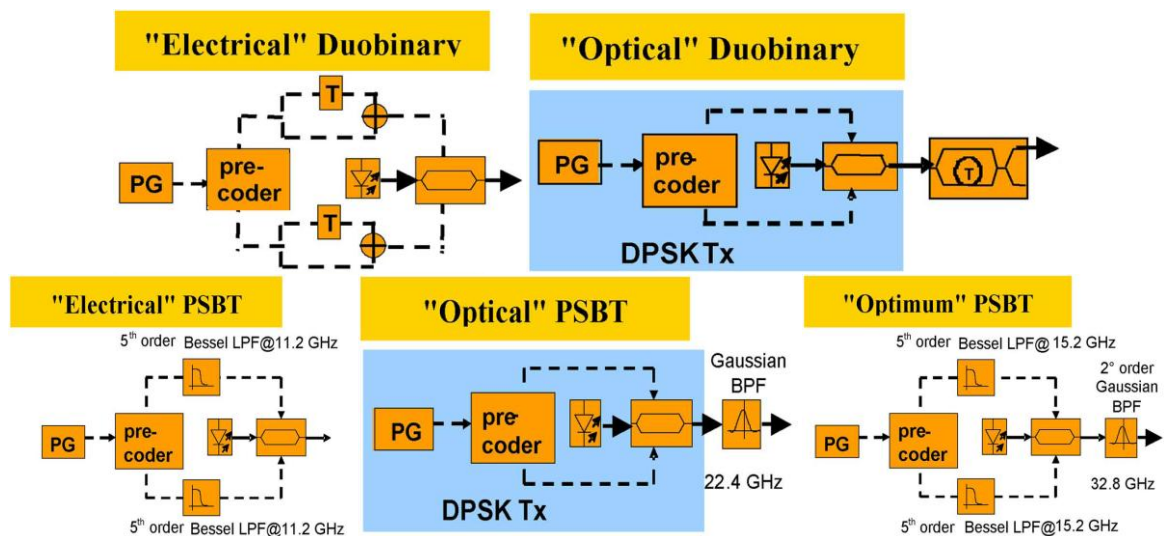


Figure 3.4.2.3 – Configuration of Different Duobinary Transmitters [45].

The first two are obtained by means of the delay-and-add filtering method, performed in the electrical or in the optical domain depending on the transmitter. To generate an “Electrical” PSBT, electrical fifth order Bessel low-pass filters are needed, while the “Optical” PSBT is obtained by assembling a DPSK transmitter and a Gaussian BPF. Regarding the “Optimum” PSBT, this is generated by combining the “Electrical” PSBT with a second order Gaussian BPF. The latter is the one which allows higher spectral compactness.

4. Proposed Architecture

4.1. Introduction

The WDM-PON scheme proposed is based on tunable devices at the users' end and a power splitter at the RN (instead of an AWG). The tunable lasers suggested are low cost ECLs based on polymer waveguide grating. Regarding the tunable receivers, these are APD-based. At the OLT were used temperature controlled DFB lasers and InGaAs APDs. All lasers were directly modulated. A 3-channel system was tested but, as regards to attenuation, the tests were performed as if 32 users were considered (by using a 1:32 splitter). Figure 4.1.1 illustrates the experimental setup of the proposed system.

In this chapter, first we present the characterization of each component composing the architecture proposed. This section is divided in 3 parts (lasers, receivers and others). RF response tests were performed using a network analyzer with frequency range from 30 kHz to 3 GHz. Files were exported and processed using Matlab®. Power and wavelength tests were performed using an optical spectrum analyzer (OSA).

After these characterizations being presented, the necessary configurations and the link budgets for both downstream and upstream transmissions, considering different scenarios, will be presented. These were based on the tests performed before.

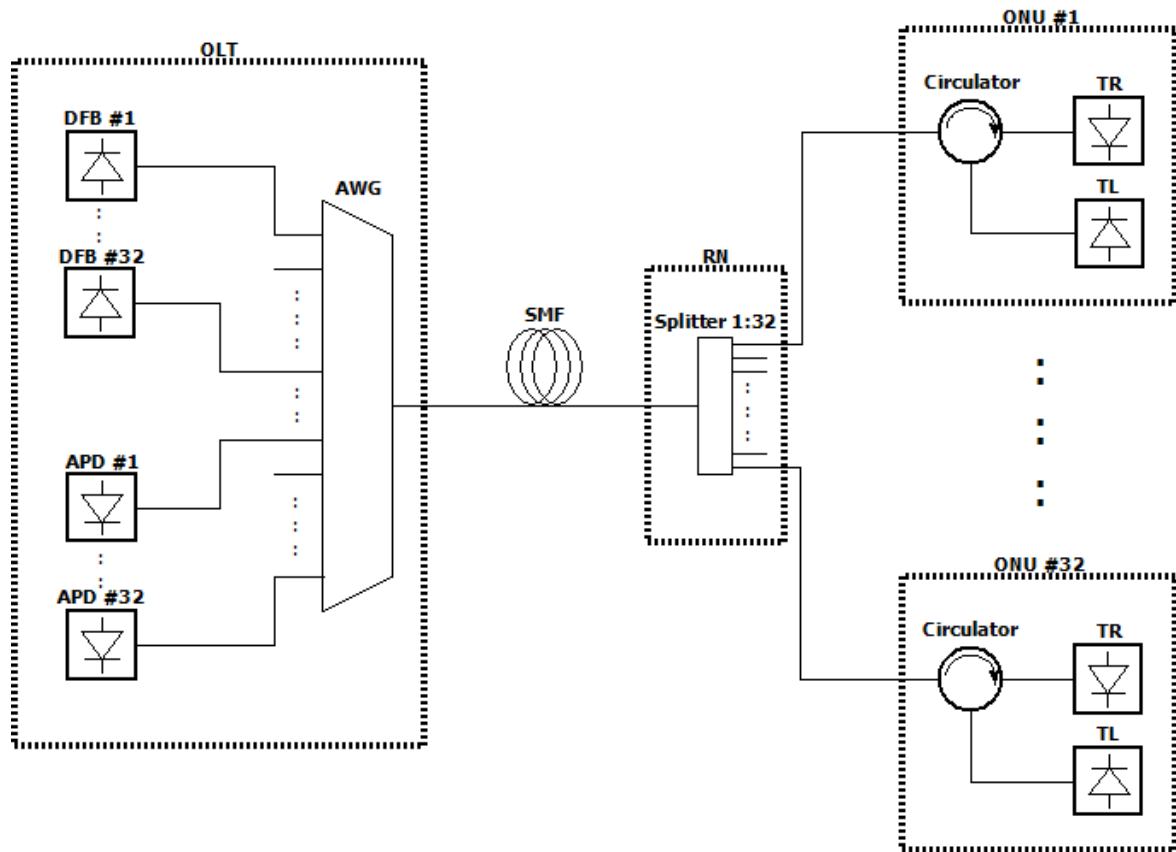


Figure 4.1.1 – Experimental Setup Proposed.

4.2. Components

4.2.1. Lasers

4.2.1.1.DFB Laser (OLT)

These temperature controlled lasers have only 2 variable parameters: temperature and bias current. Each package has 2 channels (representing 2 different wavelengths). Wavelength separation is nearly 0.8 nm. Increasing bias current leads to an increase in the output power, whereas the temperature is used to adjust the laser to the desired wavelength. The 6 different wavelengths available were tested. 2 packages are capable of reaching up to 10 mW (10 dBm) producing a signal with a good extinction ratio value and a good eye diagram, while the other one can reach up to 20 mW (about 13 dBm) with the same outcome.

First, bias current effect on both power and wavelength was checked. The highest value allowed for this parameter is 200 mA but each channel was only tested to its peak output power (10 dBm or 13 dBm). Regarding the 10 mW channels, the channel which needed the highest bias current in order to reach its peak power corresponds to 1547.7 nm (about 90 mA). Figure 4.2.1.1.1 shows the power variation with bias current for this case.

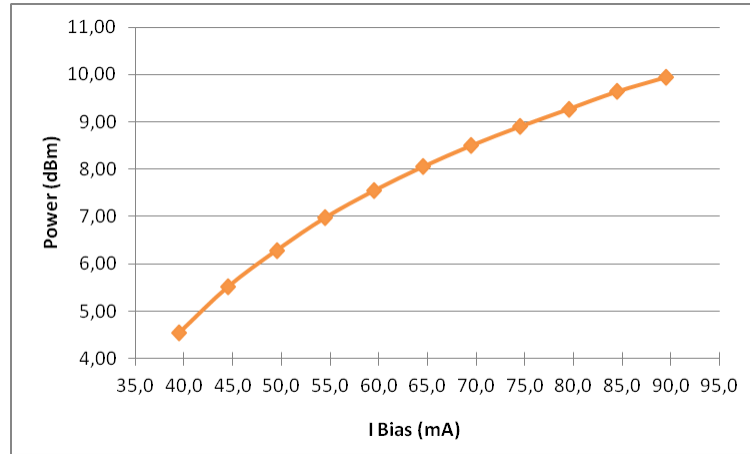


Figure 4.2.1.1.1 – Power Variation with Bias Current for the 1547.7 nm Channel.

Regarding wavelength change with bias current, all channels presented a similar behavior. This variation is not directly proportional to this parameter's increment, the slope is higher for higher currents (see Figure 4.2.1.1.2).

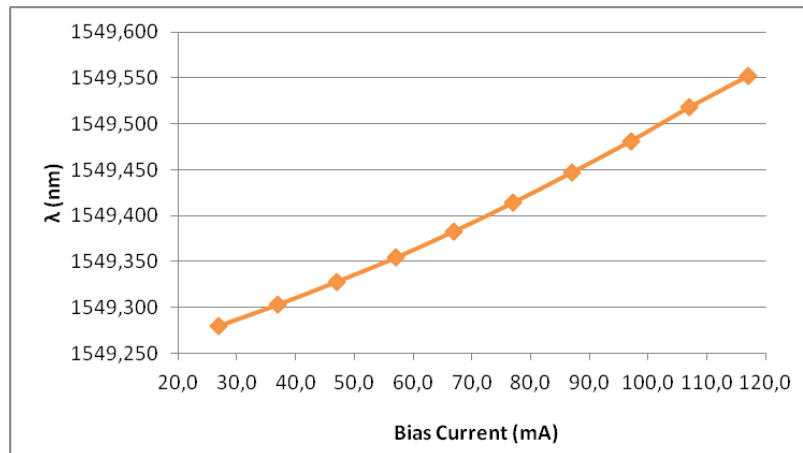


Figure 4.2.1.1.2 – Wavelength Variation with Bias Current for the 1549.3 nm Channel.

Even so, these variations will not produce a significant effect once it is possible to change the laser temperature in order to obtain the desired wavelength with an accuracy of about 0.01 nm.

Then, the RF response was studied for each wavelength, testing each of them for 3 different bias currents. As reference receiver was used a HP11982A PIN. These lasers presented a non-uniform RF response, as it is possible to see in Figure 4.2.1.1.3. Still, for the average bias current tested (corresponding to about 8 dBm CW output power), attained at least 2.5 GHz for 3 dB bandwidth.

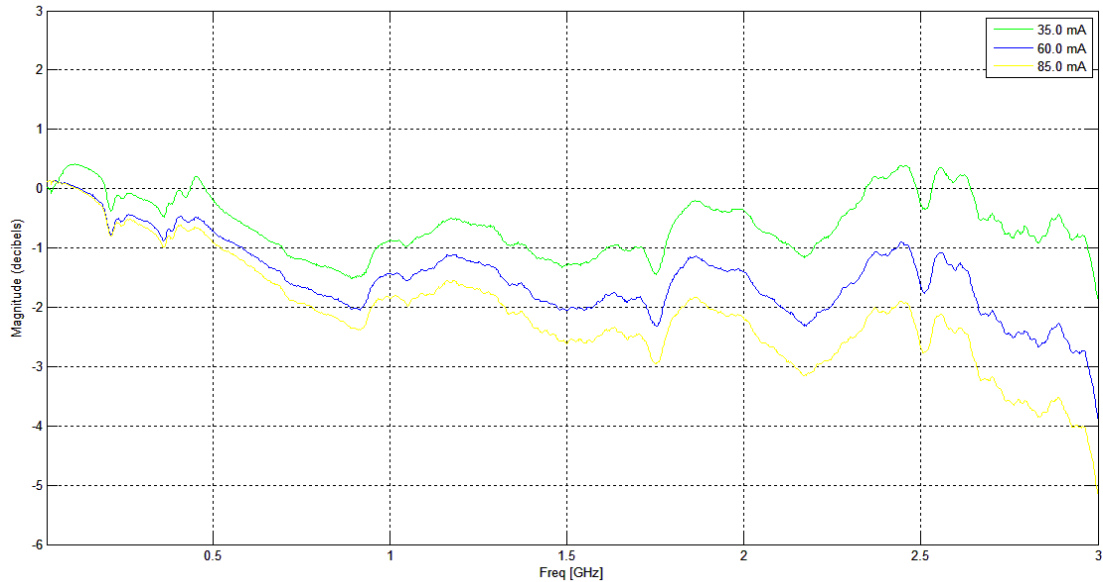


Figure 4.2.1.1.3 – RF Response for the 1546.9 nm Channel.

4.2.1.2. Tunable Laser (ONU)

The T-ECLs used have a RS232 to USB interface in order allow their parameters to be controlled via computer. The parameters are:

- LD Bias (Bias Current) – up to about 50 mA;
- LD Modulation (Modulation Current) – up to 62.5 mA;
- Heater (for sweeping all wavelengths) – from 0.00 V to 2.50 V;
- LD TEC – from 22 °C to 55 °C;
- ECL TEC (Grating TEC) – from 31 °C to 55 °C.

Each laser was tested for 4 different wavelengths (4 different Heater values – 0.00 V, 1.30 V, 2.00 V and 2.50 V) in order to check the impact of each parameter in terms of output power and wavelength variation. What was done was fixing 3 of the remaining parameters (beyond Heater) while changing the one to be tested. The fixed parameters are presented in the table below.

Table 4.2.1.2.1 – Approximate Values of the Fixed Parameters for each TL.

LD Bias (mA)	38
LD Mod (mA)	62
LD TEC (°C)	22
ECL TEC (°C)	40

The maximum bias current available was not used, although it represents a higher output power. This was because one of the lasers presented an irregular spectrum for that current value (along with the other parameters presented above).

Each laser has a tuning range of at least 17 nm (from 1525 nm to 1543 nm, approximately). It was verified that a higher value for the heater parameter corresponds to a lower wavelength. This variation is not linear, as shown below in Table 4.2.1.2.2 and Figure 4.2.1.2.1. On the other hand, different wavelengths also present different output powers, as can be observed in Figure 4.2.1.2.2. The wavelengths presenting the lowest and the highest output powers vary depending on the laser in question.

Table 4.2.1.2.2 – Wavelength Variation with Heater Parameter for TL3.

Heater (V)	λ (nm)
0,00	1543,2
1,30	1537,5
2,00	1531,1
2,50	1525,9

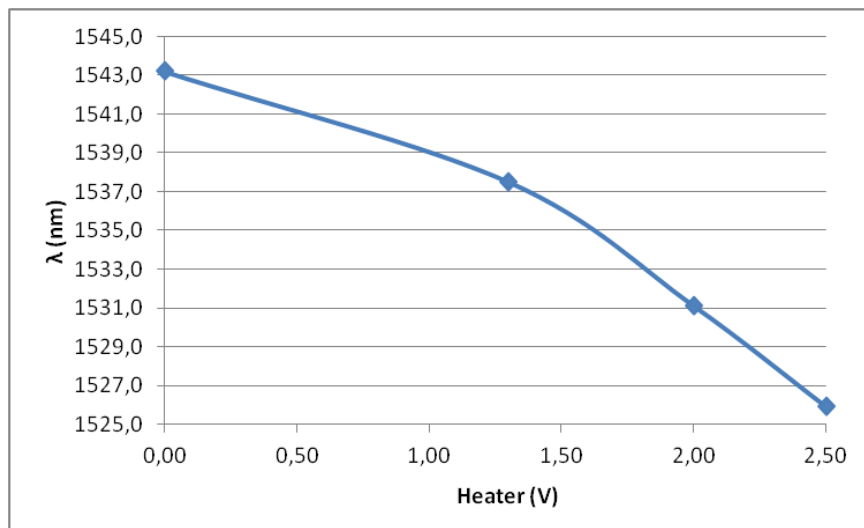


Figure 4.2.1.2.1 – Wavelength Variation with Heater Parameter for TL3.

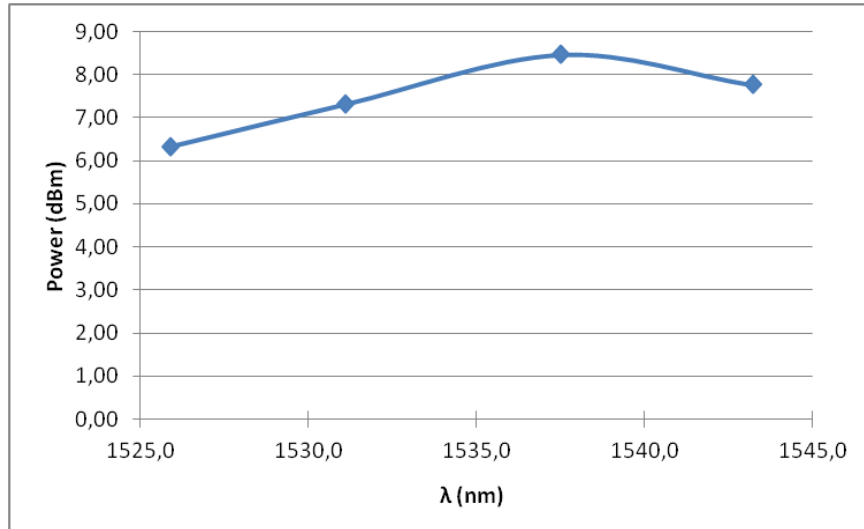


Figure 4.2.1.2.2 – Power Variation with Wavelength for TL3.

Next, tables and graphs are presented concerning the operation of the laser in CW mode. All lasers presented similar RF responses (within the tested range). As reference receiver we used the same receiver already used before, the HP11982A PIN. In Figure 4.2.1.2.3 is depicted one of these lasers' RF response for the 4 different wavelengths tested, and with the parameters set as mentioned above. It is possible to observe that the RF response presents many variations which may cause problems in the system's operation. It is also possible to observe that the laser present similar RF behavior for the different wavelengths tested.

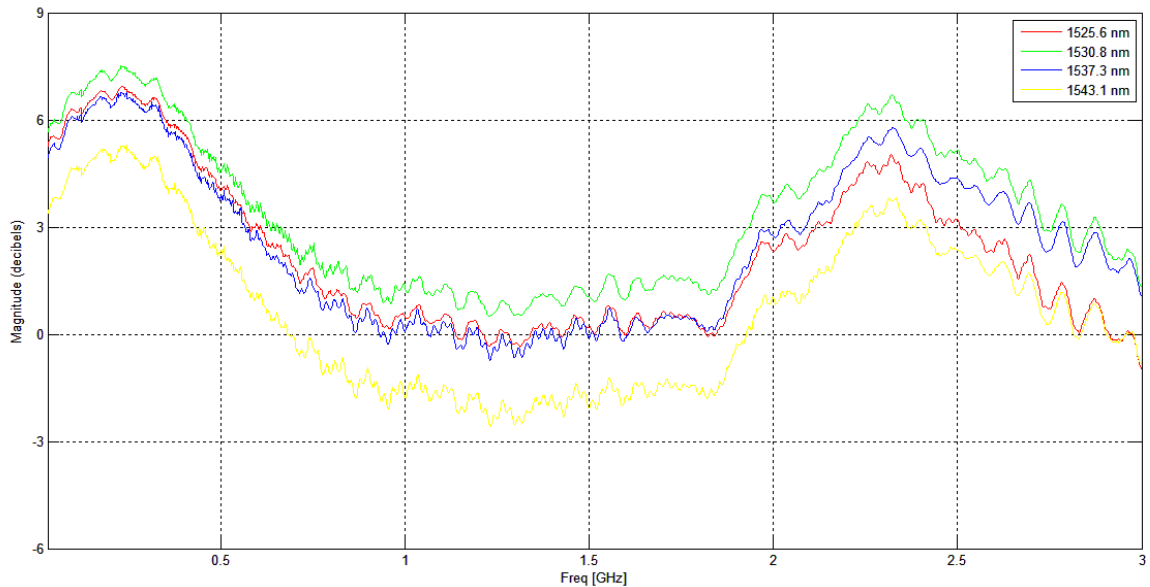


Figure 4.2.1.2.3 – RF Response for TL1.

All lasers presented identical behavior for all wavelengths when changing the other parameters. Therefore, we will only present the results obtained for one laser and one of its wavelengths.

Now let us focus on the analysis of the laser parameters. First, it was concluded that increasing LD Bias leads to increased optical power, without causing wavelength variations. The same applies to LD Modulation. The results obtained for TL3 at 1531.1 nm are presented in Table 4.2.1.2.3 and Table 4.2.1.2.4.

Table 4.2.1.2.3 – Power Variation with LD Bias for TL3 @ 1531.1 nm.

LD Bias (mA)	Power (dBm)
14,49	6,59
26,70	7,70
37,55	8,46
50,51	8,64

Table 4.2.1.2.4 – Power Variation with LD Modulation for TL3 @ 1531.1 nm.

LD Mod (mA)	Power (dBm)
14,35	6,42
25,36	7,03
36,36	7,51
48,34	7,94
62,50	8,36

The following step was to observe the outcome of LD TEC variation. Increasing LD TEC leads to decreased output power, as shown in Table 4.2.1.2.5. Wavelength drifts of more than 1 nm were also observed. Table 4.2.1.2.6 presents the wavelength variation with LD TEC for TL3 working around 1531.1 nm.

Table 4.2.1.2.5 – Power Variation with LD TEC for TL3 @ 1531.1 nm.

LD TEC (°C)	Power (dBm)
22	8,39
40	7,42
55	6,45

Table 4.2.1.2.6 – Wavelength Variation with LD TEC for TL3 @ 1531.1 nm.

LD TEC (°C)	λ (nm)
22	1531,083
40	1531,071
55	1531,123

Finally, it was concluded that ECL TEC stabilization is quite important since changing this parameter causes great wavelength variations, as shown in Table 4.2.1.2.8. As Table 4.2.1.2.7 shows, output power variations were also observed when changing this parameter's value, but these did not present a uniform behavior.

Table 4.2.1.2.7 – Power Variation with ECL TEC for TL3 @ 1531.1 nm.

LD TEC (°C)	Power (dBm)
31	8,70
40	7,96
55	8,32

Table 4.2.1.2.8 – Wavelength Variation with ECL TEC for TL3 @ 1531.1 nm.

LD TEC (°C)	λ (nm)
31	1533,062
40	1531,009
55	1527,536

Since the lasers used were low cost tunable lasers and some power and wavelength deviations were observed when using the same laser with the same set of parameters but in different moments, it was also decided to study the power and wavelength variations over time. Therefore, the behavior of each laser working at 4 different wavelengths over a 3 hour period was analyzed. In Figure 4.2.1.2.4 is illustrated the power drift for the laser which presented the lowest minimum power and in Table 4.2.1.2.9 it is shown the wavelength drift for the laser which presented the higher wavelength drift (TL2 in both cases).

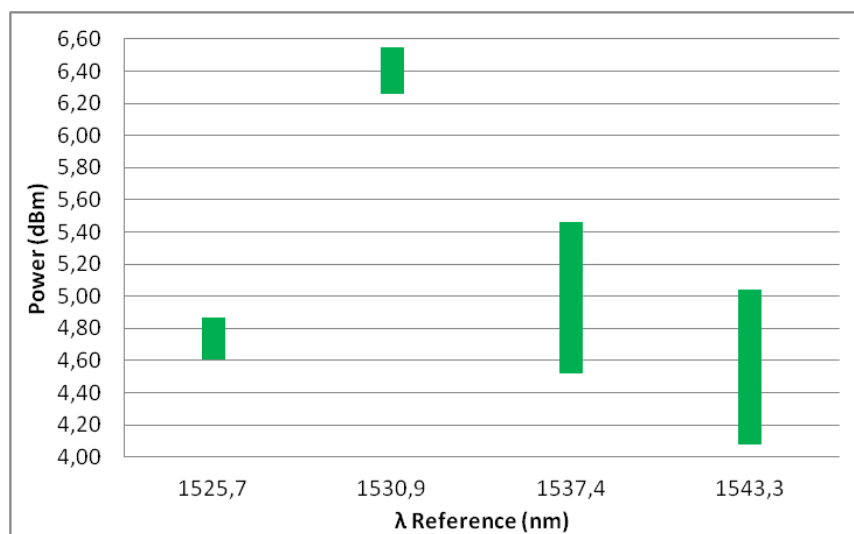


Figure 4.2.1.2.4 – Power Drift over Time for TL2.

Table 4.2.1.2.9 – Wavelength Drift over Time for TL2.

λ Ref (nm)	Min λ (nm)	Max λ (nm)	λ Drift (nm)
1525,7	1525,662	1525,733	0,071
1530,9	1530,920	1531,019	0,099
1537,4	1537,435	1537,613	0,178
1543,3	1543,361	1543,477	0,116

As it is possible to check using Figure 4.2.1.2.4, TL2 presented the lowest power (about 4.1 dBm) to a wavelength of about 1543.3 nm. Regarding wavelength drift, the worst case was verified when having the laser set to a wavelength around 1537.4 nm. Considering all lasers, none of them showed power variation greater than 1 dB and wavelength variation over 0.2 nm (during this 3 hour period). Another behavior that could be observed was the fact that not all wavelengths present the same power or wavelength drifts.

4.2.2. Receivers

4.2.2.1. Tunable Receiver (ONU)

These tunable receivers (TRs) are designed to support bit rates up to 2.5 Gbps. The tunability of these APD-based receivers is achieved by means of thin film Fabry-Pérot bandpass filters, which are thermo-optically tuned. Their working range is from 1545 nm to 1550 nm and their sensitivity using NRZ modulation is estimated to be around -29 dBm for a BER value of 10^{-9} .

First we tested the RF response of the 3 different receivers. Two different wavelengths of the DFB lasers (1546.9 nm and 1547.7 nm) were used as reference, since their RF responses were already known and, therefore, it was possible to subtract its impact on the receivers. The tests performed included using 2 different bias currents for the laser (37 mA and 62 mA) and 2 different CW output powers measured at the receivers inputs (-10 dBm and -20 dBm).

Globally, the receivers presented better response for the lowest bias current along with the highest power, what represented more than 2.5 GHz of bandwidth. The worst performance is observed for the highest bias current together with the lowest power. Figure 4.2.2.1.1 presents the RF response of one of the examined receivers at one of the wavelengths tested.

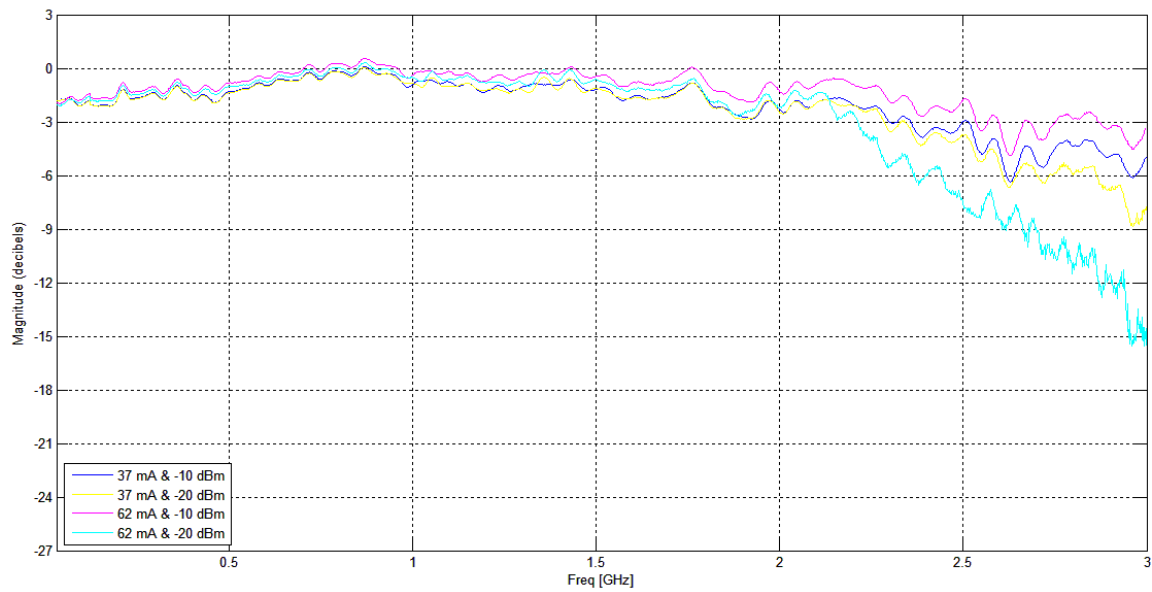


Figure 4.2.2.1.1 – RF Response for TR1 @ 1547.7 nm.

4.2.2.2. APD (OLT)

The APD receivers used at the OLT side are prepared to support bit rates up to 10 Gbps, with sensitivity about -28.5 dBm at 1550 nm using NRZ modulation (with a BER value lower than 10^{-12}). The tests performed to these receivers were the same as the ones performed to the tunable receivers and in the same conditions. Figure 4.2.2.2.1 and Figure 4.2.2.2.2 depict the results.

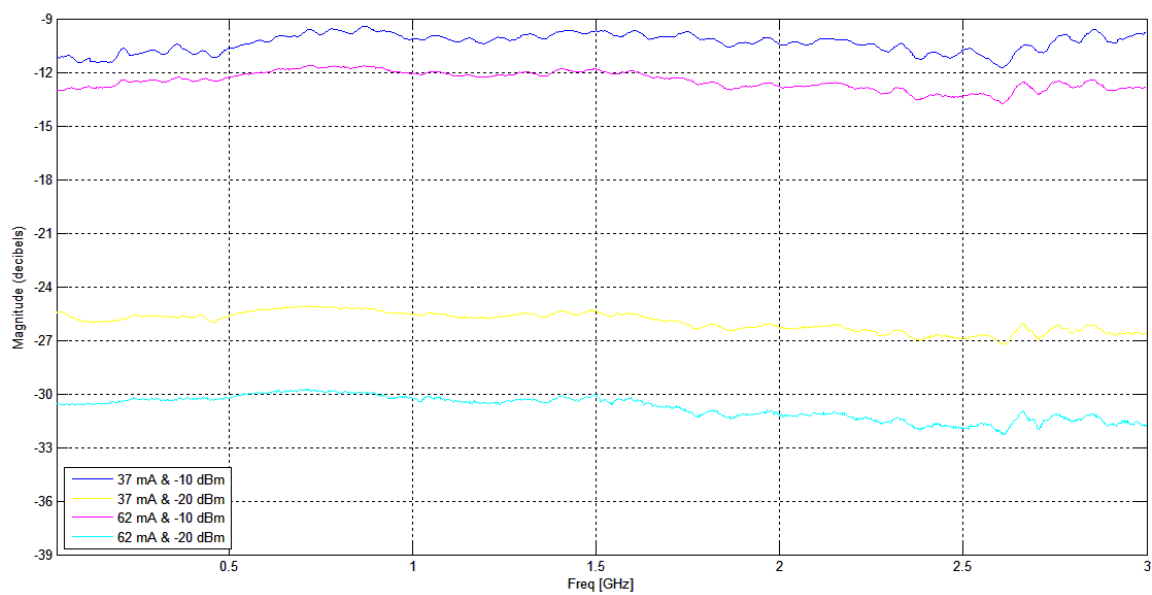


Figure 4.2.2.2.1 – RF Response for APD1 @ 1546.9 nm.

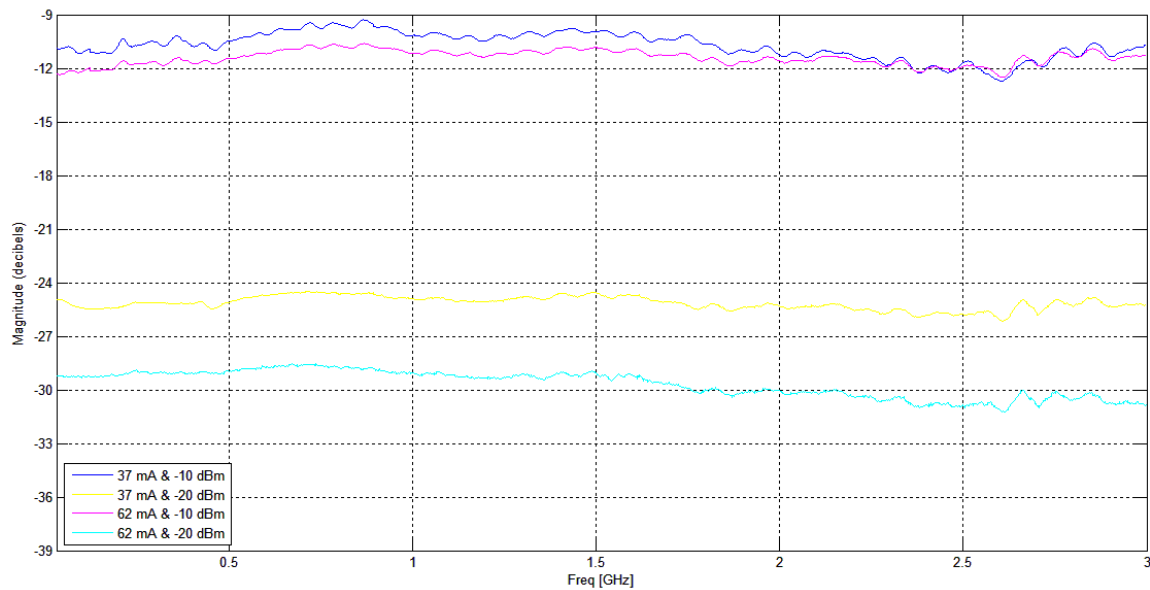


Figure 4.2.2.2.2 – RF Response for APD1 @ 1547.7 nm.

In general, as one can notice from the figures above, RF response of these APDs is quite flat. This behavior was expected since the frequency sweep goes only to 3 GHz and these APDs are prepared to work up to 10 GHz.

4.2.3. Others

4.2.3.1. AWG (OLT)

The AWG used was a 40 channel flat-top thermal AWG with 100 GHz channel spacing in C-band (starting at 1529.546 nm and ending at 1560.613 nm). To handle 32 users (thus, 64 wavelengths) would be needed 2 of these at the OLT, but in this case this is not relevant. The center wavelength accuracy of each channel comparatively to the ITU grid is ± 0.05 nm. Regarding its losses, the insertion loss for each channel is no more than 5 dB and its 0.5 dB bandwidth is greater than 0.4 nm. Considering that the DFB lasers are quite accurate and the TLs present deviations not greater than 0.2 nm, it is possible to conclude that the maximum losses on the AWG are 5.5 dB.

4.2.3.2.SMF

The measurements performed included using 2 different single mode fiber (SMF) lengths beyond the 0 km scenario (considered back-to-back): 20 km and 40 km. The 20 km fiber presented about 4.2 dB attenuation while the 40 km fiber presented about 8.0 dB attenuation, at 1550 nm in both cases.

4.2.3.3.Power Splitter

Since the objective is to prove that the system enables up to 32 users, a 1:32 power splitter was used. Whereas there was no 1:32 physical power splitter available, we used one 1:4 splitter along with four 1:8 splitter, in order to achieve 32 outputs. Figure 4.2.3.3.1 shows the configuration idealized.

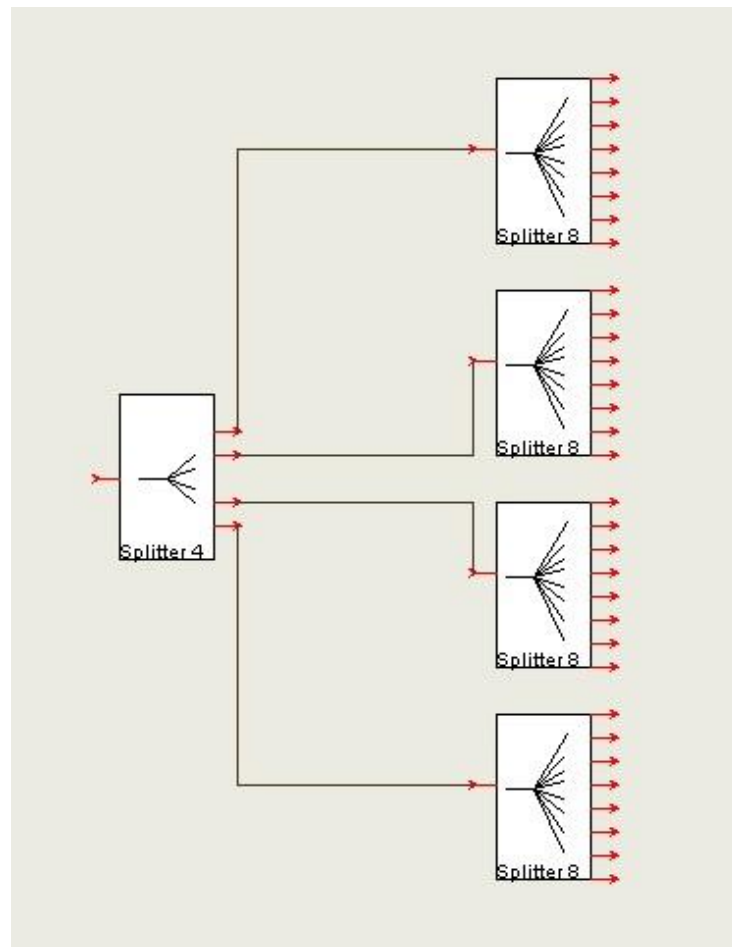


Figure 4.2.3.3.1 – 1:32 Splitter Configuration Used.

In fact, it was only used one 1:8 splitter because the system was only tested for 3 channels. The 1:4 splitter implies 7.0 dB losses while the 1:8 splitter implies 11.0 dB losses (worst case scenarios at 1550 nm). This means a total of 18 dB. The losses of each splitter port are shown in Table 4.2.3.3.1 and Table 4.2.3.3.2.

Table 4.2.3.3.1 – 1:4 Splitter Losses by Port.

Port	Losses (dB)
1	6,9
2	7,0
3	6,2
4	6,4

Table 4.2.3.3.2 – 1:8 Splitter Losses by Port.

Port	Losses (dB)
1	10,8
2	10,9
3	10,9
4	11,0
5	10,9
6	11,0
7	11,0
8	10,9

4.2.3.4. Circulator (ONU)

An optical circulator was needed at each ONU to enable uplink and downlink traffic in the fiber. As Figure 4.2.3.4.1 shows, the downstream signal enters at the IN/OUT port and exits at the next port (OUT). The upstream signal enters at the IN port and exits at IN/OUT port.

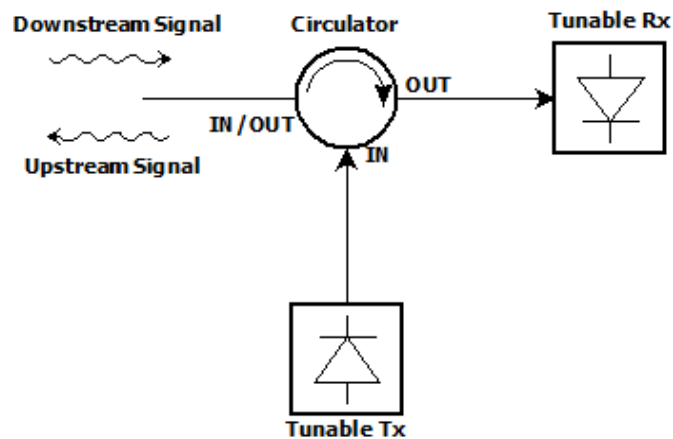


Figure 4.2.3.4.1 – Optical Circulator.

The circulator path which presented the greatest losses was the one between ports IN and IN/OUT for the circulator associated to TL1/TR1. In this case the loss was about 1.5 dB at means that this was the value considered as the worst case scenario.

4.3. Configurations and Link Budgets

4.3.1. Downstream Transmission

For downstream transmission DFB lasers were set up to generate at least 7 dBm, measured by a power meter (PM). This means that the bias currents of the lasers were different in each case. It was also needed to set up their wavelengths in order to fit the chosen AWG channels. The wavelengths used were: 1546.121 nm, 1546.916 nm and 1549.318 nm. In Table 4.3.1.1 are presented the configurations for each of the 3 lasers (and the correspondent AWG port).

Table 4.3.1.1 – Laser Configuration for Downstream Transmission.

Module	Wavelength (nm)	Temperature (°C)	Bias (mA)	AWG Port
10 mW (1)	1546,121	29,52	46,0	22
10 mW (2)	1546,916	27,11	51,0	23
20 mW	1549,318	32,54	50,0	26

Link budgets for each of the 3 different cases tested (back-to-back and 20 or 40 km length fibers) are presented in Table 4.3.1.2. Although worst case scenario losses for each component need to be considered, it was also considered a 3 dB margin for these calculations (due to losses in the fibers or the connectors, for example).

Table 4.3.1.2 – Link Budget for Downstream Transmission.

	Back-to-Back	20 KM	40 KM
Tx Power (dBm)	7,0		
AWG Losses (dB)	5,5		
SMF Losses (dB)	0,0	4,2	8,0
Splitter 1:4 Losses (dB)	7,0		
Splitter 1:8 Losses (dB)	11,0		
Circulator Losses (dB)	1,5		
Margin (dB)	3,0		
Output Power (dB)	-21,0	-25,2	-29,0
Rx Sensitivity (dBm)	-29,0		

Therefore, according to these calculations are not expected any problems regarding optical power for 0 km and 20 km, and the system may just have problems for the 40 km scenario in case of worst case scenarios occur.

4.3.2. Upstream Transmission

For upstream transmission it was decided to fix the lasers' parameters instead of opting for a minimum power, once these lasers proved to be quite unstable. Regarding their wavelengths they were set up in order to be centered to an AWG channel and the wavelengths chosen in this case were: 1529.5 nm, 1531.1 nm and 1533.5 nm. The configurations used on the lasers are presented in Table 4.3.2.1.

Table 4.3.2.1 – Laser Configuration for Upstream Transmission.

Name	Wavelength (nm)	LD Bias (mA)	LD Mod (mA)	LD TEC (°C)	ECL TEC (°C)	AWG Port
TL1	1529,5	38,7	62,5	22	40	1
TL2	1531,1	38,2	62,5	22	40	3
TL3	1533,5	37,6	62,5	22	40	6

With these laser configurations, the minimum power obtained was greater than 5 dBm (for TL2, measured by a PM) and thus this value was used as reference for link budget calculations. Again, a 3 dB margin was considered. The results are shown in Table 4.3.2.2.

Table 4.3.2.2 – Link Budget for Upstream Transmission.

	Back-to-Back	20 KM	40 KM
Tx Power (dBm)	5,0		
AWG Losses (dB)	5,5		
Fiber Losses (dB)	0,0	4,2	8,0
Splitter 1:4 Losses (dB)	7,0		
Splitter 1:8 Losses (dB)	11,0		
Circulator Losses (dB)	1,5		
Margin (dB)	3,0		
Output Power (dB)	-23,0	-27,2	-31,0
Rx Sensitivity (dBm)	-28,5		

For back-to-back and 20 km measurements there are not problems regarding optical power but with 40 km fiber length the system may experience some difficulties. This is due to lower transmitted power.

The optical power issue would be easily solved by replacing the splitter by an AWG. As it is possible to verify (using Table 4.3.2.2), the splitter losses are about 3 times greater than the losses caused by the AWG (for the considered splitting ratio). Hereupon, it could also be possible to extend the reach of this architecture at least up to 80 km (just considering the power budget analysis). Of course that changing to an AWG would also have other repercussions already discussed.

5. Experimental Results

5.1. Introduction

In this chapter it will first be presented the experimental results for the WDM-PON proposed. All procedures and conditions of measurements are detailed in the first subtopic, along with the results obtained.

After this first part, it will be presented the tests performed using a coherent QPSK system, which objective is to later on improve the architecture previously proposed in terms of transmission distance, and bit rate or spectral efficiency. At the end are presented the results obtained for a coherent UDWDM QPSK system.

5.2. Proposed Architecture

5.2.1. Conditions of Measurements

Besides the lasers configurations referred previously, other aspects shall be noted before proceeding to the results obtained. The lasers were directly modulated by a pattern generator and an oscilloscope was used to measure the Q factor in order to obtain the BER afterwards. The modulation used was NRZ and its amplitude was $1.6 V_{pp}$. The data payload was a $2^{31}-1$ PRBS. Between the circulator and the TR it was used a VOA to simulate link loss, for downstream transmission scenario. For the upstream transmission case, the VOA was inserted between the AWG and the APD. The system was also tested for 2 different bit rates: 1.25 Gbps and 2.5 Gbps.

According to [47], Q factor and BER are related by the following expression:

$$BER = \frac{1}{2} \operatorname{erfc} \left(\frac{Q}{\sqrt{2}} \right)$$

In fact, according to the same source, it is possible to find a simpler expression which provides an approximation of BER when having the Q factor, and this was the one used to estimate BER:

$$BER \approx \frac{1}{\sqrt{2\pi}Q} \exp \left(-\frac{Q^2}{2} \right)$$

5.2.2. Downstream Transmission

Downstream transmission scenario was the first to be tested. The two bit rates previously referred were tested, as well as the fiber lengths mentioned. For this purpose, the results obtained working with the 1549.3 nm channel and TR1 are presented. The values obtained for BER versus optical budget are depicted in Figure 5.2.2.1, while Figure 5.2.2.2 shows the eye diagram for 40 km and 38.0 dB optical budget at 1.25 Gbps. The lowest power measured at the receivers input when using 40 km fiber was around -25 dBm (which represents 32 dB of optical budget). The optical budget is the difference between the lasers' output power and the received power.

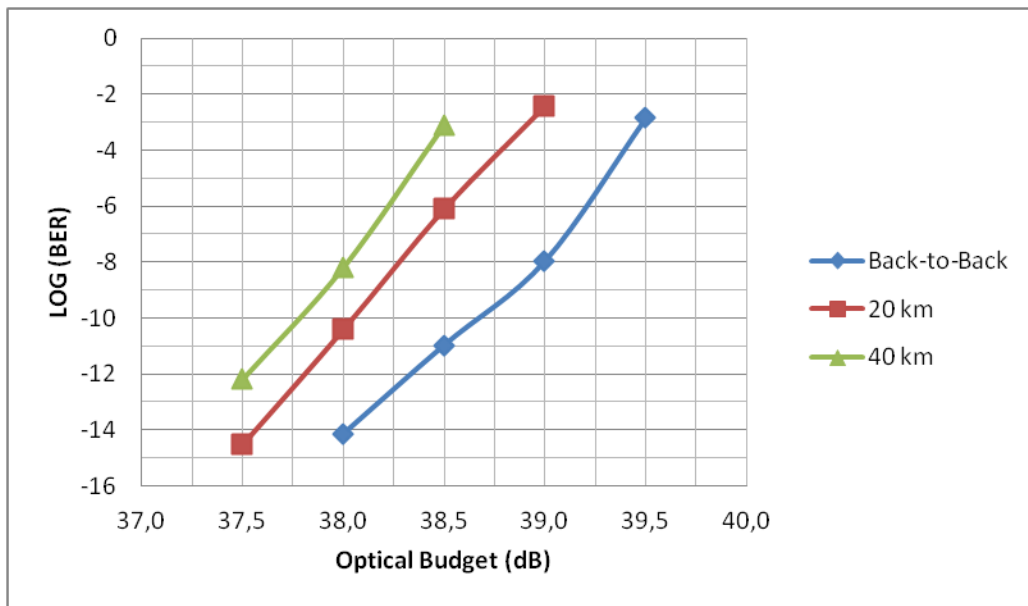


Figure 5.2.2.1 – BER vs Optical Budget for Downstream Transmission @ 1.25 Gbps.

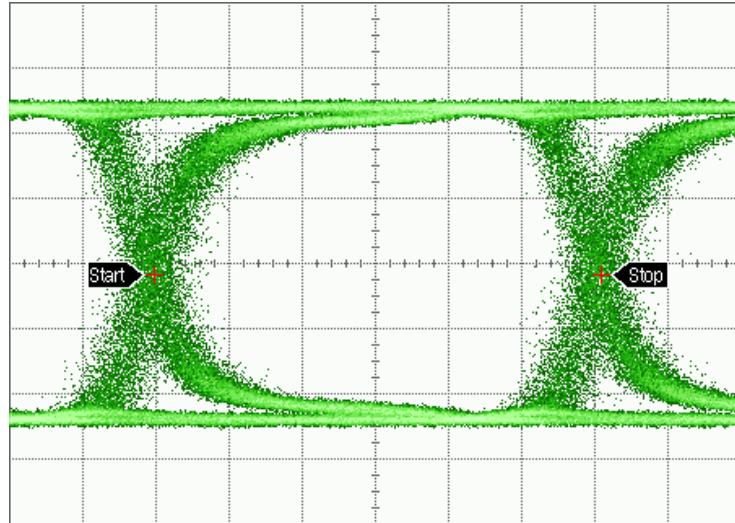


Figure 5.2.2.2 – Eye Diagram for 40 km and 38.0 dB Optical Budget @ 1.25 Gbps.

As expected, for the same optical budget value, BER value is worse for a higher fiber length (due to more accumulated chromatic dispersion). When working at 1.25 Gbps it is possible to verify that, for example for the 40 km case, 1 dB difference in optical budget implies increasing the BER from 10^{-12} to 10^{-3} . The eye diagram presents good eye opening and low jitter.

The next two figures present the same analysis as the previous but for 2.5 Gbps.

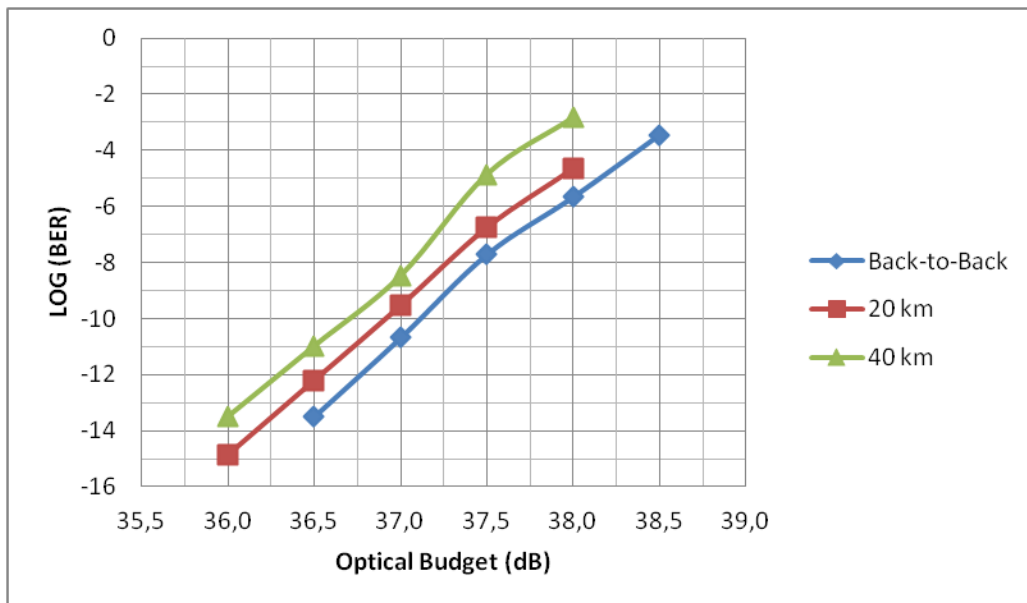


Figure 5.2.2.3 – BER vs Optical Budget for Downstream Transmission @ 2.5 Gbps.

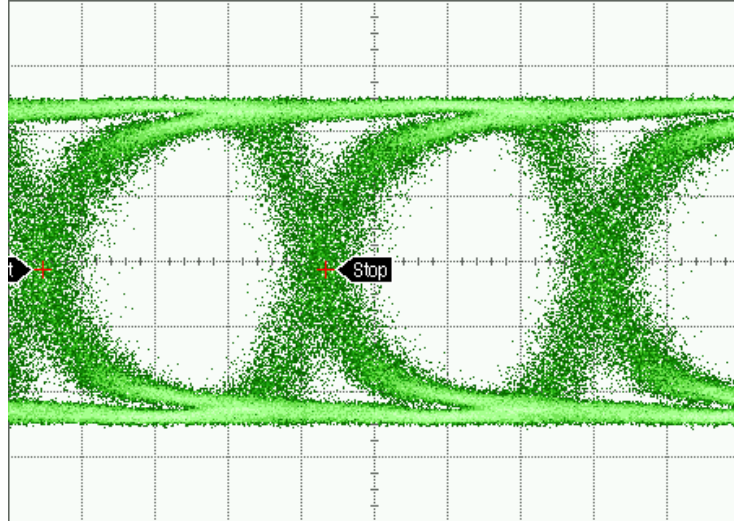


Figure 5.2.2.4 – Eye Diagram for 40 km and 37.0 dB Optical Budget @ 2.5 Gbps.

Comparing to the 1.25 Gbps case it is possible to verify that with 40 km we lose about 1.5 dB optical budget to guarantee a BER value of at least 10^{-12} (from 37.5 dB to 36 dB) and about 1 dB for 10^{-6} . It is also possible to conclude that we have a slower variation of BER while decreasing the power reaching the TR. Also in this case the eye diagram presents a good eye opening and low jitter, but not as good as for 1.25 Gbps and comparing it for lower optical budget value (1 dB less).

5.2.3. Upstream Transmission

For testing the upstream transmission scenario the procedure was the same as the one for downstream transmission: 2 different bit rates and 2 different fiber lengths (besides the back-to-back case). For this purpose, the results obtained working with TL2 (1531.1 nm) and APD2 are shown. In this case it was not possible obtain results for the 2.5 Gbps scenario. The eye diagram obtained at this bit rate will later be analyzed. Regarding transmission at 1.25 Gbps, the results obtained for BER versus optical budget are illustrated in Figure 5.2.3.1.

The lowest optical power measured at the receiver for the back-to-back setting was around -17 dBm (which represents about 22 dB of Optical Budget), for the 20 km scenario was -21 dBm and using 40 km was -25 dBm.

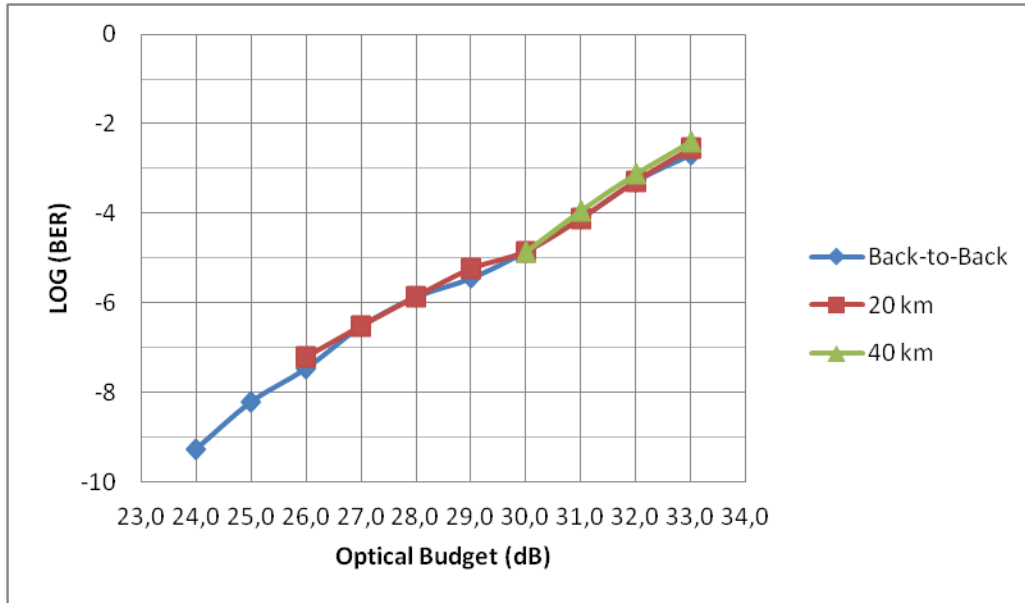


Figure 5.2.3.1 – BER vs Optical Budget for Upstream Transmission @ 1.25 Gbps.

An acceptable 10^{-6} BER value can only be achieved for the back-to-back and the 20 km scenarios (with a maximum of 27 dB optical budget). This means that it is not possible to cover a 40 km range.

As Figure 5.2.3.1 shows, increasing transmission distance did not deteriorate significantly the BER results. This results from the fact that the lasers present so wide linewidth (about 25 GHz) that the degradation imposed by this factor dominates. Additionally, there is the fact of being expected BER values lower than 10^{-12} for at least -27 dBm (32 dB optical budget). The bad behavior of the tunable lasers can also be checked by analyzing Figure 5.2.3.2 and Figure 5.2.3.3, which depict the eye diagram for the two different bit rates tested.

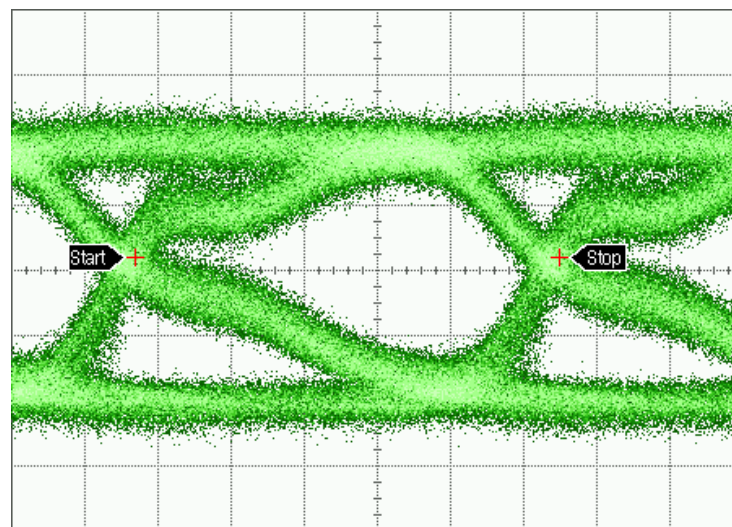


Figure 5.2.3.2 – Eye Diagram for 20 km and 26.0 dB Optical Budget @ 1.25 Gbps.

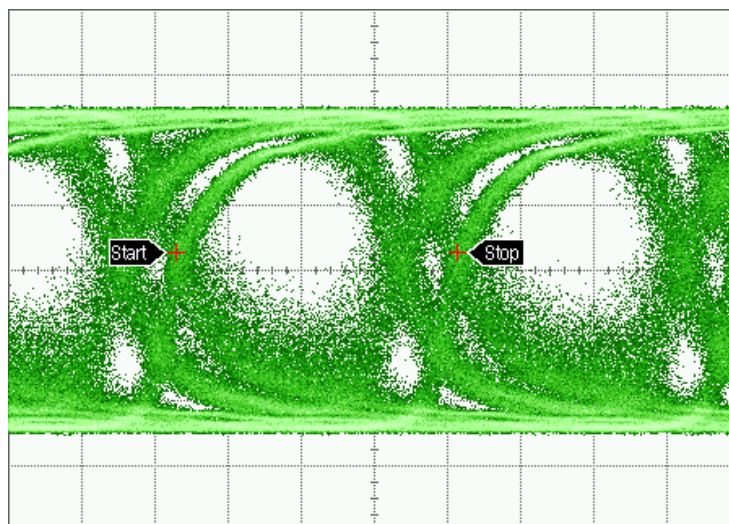


Figure 5.2.3.3 – Eye Diagram for 0 km and 22.0 dB Optical Budget @ 2.5 Gbps.

As one can see, even for 1.25 Gbps the eye diagram shape is not as regular as expected which represents higher jitter and worst eye opening. This means that system's capacity to recover the transmitted information is compromised, resulting in worse BER. Regarding the eye diagram obtained when working at 2.5 Gbps, this presents overlapping of non-synchronized samples, which means that it is impossible to recover the signal. Summarily, acquiring better TLs must be one of the priorities to improve this architecture's operation.

Since transmission at 2.5 Gbps did not work, an analysis of the eye diagram for bit rates greater than 1.25 Gbps was done in order to check the maximum possible bit rate that can be attained with these lasers. Figure 5.2.3.4 illustrates the eye diagram at 2 Gbps. This presents low jitter and the eye opening is good enough to distinguish the eye, which means that transmission at this bit rate might be achievable.

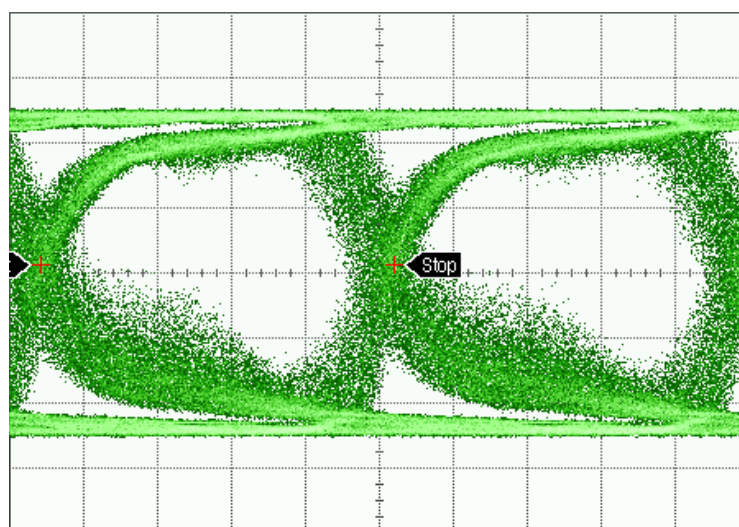


Figure 5.2.3.4 – Eye Diagram for 0 km and 22.0 dB Optical Budget @ 2 Gbps.

5.3. QPSK Systems

5.3.1. General Specifications

As stated previously, EVM is usually used as performance metric for QPSK systems. According to [48] it is possible to relate it with SNR and consequently with BER:

$$BER \approx \frac{2 \left(1 - \frac{1}{L}\right)}{\log_2 L} Q \left[\sqrt{\left| \frac{3 \log_2 L}{L^2 - 1} \right| \frac{2}{EVM_{RMS}^2 \log_2 M}} \right]$$

where:

- L is the number of signal levels identical within each dimension of (quadratic) constellation;
- Q[.] is the Gaussian co-error function;
- $\log_2 M$ is the number of bits encoded into each symbol.

Table 5.3.1.1 presents the relation between typical BER references and EVM values (presented in percentage) for a QPSK signal (L = 2 and M = 4).

Table 5.3.1.1 – Relation between BER and EVM.

LOG (BER)	EVM (%)
-3	32,4%
-6	21,0%
-9	16,7%
-12	14,2%

The mode of operation of the coherent receiver used for the experiments will be briefly described. Its configuration is shown in Figure 5.3.1.1. It is a homodyne receiver employing both phase and polarization diversities. This receiver allows recovering two different signals being transmitted in different polarizations (X and Y) by means of PBSs. Phase demodulation is performed using a 90° optical hybrid. This device has another local oscillator, whose phase is shifted 90°, in order to enable the detection of both I and Q components of the signal. In the experiments was only used X polarization. [38]

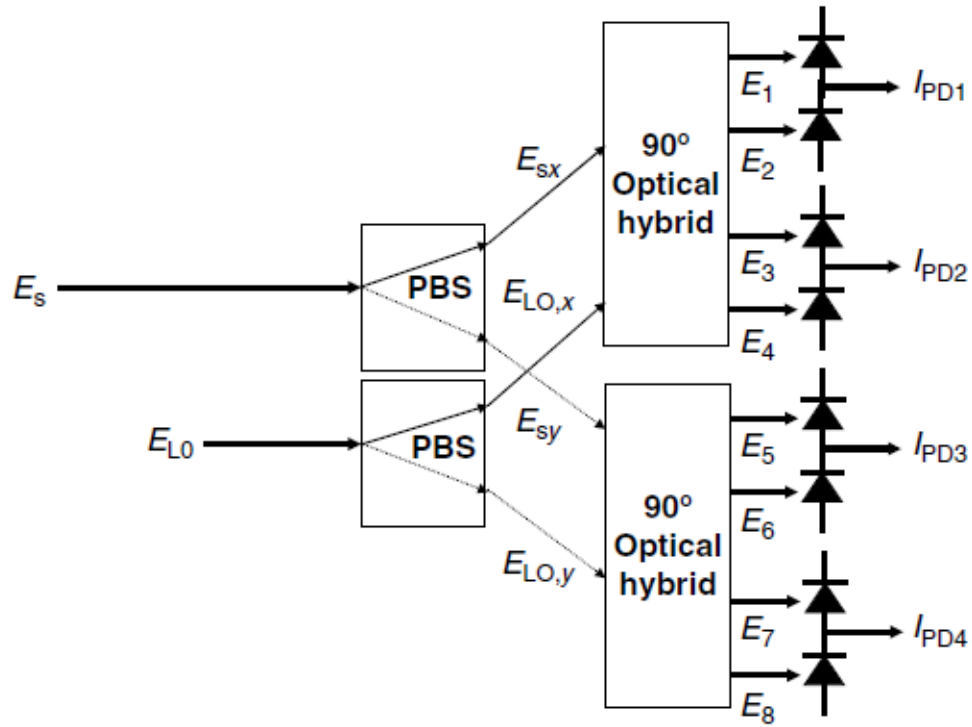


Figure 5.3.1.1 – Configuration of a Polarization/Phase Diversity Homodyne Receiver [38].

The main stages used for data recovery by means of digital signal processing were:

- Normalization and Resampling;
- Dispersion compensation;
- Equalization;
- Frequency estimation and phase recovery.

The first stage is used for signal conditioning. This block is used to normalize the samples and reshape the data that is being continuously processed to the oscilloscope sampling rate. The second stage is concerning CD compensation. A constant modulus algorithm (CMA) equalizer was used after. An equalizer is used to reverse the effects of the transmission channel, which enables reducing the ISI. The last block accomplishes frequency estimation based on [49] and phase recovery based on the Viterbi algorithm (adding feedback since this algorithm only works for a maximum phase deviation of $\pi/4$) [50].

5.3.2. Coherent QPSK System

5.3.2.1. Setup

The experimental setup used for testing the coherent QPSK system is depicted in Figure 5.3.2.1.1. As CW source was used a TLS. The signal was modulated by a Nested MZM, used to separately encode the signal components (I and Q). An adjacent channel could also be generated, in parallel, with its CW being generated by a DFB laser, modulation being performed by means of a MZM and having an EDFA managing its output power. This signal passed through a PC in order to maximize its power for the X component of the electrical field.

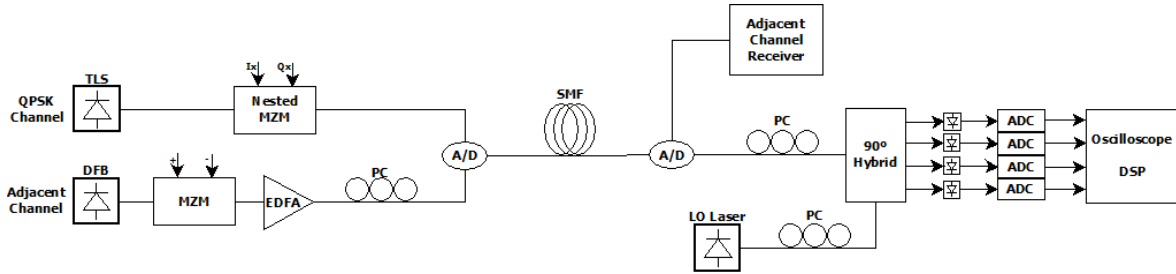


Figure 5.3.2.1.1 – Coherent QPSK System Experimental Setup.

Both channels were added by using an add-drop (A/D). These would travel through a SMF with a certain length, which was followed by another A/D to separate the two channels. The adjacent channel was directed to its dedicated receiver while the QPSK signal would pass through another PC before reaching its own receiver. The signal transmitted by the LO laser from the receiver also passed through a PC. For these tests was not focused attention to the power budget.

5.3.2.2. Results

5.3.2.2.1. Without Adjacent Channel

In these first tests the adjacent channel was not considered. The TLS used to generate the CW was working at 1550.12 nm. The QPSK signal was being transmitted at 1.244 Gbps (which means 0.622 Gsymbol/s) with 0 dBm of output power. The data payload was a $2^{15}-1$ PRBS. The sampling frequency was 50 Gsample/s (the maximum allowed by the oscilloscope). The first step

was to test the system in back-to-back configuration where 248 symbols were collected. Figure 5.3.2.2.1.1 illustrates the signal status after passing through the compensation stages.

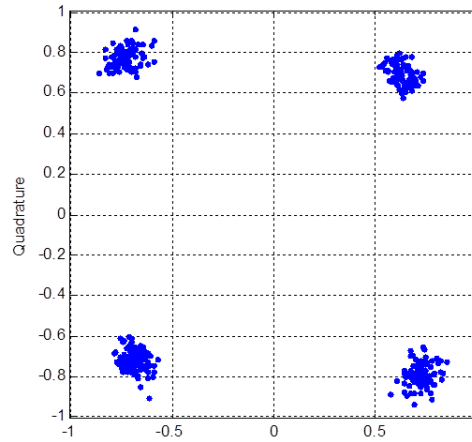


Figure 5.3.2.2.1.1 – Signal Status After Compensation for Back-to-Back (ViterbiTap = 8).

After compensation it is possible to fully detect the signal constellation. Table 5.3.2.2.1.1 presents EVM results for 3 different ViterbiTap values. The ViterbiTap value is the interval between two phase estimations.

Table 5.3.2.2.1.1 – EVM for Different ViterbiTap Values (Back-to-Back Scenario).

ViterbiTap	EVM (%)
8	6,43
16	6,98
64	8,58

After back-to-back configuration tests, the system was also tested for a 20 km length fiber. The total attenuation between the laser and the receiver was about 5 dB. The number of collected samples was the same (248 symbols). The illustration of the signal after compensation is presented in Figure 5.3.2.2.1.2.

Again, compensation allows fully detecting the constellation of the QPSK signal. Table 5.3.2.2.1.2 presents EVM results for the same 3 ViterbiTap values considered in the back-to-back scenario. Comparing these values with the ones obtained before for the back-to-back scenario, one can deduce that their difference is not much (about 1% greater).

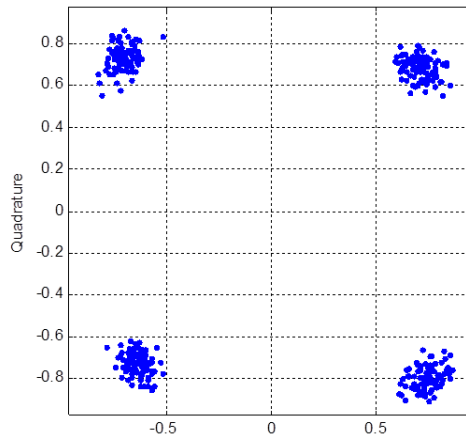


Figure 5.3.2.2.1.2 – Signal Status After Compensation for 20 km (ViterbiTap = 8).

Table 5.3.2.2.1.2 – EVM for Different ViterbiTap Values (20 km Fiber Length).

ViterbiTap	EVM (%)
8	7,25
16	8,04
64	9,84

5.3.2.2.2. With Adjacent Channel

In this case, a NRZ signal was used in the adjacent channel, and its wavelength was set at 1550.12 nm. The QPSK signal was being transmitted in the same conditions as before. The data payload of the NRZ signal was a $2^{31}-1$ PRBS. The system was tested for a 20 km length fiber.

What was done here was changing the CW wavelength of the QPSK signal, in order to examine the impact of the NRZ signal on the QPSK signal. The wavelengths used for the QPSK were: 1530.35 nm, 1535.07 nm, 1539.80 nm, 1545.35nm and 1548.55 nm. The adjacent channel was tested for 3 different values of output power (0 dBm, 8 dBm and 16 dBm), using an EDFA to control the power, as well as for 3 different bit rates (6 Gbps, 10 Gbps and 40 Gbps). To obtain the results presented below, ViterbiTap was always set at 20, and CD compensation and CMA equalization stages were removed. The total attenuation between the laser and the receiver was about 5 dB.

First, the EVM variation with QPSK signal's wavelength is presented, while having the adjacent channel transmitting at 6 Gbps. This is shown in Figure 5.3.2.2.2.1. For 0 dBm and 8 dBm, EVM values are similar to the ones obtained without having an adjacent channel, which means that in these 2 cases there was not interchannel interference.

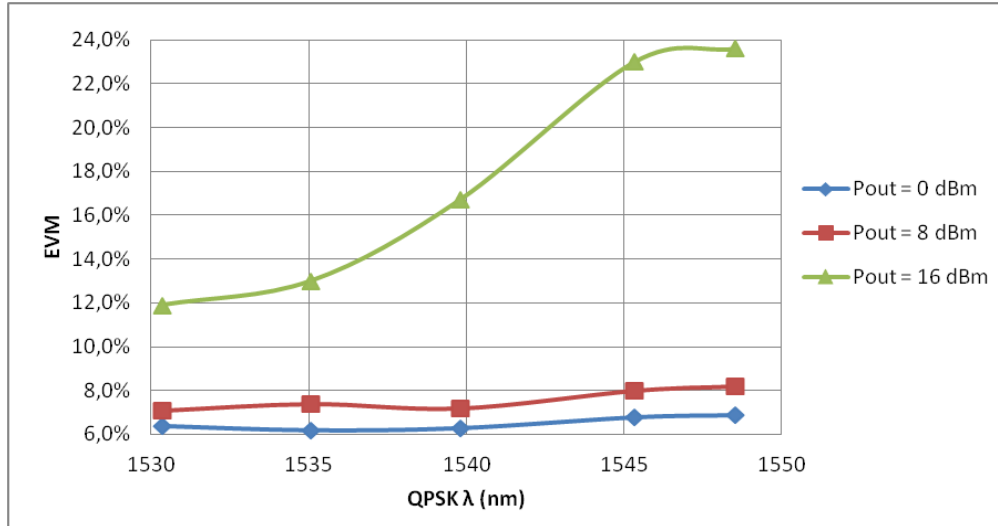


Figure 5.3.2.2.2.1 – EVM Vs. QPSK Signal Wavelength with a NRZ Adjacent Channel @ 1550.12 nm and Working @ 6 Gbps (for 3 Different Output Powers of this Channel).

For 16 dBm of output power it is possible to verify that there was interchannel interference since EVM increases from about 12%, with nearly 20 nm channel spacing, to almost 24%, with a channel spacing of approximately 1.6 nm. This means that the BER increases from a value lower than 10^{-12} to a value greater than 10^{-6} .

Figure 5.3.2.2.2.2 and Figure 5.3.2.2.2.3 depict the same analysis as the one before but for the NRZ signal on the adjacent channel working at 10 Gbps and 40 Gbps, respectively. For a 10 Gbps NRZ signal on the adjacent channel, having approximately 1.6 nm spacing, EVM is about 17.5%, which represents a BER value not much greater than 10^{-9} .

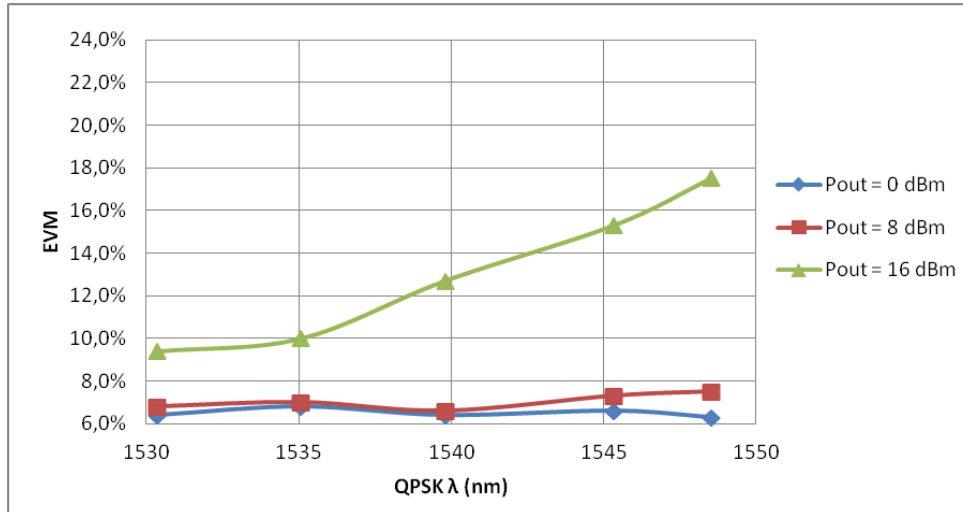


Figure 5.3.2.2.2.2 – EVM Vs. QPSK Signal Wavelength with a NRZ Adjacent Channel @ 1550.12 nm and Working @ 10 Gbps (for 3 Different Output Powers of this Channel).

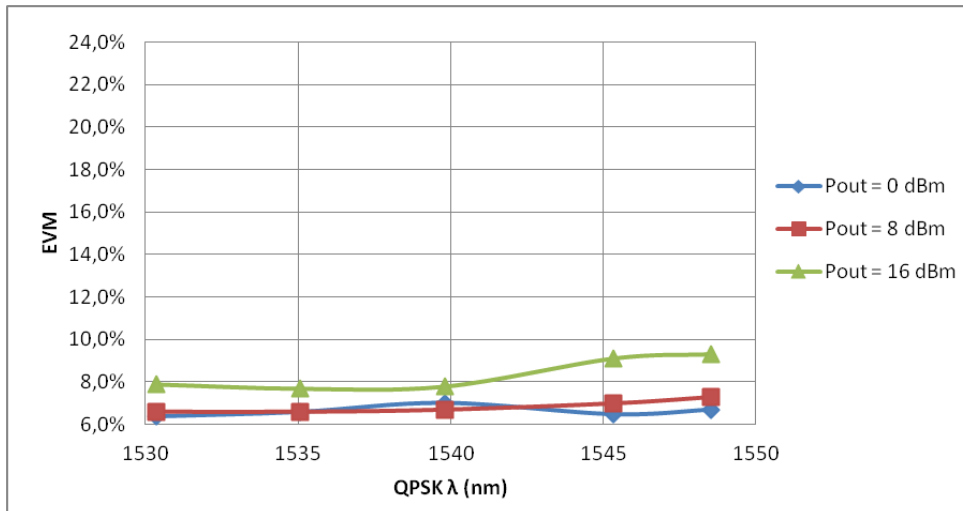


Figure 5.3.2.2.2.3 – EVM Vs. QPSK Signal Wavelength with a NRZ Adjacent Channel @ 1550.12 nm and Working @ 40 Gbps (for 3 Different Output Powers of this Channel).

For the 40 Gbps scenario, shown in Figure 5.3.2.2.2.3, it is possible to verify that, for the 16 dBm case, EVM values are not far from the ones obtained for 0 dBm and 8 dBm (which are, in fact, similar to the ones obtained without having an adjacent channel transmitting). The highest EVM value obtained for this case was 9.3%, representing a BER value much lower than 10^{-12} .

The figures presented before allow concluding that increasing the bit rate of the adjacent channel reduces the interference caused by this channel on the QPSK channel. This is proved by Figure 5.3.2.2.2.4, where the comparison for different bit rates at the same output power is presented. The output power selected was, logically, 16 dBm (since interchannel interference was only verified for this output power value). Lower bit rates channels are more susceptible to

interchannel effects (like cross-phase modulation and four-wave mixing) while higher bit rate channels are more susceptible to intrachannel effects (like self-phase modulation).

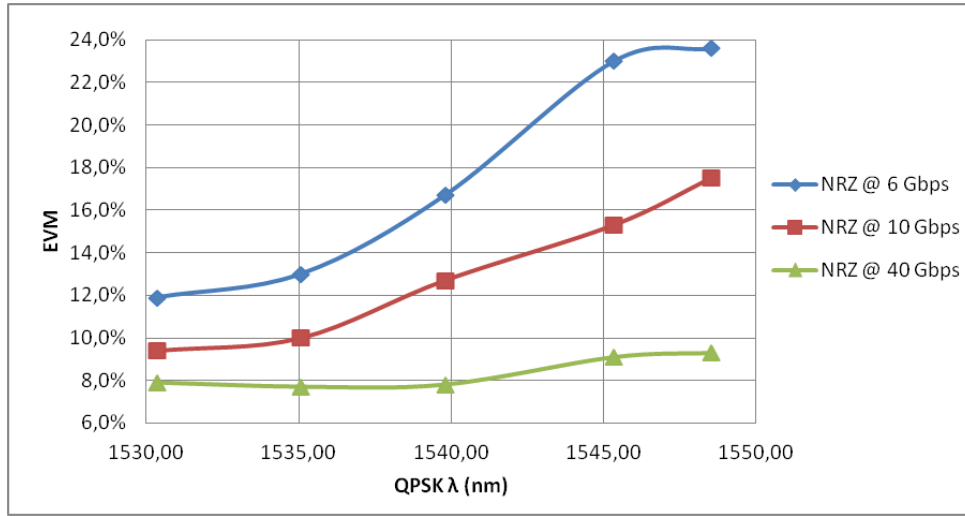


Figure 5.3.2.2.4 – EVM Vs. QPSK Signal Wavelength with a NRZ Adjacent Channel @ 1550.12 nm and for 16 dBm Output Power (for 3 Different Bit Rates of this Channel).

This allows concluding that using a WDM-PON system with QPSK signals at 1.25 Gbps enables coexistence with systems based on the already ratified 10 Gbps PON standards, XG-PON and 10G-EPON, as well as with future higher bit-rate systems. It also allows concluding that for an average output power value of 8 dBm there is no interchannel interference, at least for bit rates equal or greater than 6 Gbps.

5.3.3. Coherent UDWDM QPSK System

5.3.3.1. Setup

The experimental setup used for this part is depicted in Figure 5.3.3.1.1. The CW was generated by a TLS and a PC was used to maximize its output power. The MZM was responsible for creating the WDM channels the same way as demonstrated in [51]. In this case, 16 channels were generated, with 3.125 GHz spacing between them. For this purpose, the phase shifter was set to 190° and the RF signal's frequency was set to 3.125 GHz. Not all the 16 channels were obtained since their quality was not as good as expected, and it was decided to filter only 13 channels using a BFP.

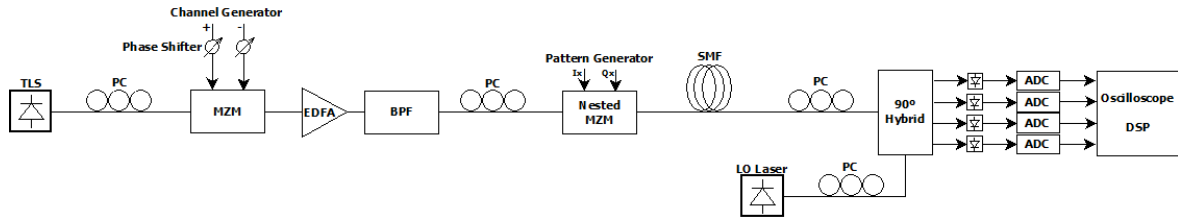


Figure 5.3.3.1.1 – Coherent UDWDM QPSK System Experimental Setup.

The EDFA was used for amplification before the BPF. Another PC was used with the same purpose as the one before. After, the Nested MZM would perform QPSK modulation in each of the channels, before transmission in a SMF with a determined length.

The channels would pass through another PC before reaching the coherent receiver. The signal transmitted by the LO laser from the receiver also passed through a PC. For these tests was also not focused attention to the power budget. Comparing to the coherent QPSK system, it was added a recovery stage responsible for filtering one of the channels for further analysis.

5.3.3.2. Results

The QPSK signals were being transmitted at 1.244 Gbps (which means 0.622 Gsymbol/s). Their output power was 0 dBm. The data payload was a $2^{15}-1$ PRBS. The sampling frequency was 50 Gsample/s (the maximum allowed by the oscilloscope). Figure 5.3.3.2.1 depicts the spectrum of the carrier (containing the 13 channels) and the spectrum of a chosen channel.

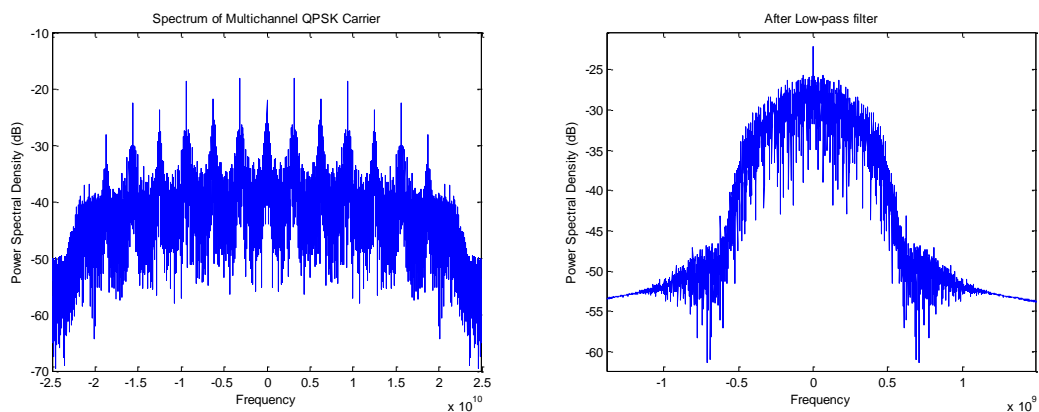


Figure 5.3.3.2.1 – Carrier's Spectrum; One of the Channel's Spectrum After Filtering (Cutoff Frequency = 0.75×622 MHz)

It makes no sense to compare these results to those obtained for the coherent QPSK system since this system presented signal degradation at the output of the Nested MZM. This is due to the fact that, while in the system presented before the data payload was driven by an electrical drive, in this case the electrical drive was used to generate the WDM channels, meaning lower quality of the PRBS.

The system was first tested in back-to-back configuration where 621 symbols were collected. The best results were obtained for a cutoff frequency of 1.8 times the symbol bit rate (622 MHz). Figure 5.3.3.2.2 illustrates the signal status after passing through all compensation stages. It is possible to verify that the system presents more distortion when compared to the coherent QPSK system. The cause was already explained, being related to the electrical drive.

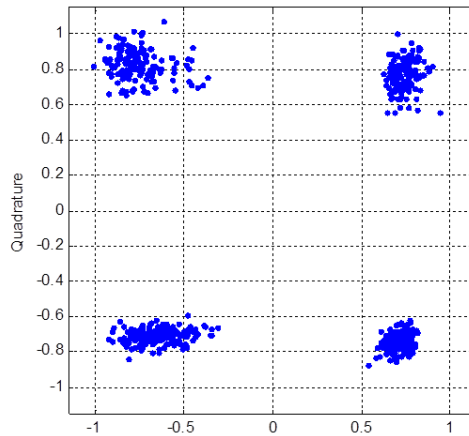


Figure 5.3.3.2.2 – Signal Status After Compensation for Back-to-Back (ViterbiTap = 8).

Once it was not possible to compare this system's results with the ones obtained for the coherent QPSK system, this system was also tested in a single channel configuration in order to measure the penalty caused by having multi channels. Table 5.3.3.2.1 presents EVM results for 3 different ViterbiTap values in both cases (single channel and multi channel).

Table 5.3.3.2.1 – Single Channel and Multi Channel EVM Results for Different ViterbiTap Values (Back-to-Back Scenario).

ViterbiTap	EVM (%)	
	Single Channel	Multi Channel
8	7,80	10,47
16	7,92	10,50
64	9,30	11,19

This system was also tested for a 20 km length fiber. Again, 621 symbols were collected. The best cutoff frequency was the same as before, 1.8 times 622 MHz. Figure 5.3.3.2.3 illustrates the status of the chosen channel after compensation. Table 5.3.3.2.2 presents EVM results for both single channel and multi channel cases, using 3 different ViterbiTap values.

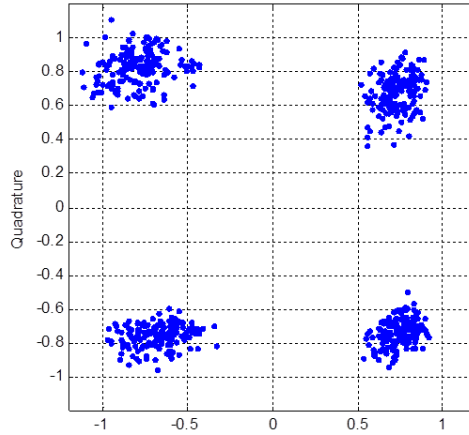


Figure 5.3.3.2.3 – Signal Status After Compensation for 20 km (ViterbiTap = 8).

Table 5.3.3.2.2 – Single Channel and Multi Channel EVM Results for Different ViterbiTap Values (20 km Fiber Length).

ViterbiTap	EVM (%)	
	Single Channel	Multi Channel
8	9,67	11,38
16	9,52	11,52
64	10,43	12,42

In both cases (back-to-back and 20 km fiber), the EVM results obtained for the multi channel scenario were about 2% greater than for the single channel scenario. It is not possible to draw major conclusions for the multi channel scenario comparing the back-to-back configuration with the 20 km length fiber configuration because the system is too noisy, not being possible to distinguish the effects of interchannel interference. This noise is also responsible for the penalty obtained for the single channel scenario because it complicates the compensation processes.

6. Conclusions and Future Work

6.1. Conclusions

This work has been presented in a set of 6 chapters. The first chapter included context, motivation, structure, objectives and the main contributions.

Chapter 2 presented an overview on WDM-PON, starting by its main advantages, namely, higher bit rates and more effective use of fiber, no need for bandwidth scheduling and capability of achieving greater transmission distances by allowing greater optical budgets. The obstacles to overcome were also discussed, including, standardization, equipment cost and investment. After, a set of guidelines that can make this technology dominate the market in the future was addressed. The possible approaches for WDM-PON architectures were described, along with the pros and cons for each case, and reported examples were presented. This technology's market status was included in the last subchapter, regarding both vendors – with particular emphasis on the use of SFPs and implementation of a UDWDM system – and service providers.

The main purpose of the third chapter was to conclude on the benefits of using advanced modulation formats in an optical network, and their impact in terms of complexity and hardware. It starts by differentiating direct modulation and external modulation, also naming the benefits and drawbacks associated to each of them. Two different types of external modulators – EAMs and EOMs – were also described. After, direct detection and coherent detection were discussed. Finally, QPSK and Duobinary modulation formats were addressed.

In chapter 4 was proposed an architecture based on tunable devices at the ONUs and a splitter at the RN, enabling up to 32 users. Each component constituting the proposed network was described and tested. After realizing the impact of each component, their settings were defined and calculations allowing obtaining an estimate in terms of optical budget were carried out.

Finally, the fifth chapter presented the experimental results obtained in the lab. The proposed architecture was tested, allowing a minimum transmission distance of 20 km. This was limited by the upstream transmission scenario, which presented a BER value of approximately 10^{-6} for an optical budget of 28 dB at 1.25 Gbps. It was possible to conclude that upstream transmission at 2.0 Gbps would also be achievable by analyzing the eye diagram at this bit rate. The results obtained for downstream transmission were much more satisfactory, leading to conclude that error free operation (BER lower than 10^{-9}) is possible to be performed at 2.5 Gbps for a 20 km length fiber (implying an optical budget of 37 dB).

The fifth chapter also included tests with coherent QPSK systems. In the first case the main goal was to investigate the possibility of using QPSK modulation, taking into account the recovery of the transmitted signal. A single QPSK channel at 1.25 Gbps was tested in two scenarios: back-to-back and 20 km fiber. The results obtained after the compensation stages were identical in both cases and the EVM values obtained were around 8% (which means a BER value much lower than 10^{-12}). After, the QPSK signal was coupled to a NRZ signal to measure the interchannel interference caused by the second on the first. The NRZ signal was tested at three different bit rates – 6 Gbps, 10 Gbps and 40 Gbps – and for 3 different output power values – 0 dBm, 8 dBm and 16 dBm. The main objective of this part was to evaluate the possibility of joining a QPSK system with 10 Gbps systems (like 10G-EPON and XG-PON) and future 40 Gbps systems. The coexistence was proved possible since increasing the bit rate resulted in less interference in the QPSK signal. Besides, it was observed that the interchannel interference only happened for the greatest output power value of the adjacent channel (16 dBm), independently of its bit rate.

In the last section of the fifth chapter were presented experimental results for a coherent UDWDM system with QPSK channels. This system was proved as a viable solution for NGPON2. The EVM results obtained for a 20 km fiber length were around 12%, meaning a BER value lower than 10^{-12} .

6.2. Future Work

The first proposal is testing the proposed WDM-PON architecture for an AWG, instead of a power splitter, at the RN. It was proved that for 1:32 splitting ratio, splitter losses are about 3 times greater than the losses caused by an AWG. This means that using an AWG at the RN would significantly reduce the total attenuation of the system (meaning an increased power budget), allowing to increase the transmission distance.

Another proposal related to the proposed architecture is changing the TLs used for better ones, in order to be possible attaining greater power budget, as well as higher bit rates, for upstream transmission.

The WDM-PON architecture demonstrated allows integration with GPON/EPON and video transmission, since the wavelengths can be chosen so as not to occupy the transmission windows used by these standards. Still, the coexistence with GPON/EPON systems shall be tested.

Regarding the use of advanced modulation formats, it is proposed testing the NRZ channels used in the proposed architecture (at 1.25 Gbps and 2.5 Gbps) along with the 1.25 Gbps QPSK channels (and for higher bit rates as well). Another proposal related to this topic is to perform tests using the duobinary modulation format. Testing a coherent UDWDM QPSK system that allows drawing conclusions on the interchannel interference might also be important. The last proposal is testing all these systems in a PON environment, where the impact of all the elements of an access network would be considered.

References

- [1] L. G. Kazovsky, W.-T. Shaw, D. Gutierrez, N. Cheng, and S.-W. Wong, "Broadband Optical Access Networks", Hoboken, New Jersey: Wiley, 2011.
- [2] M. Hajduczenia, and J. A. da Silva, "Next generation PON systems – current status", 11th International Conference on Transparent Optical Networks (ICTON 2009), June 2009.
- [3] "Fibre capacity limitations in access networks – Final report", Report for Ofcom, Analysys Mason, Jan. 2010.
- [4] "FTTH Business Guide – Edition 3", FTTH Council Europe, Feb. 2012.
- [5] "WDM-PON: A key component in next generation access" [White Paper], Transmode, Sept. 2011.
- [6] "Upgrade Strategies for GPON2 – The WDM-PON Solution" [White Paper], ADC Telecommunications, July 2008.
- [7] P. Rigby, "WDM-PON Standards: Playing the Long Game", Technically Speaking, ADVA Optical Networking, Mar. 2012 [Online]. Available: <http://blog.advaoptical.com/wdm-pon-standards-playing-the-long-game/>
- [8] FSAN (Full Service Access Network) website [Online]. Available: <http://www.fsan.org/>
- [9] A. Najam, "WDM PON: How Long Is It Going To Take?", Frost Sullivan, Nov. 2009 [Online]. Available: <http://www.frost.com/prod/servlet/market-insight-top.pag?docid=184986442>
- [10] K. Prince, T. B. Gibbon, R. Rodes, E. Hviid, C. I. Mikkelsen, C. Neumeyr, M. Ortsiefer, E. Rönneberg, J. Rosskopf, P. Öhlén, E. I. de Betou, B. Stoltz, E. Goobar, J. Olsson, R. Fletcher, C. Abbott, M. Rask, N. Plappert, G. Vollrath, and I. T. Monroy, "GigaWaM – Next-Generation WDM-PON Enabling Gigabit Per-User Data Bandwidth", J. Lightw. Technol., vol. 30, no. 10, pp. 1444-1454, May 2012.
- [11] "WDM-PON: Can it save operators over €10bn in total cost of ownership?", Gazettabyte, Oct. 2009 [Online]. Available: <http://www.gazettabyte.com/home/2009/10/30/wdm-pon-can-it-save-operators-over-10bn-in-total-cost-of-own.html>
- [12] K. Iwatsuki, and J.-i. Kani, "Applications and technical issues of Wavelength-Division Multiplexing Passive Optical Networks with colorless optical network units", IEEE/OSA J. of Opt. Commun. and Netw., vol. 1, no. 4, pp. C17-C24, Sept. 2009.
- [13] N. Cheng, and F. Effenberger, "WDM PON: Systems and Technologies" [Presentation], ECOC Workshop, Huawei Technologies, Sept. 2010.
- [14] R. Chen, H. Chin, D. A. B. Miller, K. Ma, and J. S. Harris Jr., "MSM-based integrated CMOS wavelength-tunable optical receiver", IEEE Photon. Technol. Lett., vol. 17, no. 6, pp. 1271-1273, June 2005.

- [15] F. Raharimanitra, P. Chaclo, and R. Murano, "40 Gb/s NG-PON system using low electrical bandwidth tunable receiver and emitter at 10 Gb/s", ECOC Technical Digest, Sept. 2011.
- [16] D. K. Jung, S. K. Shin, C.-H. Lee, and Y. C. Chung, "Wavelength-Division-Multiplexed passive optical network based on spectrum-slicing techniques", IEEE Photon. Technol. Lett., vol. 10, no. 9, pp. 1334-1336, Sept. 1998.
- [17] K. H. Han, E. S. Son, H. Y. Choi, K. W. Lim, and Y. C. Chung, "Bidirectional WDM PON using light-emitting diodes spectrum-sliced with cyclic Arrayed-Waveguide Grating", IEEE Photon. Technol. Lett., vol. 16, no. 10, pp. 2380-2382, Oct. 2004.
- [18] S.-M. Lee, K.-M. Choi, S.-G. Mun, J.-H. Moon, and C.-H. Lee, "Dense WDM-PON based on wavelength locked Fabry-Perot lasers", IEEE Photon. Technol. Lett., vol. 17, no. 7, pp. 1579-1581, July 2005.
- [19] L. Y. Chan, C. K. Chan, D. T. K. Tong, F. Tong, and L. K. Chen, "Upstream traffic transmitter using injection-locked Fabry-Perot laser diode as modulator for WDM access networks", Electron. Lett., vol. 38, no. 1, pp. 43-45, Jan. 2002.
- [20] P. Healey, P. Townsend, C. Ford, L. Johnston, P. Townley, I. Lealman, L. Rivers, S. Perrin, and R. Moore, "Spectral slicing WDM-PON using wavelength-seeded reflective SOAs", Electron. Lett., vol. 37, no. 19, pp. 1181-1182, Sept. 2001.
- [21] W. T. Holloway, A. J. Keating, and D. D. Sampson, "Multiwavelength source for spectrum-sliced WDM access networks and LAN's", IEEE Photon. Technol. Lett., vol. 9, no. 7, pp. 1014-1016, July 1997.
- [22] C. H. Yeh, C. W. Chow, C. H. Wang, F. Y. Shih, H. C. Chien, and S. Chi, "A self-protected colorless WDM-PON with 2.5 Gbs upstream signal based on RSOA", Optics Express, vol. 16, no. 6, Aug. 2008.
- [23] E. Wong, K. L. Lee, and T. B. Anderson, "Directly modulated self-seeding reflective semiconductor optical amplifiers as colorless transmitters in wavelength division multiplexed passive optical networks", J. of Lightw. Technol., vol. 25, no. 1, pp. 67-74, Jan. 2007.
- [24] F. Payoux, P. Chanclow, T. Soret, N. Genay, and R. Brenot, "Demonstration of a RSOA-based wavelength remodulation scheme in 1.25 Gbits bidirectional hybrid WDM-TDM PON", Optical Fiber Communication Conference (OFCC), Anaheim, CA, Mar. 2006.
- [25] R. Heron "Future technologies for the mass market residential access network – Alcatel-Lucent", European Conference on Optical Communication (ECOC), Sept. 2010.
- [26] "PONy Express – Cost-effective Optical Transport Solutions for Access Networks" [White Paper], ADC Telecommunications, Nov. 2007.
- [27] "Transmode iWDM-PON: Flexible, Open Standards Based Approach" [Application Note], Transmode, Sept. 2011.
- [28] MEL Inc. website [Online]. Available: <http://www.mel-wdmpon.com/index.html>
- [29] H. Suzuki, M. Fujiwara, T. Suzuki, N. Yoshimoto, H. Kimura, and M. Tsubokawa, "Wavelength-tunable DWDM-SFP transceiver with a signal monitoring interface and

its application to coexistence-type colorless WDM-PON", 2007 33rd European Conference and Exhibition of Optical Communication – Post Deadline Papers (published 2008).

[30] "UDWDM" [White Paper], Nokia Siemens Networks, Apr. 2012.

[31] J. S. Wey, "UDWDM PON – the clear technology winner for NG-PON2" [Presentation], NFOEC Workshop, Nokia Siemens Networks, Mar. 2012.

[32] M. Jackson, "UK Still Missing from Global Ranking of Ultrafast FTTH Broadband Countries", ISPreview, Feb. 2012 [Online]. Available:

<http://www.ispreview.co.uk/story/2012/02/17/uk-still-missing-from-global-ranking-of-ultrafast-ftth-broadband-countries.html>

[33] J. Chen, L. Wosinska, M. Forzati, A. Gavler, and E. Malésys, "Overview and assessment of existent optical access network architectures", OASE, Dec. 2010.

[34] "LG-Nortel WDM-PON Technology Gains Momentum" [Press Release], LG-Ericsson, Nov, 2009 [Online]. Available:

<http://www.lgericsson.com/global.press.viewReleases.laf?wrld=828&mid=5&openId=0>

[35] C. Peucheret, "Direct and External Modulation of Light", Experimental Course in Optical Communication, Technical University of Denmark – DTU Fotonik, Nov. 2009.

[36] G. P. Agrawal, "Fiber-Optic Communication Systems – Third Edition", Rochester, New York: Wiley, 2002.

[37] G. L. Li, and P. K. L. Yu, "Optical Intensity Modulators for Digital and Analog Applications", J. of Lightw. Technol., vol. 21, no. 9, pp. 2010-2030, Sept. 2003.

[38] I. V. Kaminow, T. Li, and A. E. Willner, "Optical Fiber Telecommunications V B: Systems and Networks", Oxford, UK: Elsevier, 2008.

[39] S. J. Savory, "Digital coherent optical receivers: algorithm and subsystems", IEEE J. of Select. Topics Quantum Electron., vol. 16, no.5, pp. 1164-1179, Sept./Oct. 2010.

[40] S. J. Savory, "Digital coherent optical receivers", Optics Express., vol. 16, no. 2, pp. 804-817, Jan. 2008.

[41] L. Zhao, H. Shankar, and A. Nachum, "40G QPSK and DQPSK Modulation" [White Paper], Inphi Corporation.

[42] "The common digital modulation techniques Phase-shift keying", Broadband India, Jan 2010 [Online]. Available: <http://www.broadbandindiamagazine.com/>

[43] "10 Steps to a Perfect Digital Demodulation Measurement" [Product Note], Agilent PN 89400-14A, Agilent Technologies.

[44] H. Shankar, "Duobinary Modulation for Optical Systems" [White Paper], Inphi Corporation.

[45] A. Tan, and E. Pincemin, "Performance Comparison of Duobinary Formats for 40-Gb/s and Mixed 10/40-Gb/s Long-Haul WDM Transmission on SSMF and LEAF Fibers" J. of Lightw. Technol., vol. 27, no. 4, pp. 396-408, Feb. 2009.

[46] VPI Photonics. Available: <http://www.vpiphotonics.com/>

- [47] M. Summerfield, "Minding Your BER's and Q's – Bit-Error-Rate and Q Factor Measurement: Theory and Practice", University of California Santa Barbara – Electrical and Computer Engineering, Nov. 1999.
- [48] R. H. Shafik, M. S. Rahman, and A. H. M. R. Islam, "On the Extended Relationships Among EVM, BER and SNR as Performance Metrics", 4th International Conference on Electrical and Computer Engineering, ICECE 2006, pp. 19-21, Dec. 2006.
- [49] A. Leven, N. Kaneda, U.-V. Koc, and Y.-K. Chen, "Frequency estimation in intradyne reception", IEEE Photon. Technol. Lett., vol. 19, no. 6, pp. 366–368, Mar. 15, 2007.
- [50] A. J. Viterbi and A. M. Viterbi, "Nonlinear estimation of PSK-modulated carrier phase with application to burst digital transmission," IEEE Trans. Inf. Theory, vol. 29, no. 4, pp. 543–551, Jul. 1983.
- [51] T. Sakamoto, T. Kawanishi, and M. Izulsu, "Optimization of electro-optic comb generation using conventional Mach-Zehnder modulator," 2007 IEEE International Topical Meeting on Microwave Photonics, pp. 50-53, Oct. 2007.